Identification of the Transcriptional Regulators of ATP7B gene by Genomic Locus Proteomics and Their Effect on Cisplatin Resistance

by

Ayça Açar

A Dissertation Submitted to the
Graduate School of Health Sciences
in Partial Fulfillment of the Requirements for
the Degree of

Master of Science

in

Cellular and Molecular Medicine

KOÇ
ÜNİVERSİTESİ

July 24, 2023

ABSTRACT

Identification of the Transcriptional Regulators of ATP7B gene by Genomic Locus Proteomics and Their Effect on Cisplatin Resistance

Ayça Açar

Master of Science in Cellular and Molecular Medicine

July 24, 2023

ATP7B is a copper pump that plays a vital part in cellular homeostasis. It removes the excess metal from the cells to prevent the toxic results of copper accumulation. Insufficient ATP7B activity results in copper gathering in the body, culminating in Wilson's disease. Upregulation of ATP7B conversely causes the removal of platinum-based drugs along with copper, leading to drug resistance. Understanding the transcriptional regulation of ATP7B may shed light on the mechanisms of disease progression.

Metal Regulatory Transcription Factor 1 (MTF1) is a well-studied regulator of ATP7B; however, its expression does not always correlate with ATP7B expression in cancers. The expression of a transcription factor does not always have to be correlated with the expression of the target gene. But the probability that ATP7B is regulated by a single transcription factor is also very low, thus indicating the necessity to identify novel regulators of ATP7B. An in-silico analysis using TRANSFAC/PROMO software was performed to find these additional factors. It was found that several transcription factors may bind to the ATP7B promoter, which was focused around -3000 to +1, indicating that the regulatory sequences are most likely located in this region.

A novel proximity labeling methodology called "Genomic Locus Proteomics" was used in this thesis to identify the transcription factors that regulate ATP7B expression. In this technique, the deadCas9 (dCas9) protein is fused to the APEX2 enzyme, and the protein is guided to the ATP7B promoter via specific gRNAs. The efficient gRNAs spanning the -3000 to +1 region were determined by T7E assay and ChIP-qPCR experiments. The proteins near the dCas9-targeted regions of the ATP7B promoter were subsequently biotinylated with the APEX2 enzyme and pulled down with streptavidin-magnetic beads. The marked proteins were then identified with mass spectrometry, and several proteins were selected based on their enrichment scores and their associations with cancer progression and drug resistance in cancers.

The target gene PINX1 (Pin2/TRF1-Interacting Protein) was analyzed to illuminate its relationship with ATP7B activity, and it was shown that overexpression of this gene leads to an increase in ATP7B expression. Furthermore, PINX1 overexpression in the HEK293T and Huh7 cells increased the cell viability against cisplatin treatment. This resistance to cisplatin is attributed to the heightened ATP7B activity in the cells. Our findings indicate a transcriptional connection between PINX1 and ATP7B. This relationship may play a role in the progression of the disease and could potentially be utilized to develop more effective therapies.

Keywords: ATP7B, copper, cisplatin resistance, Wilson's disease, proximity labeling assay, mass spectrometry

ÖZETÇE

ATP7B Geninin Transkripsiyonel Regülatörlerinin Genomik Lokus Proteomik Yöntemi ile Tanımlanması ve Cisplatin Direncine Etkilerinin Araştırılması

Ayça Açar

Hücresel ve Moleküler Tıp, Yüksek Lisans

24 Temmuz 2023

ATP7B, hücresel homeostazda hayati bir rol oynayan bir bakır pompasıdır. Bakır birikiminin toksik sonuçlarını önlemek için hücrede biriken fazla metali ekzositoz yolu ile hücreden uzaklaştırır. Yetersiz ATP7B aktivitesi, vücutta bakır toplanmasına neden olarak Wilson hastalığına neden olur. ATP7B'nin expresyonundaki artış ise tam tersine, platin bazlı ilaçların bakırla birlikte hücreden atılmasına neden olarak ilaç direncine yol açar. ATP7B'nin transkripsiyonel seviyede regülasyonunu anlamak, bu genin disregülasyonu sonucu oluşan hastalıkların mekanizmalarını anlamaya yardımcı olabilir.

Metal Düzenleyici Transkripsiyon Faktörü 1 (MTF1), ATP7B'nin en çok çalışılmış transkripsiyonel düzenleyicisidir, ancak ekspresyonu, kanserlerde ATP7B ekspresyonu ile her zaman ilişkili değildir. Bir transkripsiyon faktörünün ekspresyonu her zaman hedef genin ekspresyonu ile ilişkili olmak zorunda değildir. Ancak ATP7B'nin tek bir transkripsiyon faktörü tarafından düzenlenme olasılığı da çok düşüktür, bu da ATP7B'nin düzenleyicilerinin tanımlanması gerekliliğini göstermektedir. ATP7B anlatımını düzenleyen ek faktörleri bulmak için, TRANSFAC/PROMO yazılımı kullanılarak bir in-silico analiz gerçekleştirildi ve birkaç transkripsiyon faktörünün -3000 ila +1 civarında odaklanan ATP7B promotörüne bağlanabileceği bulundu, bu da düzenleyici dizilerin en çok bu bölgede toplandığını göstermektedir.

ATP7B ekspresyonunu düzenleyen transkripsiyon faktörlerini tanımlamak için bu tezde "Genomik Lokus Proteomik" adlı yeni bir proximity-labeling metodolojisi kullanılmıştır. Bu teknikte, dCas9 proteini APEX2 enzimi ile birleştirilmiş ve protein, spesifik gRNA'lar aracılığıyla ATP7B promotörüne yönlendirilir. -3000 ila +1 bölgesini kapsayan gRNA'lar, T7E ve ChIP-qPCR deneyleri ile belirlendi. ATP7B promotörünün dCas9 hedefli bölgelerinin yakınındaki proteinler daha sonra APEX2 enzimi ile biyotinlendi ve streptavidin-manyetik bead ile çöktürüldü. İşaretlenen proteinler daha sonra kütle spektrometresi ile tanımlandı ve zenginleştirme puanlarına ve kanserlerde ilaç direnci ile ilişkilerine göre birkaç protein hedef olarak seçildi.

ATP7B aktivitesi ile ilişkisini aydınlatmak için hedef gen PINX1 (Pin2/TRF1-Interacting Protein) analiz edildi ve bu genin aşırı ekspresyonunun ATP7B ekspresyonunda bir artışa yol açtığı gösterildi. Ayrıca, HEK293T ve Huh7 hücrelerinde PINX1 aşırı ekspresyonu, sisplatin tedavisine karşı hücre canlılığını arttırdı. Analiz sonuçları PINX1 ve ATP7B arasında transkripsiyonel bir şekilde bir bağlantı olduğunu göstermektedir. Bu ilişki hastalığın ilerlemesine sebep olabilir ve daha etkili tedaviler geliştirmek için kullanılabilir.

Anahtar kelimeler: ATP7B, bakır, cisplatin direnci, Wilson's hastalığı, kütle spektrometrisi

ACKNOWLEDGEMENTS

I would like to express my gratitude to my advisor Prof. Ceyda Acılan Ayhan for her mentorship and guidance throughout my studies. Her expertise and support have played a crucial role in the success of this thesis. I would also like to thank my committee members Assist. Prof. Gözde Korkmaz and Assoc. Prof Kirill Kiselyov for their comments and suggestions.

I would like to express my heartfelt appreciation to my lab mate and project mate MSc. student Batuhan Altay whose support, friendship, and collaboration have been invaluable throughout our research journey. In addition, I would like to thank Dr. Selahattin Can Ozcan and Ph.D. Student Barış Sergi for their assistance and guidance throughout my research. I am also grateful to my lab mates for their moral support and inspiration. The collaborative research environment in our lab has made our studies truly enjoyable.

This thesis is the output of the project titled “Characterization of the Transcriptional Regulation of ATP7B Gene by Genomic Locus Proteomics and the Role of ATP7B Regulators on Cisplatin Resistance in Cancer” funded by TÜBİTAK. I would like to express my gratitude to TÜBİTAK for their support.

Lastly, I would like to thank my family for their unwavering support. I could not have undertaken this journey without their encouragement and motivation.

Thank you all,

Ayça Açar

TABLE OF CONTENTS

LIST OF TABLES

LIST OF FIGURES

ABBREVIATIONS

APEX	Ascorbate peroxidase
ATP7A	ATPase copper transporting alpha
ATP7B	ATPase copper transporting beta
BCA	Bicinchoninic Acid
BET	Bromodomain and extra-terminal domain
BSA	Bovine Serum Albumin
CASPEX	dCas9-APEX2
cDNA	Complementary Deoxyribonucleic Acid
ChIP	Chromatin Immunoprecipitation
CRISPR	Clustered Regularly Interspaced Short Palindromic Repeats
dCas9	Dead CRISPR-associated protein
DMEM	Dulbecco's Modified Eagle Medium
DMSO	Dimethyl sulfoxide
DNA	Deoxyribonucleic Acid
EDTA	Etheylenediaminetetraacetic Acid
FBS	Fetal Bovine Serum
GAPDH	Glyceraldehyde-3-Phosphate Dehydrogenase
GBM	Glioblastoma
GD	Gene desert
GFP	Green Fluorescent Protein
gRNA	Guide RNA
HAT	Histone acetyltransferase
HDAC	Histone deacetylase
HRP	Horseradish peroxidase
INDEL	Insertion-deletion
KO	Knock-out
LFQ	Label-free quantification
LIHC	Liver hepatocellular carcinoma
LOH	Loss of heterozygosity
MMLV	Moloney Murine Leukemia Virus
MRE	Metal responsive element

MTF1	Metal regulatory transcription factor 1
NAC	N-acetyl-L-cysteine
NHEJ	Non-homologous end-joining
NP40	Nonylphenoxypolyethonxyethanol
NT	Non targeting
OX	Overexpression
PAGE	Poly acrylamide gel electrophoresis
PBS	Phosphate-Buffered Saline
PCR	Polymerase Chain Reaction
PINX1	Pin2/TERF1 interacting telomerase inhibitor 1
PNK	Polynucleotide Kinase
PVDF	Polyvinylidene difluoride
qPCR	Quantitative polymerase chain reaction
RNA	Ribonucleic Acid
ROS	Reactive oxygen species
SDS	Sodium dodecyl sulfate
SNP	Single nucleotide polymorphism
SRB	Sulforhodamine B
T7E	T7 Endonuclease
TBST	Tris Buffered Saline Tween-20
TCA	Trichloroacetic Acid
TERT	Telomerase reverse transcriptase
TFEB	Transcription factor EB
THCA	Thyroid carcinoma
TID	Telomerase inhibiting domain
TRF1	Telomeric repeat binding factor 1
TSS	Transcription start site

Chapter 1:
INTRODUCTION

1.1 ATP7B function in copper metabolism

Copper is a metal utilized in cells during many essential processes such as tissue generation and cellular respiration. Oxidation of this metal however gives rise to the formation of oxygen radicals. Copper metabolism is strictly controlled in the cells via various pathways to ensure they obtain sufficient copper to maintain their homeostasis while preventing the copper amounts from reaching toxic levels (Polishchuk & Lutsenko, 2013). ATP7B is a P-type ATPase that plays an essential part in copper metabolism in the cell and secures the correct trafficking of copper. ATP7B resides in Golgi and gets located in lysosomes when the copper levels are increased in the cell to hinder harmful copper accumulation (Polishchuk & Lutsenko, 2013).

1.1.1 ATP7B and Wilson's Disease

Such a significant role requires strict control and maintaining the balance between gene expression, and the copper levels in the cells is crucial for stable homeostasis. As expected, the dysregulation of ATP7B activity results in several physiological problems (Figure *1.1*). A deficiency of ATP7B expression leads to copper gathering in the brain and liver and inevitably leads to the progression of a rare disease called Wilson's Disease (Ala, Walker, Ashkan, Dooley, & Schilsky, 2007). The disease symptoms vary from liver failures to neurological defects while the beginning of the symptoms ranges from childhood to 40 years of age based on the genetic background and epigenetic changes (Poujois & Woimant, 2019).

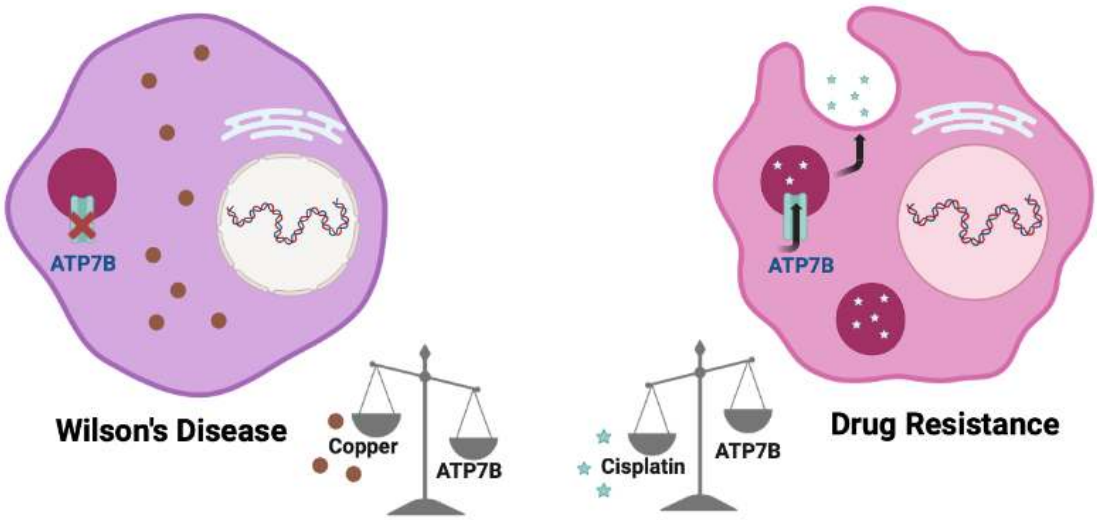

Figure 1.1: Schematic representation of the relationship between dysregulation of ATP7B activity and physiological disorders.

A study of next-generation sequencing data conducted in 2019 revealed that the prevalence of Wilson's disease is 13.9 per 100.000. However, this ratio increases dramatically in isolated regions such as Crete and the Canary Islands, where the occurrence of the disease rises to 35 per 100.000 (Gao, Brackley, & Mann, 2018). The current common therapy for Wilson's disease includes the use of a chelator agent to remove heavy metals such as copper from the body; however, this method does not correct the copper metabolism in the body and could result in unfavorable outcomes (Greig et al., 2019). Gene therapy approaches propose a permanent solution to the disease by utilizing adenoviral vectors to restore ATP7B expression activity for patients suffering from Wilson's disease (Greig et al., 2019). Understanding the molecular basis behind the disease could provide new approaches to developing treatments for the disease.

Another P-type ATPase, ATP7A is also involved in the maintenance of copper homeostasis in the cell and resembles ATP7B in structure. Both ATP7A and ATP7B function in the removal of copper via exocytosis. Deficiency in ATP7A activity also results in a genetic disease called Menkes disease (Linz & Lutsenko, 2007). Mutations in ATP7A lead to copper accumulation in the intestine, however, copper absorbance is limited, and results in a copper deficiency in the liver and brain, similar to Wilson's disease (Fujisawa et al., 2022). When copper levels are elevated in the cells, both of these

proteins get transported to the vesicular components adjacent to the plasma membrane (La Fontaine & Mercer, 2007).

1.2 Role of ATP7B in cisplatin resistance

1.2.1 Cisplatin

Cisplatin is a platinum-based chemotherapeutic drug used in the treatment of several cancer types such as lung, ovarian, head, and neck cancers. Cisplatin affects the cells either by damaging DNA by the formation of DNA adducts or generating oxidative stress in the cells and resulting in apoptosis (Dasari & Bernard Tchounwou, 2014). The cellular uptake of cisplatin induces the reaction between the drug and the purine residues on the nucleic acids and then causes the generation of cross-links in DNA. This may activate the DNA repair mechanisms in the cells, and hinder the cell cycle (Yimit, Adebali, Sancar, & Jiang, 2019).

Reactive oxygen species (ROS) are the byproducts of oxidative phosphorylation in mitochondria. Incomplete reduction of oxygen generates ROS complexes and may undercome the ROS-scavenging systems in the cells and leads to oxidative stress (Ray, Huang, & Tsuji, 2012). The cisplatin treatment disrupts the antioxidant components in the cells and results in an increase in oxidative stress (Saad, Najjar, & Alashari, 2004).

1.2.2 ATP7B plays a role in cisplatin resistance

Many patients develop resistance against cisplatin treatment over time which leads to poor prognosis and disease recurrence. The drug resistance may stem from alterations of cisplatin efflux in the cells or detoxification of the drug via various mechanisms (Dasari & Bernard Tchounwou, 2014). *In vitro* experiments demonstrate that in ovarian carcinomas, ATP7B expression was shown to be higher compared to normal ovarian cells. Due to its role as a metal pump, it was suggested that ATP7B is involved in the efflux of cisplatin from the cells and leads to resistance to the cisplatin therapy (Nakayama et al., n.d.). In cisplatin-resistant cells, ATP7A and ATP7B are mostly shuttled to the cell periphery from the Golgi network to export cisplatin. Thus, inaccurate localization of ATP7B hinders the cisplatin to interact with its target nuclear DNA and

eventually results in chemotherapeutic resistance (Kalayda, Wagner, Buß, Reedijk, & Jaehde, 2008).

In addition to the increased drug efflux by the copper pumps ATP7A and ATP7B, high-affinity copper uptake protein CTR1 could also be involved in the decreased influx of the cisplatin (Schoeberl et al., 2022). However, only the alterations in the ATP7A and ATP7B levels in the cells were linked with the platinum-based drug resistance (Lukanović, Herzog, Kobal, & Černe, 2020). Moreover, the knock-down of ATP7A did not reverse the cisplatin resistance, but suppressed ATP7B expression led to the DNA adduct formation, and could significantly reverse the drug resistance phenotype (Mangala et al., 2009).

The relationship between platinum drug resistance and ATP7B expression was also indicated with the localization shift of ATP7B from Golgi to the vesicles in drug-resistant cancer cell lines (Kalayda et al., 2008). Targeting the copper pump of the cells thus may increase the efficiency of drug-based therapies for cancer via manipulating the mechanisms that would lead to resistance phenotypes.

1.3 Regulation of ATP7B expression

ATP7B gene is located on the 13th chromosome and consists of 21 exons (Telianidis, Hung, Materia, & Fontaine, 2013). The core promoter sequence of the ATP7B gene was proposed to reside in the bidirectional promoter region between ATP7B and ALG11 genes which host several transcription factor binding motifs (Höflich, Brieger, Zeuzem, & Plotz, 2021). So far, a few potential transcription factors which could regulate ATP7B activity were proposed, and their binding sequences were analyzed.

1.3.1 Transcriptional Regulation

The transcriptional regulation process aids the cells to respond and adapt to the changes in their environment by controlling the transcription activity of a gene and therefore organizing the cellular signaling mechanisms. Numerous proteins are involved in the regulation via DNA-protein interactions to either recruit the transcriptional machinery to the target site or initiate epigenetic mechanisms such as histone modifications (Casamassimi & Ciccodicola, 2019). Transcription factors control a gene's expression by binding to the target gene and then recruiting necessary components of

transcriptional machinery such as polymerases and regulatory proteins (Lee & Young, 2013).

1.3.2 Transcription factors controlling ATP7B activity.

The presence of metal-responsive elements (MREs) in the ATP7B promoter region suggests that transcription factors could bind to the region upon the increase in metal levels (Oh, Kim, Park, Hahn, & Yoo, 1999)(Culotta & Hamer, 1989). Metal Regulatory Transcription Factor 1 (MTF1) binds to the consensus sequences of MREs located near the promoter of genes that are involved in mediating the metal levels in the cells. The binding is induced by the efflux of metal ions such as zinc into the cells and MTF1 gets located in the nucleus to activate the transcription of the target genes (Tavera-Montañez et al., 2019). The binding of MTF1 to the ATP7B promoter was verified and shown that this binding enhances the ATP7B gene activity (Stalke et al., 2020).

Figure 1.2: Metal responsive element (MRE) on the promoter region of a target gene, occupied by MRE-binding transcription factor 1 (MTF1).

Represented data adapted from Fujie, Hara, & Kaji, 2016.

Dysregulations in MTF1 activity also disrupt ATP7B expression. It had been demonstrated in a study that a homozygous variant that distorts the MTF1 binding site on the ATP7B promoter region leads to reduced ATP7B activity and Wilson's Disease (H. I. Chen et al., 2018). However, in cancers, ATP7B levels are not always correlated with MTF1 levels (H. Liu, 2022). Expression of a transcription factor does not always have to be correlated with the expression of the target gene. But the probability that ATP7B is regulated by a single transcription factor is also very low, thus indicating the necessity to identify novel regulators of ATP7B to shed light on the mechanisms leading to cisplatin drug resistance.

Possible binding sites of several liver-specified transcription factors such as HNF1, HNF2, and CTF were also identified at the upstream of ATP7B coding region (Loudianos et al., 1999). Transcription factor EB (TFEB) is also a major regulator of lysosomal genes and its binding to specific loci on ATP7B promoter region was demonstrated only by the presence of platinum-based drugs in the medium and as a result, increases ATP7B activity and maintains the resistance phenotype (Petruzzelli et al., 2022). The binding of these factors and how their effects induce cisplatin resistance via the ATP7B activation pathway remains a current interest in the field.

1.3.3 Epigenetics

Epigenetics are defined as the inheritance of genetic information without altering the DNA sequence. Chromatin structure contains DNA and histones and the change in this structure affects the gene activity. If the modifications on DNA and histones result in a more open structure, the transcriptional machinery can be recruited to the target sequence, and the gene is turned on. On the other hand, if the chromatin structure is more condensed, the transcription activity is diminished (Hess-Stumpp, Bracker, Henderson, & Politz, 2007). These epigenetic changes are controlled by histone-modifying enzymes by the addition or detachment of chemical groups through the processes such as acetylation or methylation (Cohen, Poręba, Kamieniarz, & Schneider, 2011).

1.3.4 Histone Deacetylation

Post-translational modifications on histones could affect the expression of a target gene. Several histone modifications have been identified and one of the commonly studied modifications is the acetylation of the amino groups on lysine residues on the histone tails. This reversible process is maintained by the two classes of enzymes called histone acetyltransferases (HATs) and histone deacetylases (HDACs). Removing the acetyl group on the histone tails by HDAC activity usually results in the suppression of the gene expression by the enhancement of the DNA-histone interaction and by inhibiting the access of the transcriptional proteins binding to the DNA (Gallinari, Di Marco, Jones, Pallaoro, & Steinkühler, 2007). Histone deacetylation could also lead to additional posttranslational modifications such as methylation or ubiquitination and unbalanced HDAC activity would result in some physiological problems (Seto & Yoshida, 2014).

HDAC family of proteins is divided into four categories based on their sequence homologies. Class I proteins are labeled as HDAC1, HDAC2, HDAC3, and HDAC8. Class II proteins are labeled as HDAC4, HDAC5, HDAC6, HDAC7, HDAC9, and HDAC10. Class III proteins are labeled as sirtuins and have NAD-dependent deacetylase activity. Class IV protein is labeled as HDAC11 (Seto & Yoshida, 2014).

1.3.5 Bromodomains

Histone acetylation mark could result in the recruitment of bromodomain-containing proteins and bromodomain extra-terminal proteins (BETs) to the site and enhances transcriptional activity by the further recruitment of transcriptional machinery (Cochran, Conery, & Sims, 2019). BET inhibitors are chemical drugs that block the 'reading' activity of the bromodomain proteins on the acetylated residues on the histone tails and could alter the transcriptional activity (Chueh, Tse, Tögel, & Mariadason, 2015).

1.3.6 Epigenetic changes alter gene (ATP7B) expression

Evidence suggests that epigenetic regulation of ATP7B plays a vital role in Wilson's disease progression. Epigenetic changes consist of alterations in gene expression level without any change or mutation in the nucleotide sequence itself (Jaenisch & Bird, 2003). In mouse disease models, histone deacetylases HDAC4 and HDAC5 levels were diminished when the copper amounts are increased. As a result, histone acetylation marks are imbalanced in the cells, disrupting the gene regulation (Sarode et al., 2021). Investigating the epigenetic alterations in the ATP7B gene is also crucial to shed light on the mechanism of the gene's regulation.

1.4 Proximity Labeling Assays

Proximity labeling assays are used to demonstrate protein-protein interactions which employ the biotin tag to label adjacent proteins interacting with a target protein or a genomic locus (Trinkle-Mulcahy, 2019). These techniques are usually coupled with mass spectrometry to identify the target proteins, also as an advantage, compared to the prior labeling protocols, these assays allow the researchers to study these interactions in their native state (Ummethum & Hamperl, 2020).

The main component of proximity labeling assay is derivatives of peroxidases that oxidize compounds using hydrogen peroxide in the medium. The initial protocols involved horseradish peroxidases (HRP) which were useful to perform immunofluorescence experiments (Mayer & Bendayan, 1997). A modified version of ascorbate peroxidase (APEX) obtained from peas took over the stage and was utilized by its smaller size and ability to remain active in the cytosolic medium. The enzyme adds biotin tags to the adjacent proteins in the presence of hydrogen peroxide and biotin-phenol, specifically reacting with tyrosine residues (Lam et al., 2014)(Ummethum & Hamperl, 2020).

1.4.1 CRISPR- guided assays

Combining genome editing technologies with proximity labeling assays has been a great tool to shed light on DNA-protein interactions. In genome editing techniques, a double-strand break is introduced and the repair pathways in the cell are activated to repair the break without a major loss of the genomic sequence (D. B. T. Cox, Platt, & Zhang, 2015). In CRISPR-Cas9 systems, Cas9 protein is recruited to the desired genomic locus by a guide RNA and performs a cleavage at the site. When a DNA template was introduced in the cell, the machinery could perform a homology-directed repair to fill in the cleavage site thus creating a customized sequence. A directed targeting of Cas9 can result in the loss of the sequence and could affect the transcription efficiency or result in an inactive protein translation, thus producing a knock-out of the gene (Doudna, 2020). On the other hand, dead Cas9 (dCas9) proteins that have no endonuclease activity are solely used to target a specific genomic locus. These techniques can be used to monitor gene regulation both in a transcriptional and epigenetic manner. In different experimental setups, dCas9 can be fused with specific enzymes to visualize protein relations by microscopy techniques or investigate their binding partners with immunoprecipitation (Saifaldeen, Al-Ansari, Ramotar, & Aouida, 2020)(Kanafi & Tavallaei, 2022).

A novel technique termed “Genomic Locus Proteomics” was introduced recently which utilizes an APEX2 enzyme fused with dCas9 (CASPEX), and it can be targeted to a specific locus with designed guide RNAs and can add a biotin tag to all the adjacent proteins (Figure *1.3*). The strong interaction between biotin and streptavidin assists in performing pulldown experiments with streptavidin-coated beads, then the labeled

proteins can be identified by mass spectrometry and their enrichment scores can be evaluated (Myers et al., 2018).

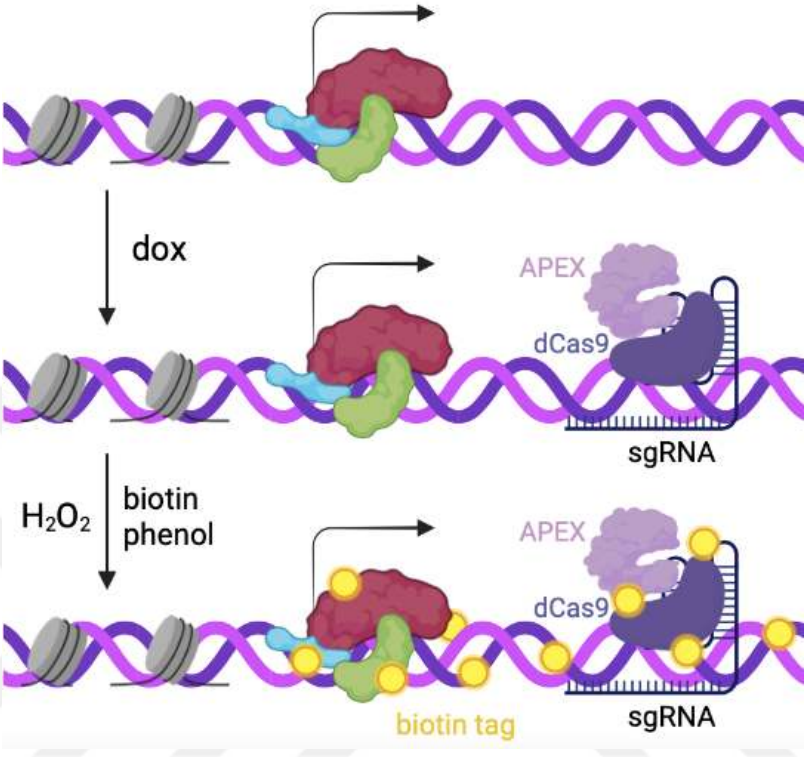

Figure 1.3: dCas9-APEX2 mediated proximity labeling assay

Represented data adapted from (Myers et al., 2018).

In this thesis, the "Genomic Locus Proteomics" method was used to examine the transcriptional regulation of ATP7B. 15 different gRNAs that target the ATP7B promoter region from the transcription start site (TSS) to the upstream region of 3000 base pairs (bp) were designed initially and transfected to HEK293T cell lines that express CASPEX protein. The choice for that region stems from the presence of putative promoter sequences and regulatory sequences in that area (Höflich et al., 2021). The proteins near the dCas9-targeted regions of the ATP7B promoter were subsequently biotinylated with the APEX2 enzyme and identified with mass spectrometry. Several transcription factors were selected based on their enrichment scores and their association with cancer progression. The relationship between the target proteins and the ATP7B expression was analyzed with *in vitro* experiments. qPCR analysis showed that overexpression of PINX1 (Pin2/TRF1-Interacting Protein) leads to an increase in ATP7B activity. The overexpression of this gene also increases the cell viability against cisplatin treatment in

hepatocellular cancer cell lines. Thus, PINX1 is proposed as a potential regulator of ATP7B in a transcriptional manner.

Chapter 2:
MATERIALS AND METHODS

2.1 Cell Culture and Cell Lines

HEK293T, Huh7, and Du145 cell lines (ATCC, CRL-3216, HTB-81) were grown at 37℃ and 5% CO_2 conditions. HEK293T and Huh7 cell lines were grown in DMEM-high glucose (Sigma Aldrich, D5796), heat-inactivated 10% fetal bovine serum, 100 U/ml of penicillin, and 100 µg/ml of streptomycin. Du145 cells were grown in RPMI-1640 (Sigma Aldrich, R8758), heat-inactivated 10% fetal bovine serum, 100 U/ml of penicillin, and 100 µg/ml of streptomycin.

2.2 Generation of HEK293T-CASPEX cell lines

2.2.1 Generation of a stable dCas9-APEX2 expressing cell line and confirmation with flow cytometry

HEK293T cells were seeded as $5x10^4$ in a 6-well plate. After 24 hours, the cells were transfected with dCas9-APEX2 (Addgene; 97421) and Piggy-Bac Transposase (System Biosciences; PB210PA-1) using Lipofectamine 3000 (Thermo; L300015). After 24 hours, their media were changed with fresh media, and the cells were treated with 2 µg/ml puromycin. At the end of the selection, which was marked by the 100% of non-transfected control HEK293T cells were dead, the cell medium was changed again. The cells were treated with 2 mg/ml doxycycline for 48 hours. Then, the cells were trypsinized and sorted by Sony Cell Sorter (SH800S) based on their GFP positive signals into a 96-well plate as 1 cell/1 well.

When microscopically observable colonies were formed, the cells were trypsinized and passaged into 12-well plates. Then they were divided into 2 when the cells reached optimum confluency, and one group was treated with 2 µg/ml doxycycline for 48 hours. The cells were again sorted by the Cell Sorter to calculate the GFP-positive cells in the population.

2.2.2 Immunofluorescence Staining

HEK293T cells were placed on coverslips and fixed using ice-cold methanol for 20 minutes at -20°C. Following this, they were permeabilized with 0.1% Triton X-100 for 15 minutes at room temperature and then blocked with 1% BSA for 15 minutes at room temperature. The samples were subjected to overnight treatment with a 1:100 dilution of anti-V5 antibody (Invitrogen, R960) at 4°C. Next, the samples were washed with PBS and exposed to goat anti-mouse IgG H&L - Alexa Fluor 594 secondary antibody (Abcam, ab150116) for 1 hour at room temperature. After a 5-minute PBS wash, the coverslip was mounted with DAPI (Abcam, ab228549) on a glass slide. Finally, the specimen was observed under a fluorescence microscope (Axiocam 506 mono Imager M1 from Zeiss).

2.2.3 Immunoprecipitation

HEK293T and HEK293T-CASPEX cells were treated with 2 mg/mL doxycycline for 48 hours and then lysed with RIPA buffer (EcoTech Biotechnology, Sigma Aldrich, #R0278) for 30 minutes at 4°C. They were centrifuged for 10 minutes at 10000g. The supernatant was collected and analyzed with a BCA assay to determine protein quantification. The lysates were mixed with anti-FLAG antibody (Sigma, F1804) and magnetic beads. Then the Laemmli buffer was added to elute the antibody-protein complexes from the beads. The samples were incubated for 10 minutes at 95°C and loaded onto an SDS-PAGE gel. After electrophoresis, they were transferred onto a PVDF membrane, blocked with 5% NFDM (BioRad, 1706404), and incubated with suitable secondary antibodies which are goat anti-rabbit IgG (Abcam, ab97051) or goat anti-mouse IgG (Abcam, ab97023). The membrane was imaged by the LI-COR Odyssey FC Imaging system (LI-COR Biosciences).

2.2.4 Western blot

Cell pellets were lysed with RIPA buffer (EcoTech Biotechnology, Sigma Aldrich, #R0278) for 30 minutes at 4°C and centrifuged at 15.000 g for 15 minutes at 4°C. The supernatant was quantified with Pierce™ BCA Protein Assay Kit (Thermo Fischer Scientific, 23225) to determine the protein concentrations. 2mg/ml Bovine Serum Albumin (BSA) was diluted with dH_2O in several concentrations ranging from 0.4 to 2 mg/ml to use as a standard control for quantification. Reagent A and Reagent B from the

kit were mixed at a 50:1 ratio to generate the working solution. BSA standards and proteins were added to a 96-well plate (25 µL/well) and mixed with the working solution (200 µL/well) and incubated for 30 minutes at 37 ˚C. Their absorbance at 562 nm was measured with a Bio-Tek H1 Synergy microplate reader. Protein concentrations were calculated by subtracting blank values and normalizing them to the standard curve.

The Laemmli sample buffer (BioRad, 1610747) was added to the protein samples and incubated for 10 minutes at 95°C. 30 µg protein for each sample was loaded and separated in 4-15% Mini-PROTEAN Precast SDS-PAGE gel (BioRad, 4561083). They were transferred onto the PVDF membrane (Bio-Rad #1620177) for 120 minutes at 200 mA at 4 ˚C. Then the membranes were blocked with 5% NFDM (BioRad, 1706404) for 1 hour at room temperature. The membranes were blotted with primary antibodies for target proteins at 4°C overnight. The antibodies used in this thesis are GAPDH (Abcam, ab9485), ATP7B (ABclonal, A5676), ATP7B (Santa Cruz, sc-373964), ATP7B (Novus, NB100-360), MTF1 (Santa Cruz, sc365090), FLAG (Sigma, F1804), V5 (Invitrogen, R960), TP53 (Abcam, ab131442). Then the membranes were washed with TBST and blotted with the HRP-conjugated secondary antibodies Goat anti-Rabbit (Abcam, ab205718) and Goat anti-Mouse IgG (Abcam, ab97023) at 1:5.000 dilution for 1 hour in room temperature. The membranes were washed with TBST 3 times, and their signal was detected with Immobilon Forte Western HRP substrate (Millipore, WBKLS0500) and imaged by LI-COR Odyssey FC Imaging system (LI-COR Biosciences).

2.3 Cloning of gRNAs targeting ATP7B promoter into HEK293T cells

Lenti-guide hygro plasmid (Addgene, 139462) was digested with BsmBI enzyme (NEB, R0739) and dephosphorylated with Antarctic Phosphatase enzyme (NEB, 0289). Guide RNAs (gRNAs) targeting the ATP7B promoter region were designed using the Benchling database (https://benchling.com) (Table *2.1*). NT guide RNAs were designed based on literature, where the targeting activity of gRNAs was investigated and the gRNA sequences with no targets were determined (Doench et al., 2016). gRNAs were annealed with T4 PNK enzyme (NEB, M0201) and ligated into the cut Lenti-guide hygro backbone by T4 Ligase (NEB, M0202). Then, the samples were transformed into competent bacteria and streaked onto LB-agar plates containing ampicillin. Upon the formation of

bacterial colonies, plasmid DNA was isolated, and the cloning of correct gRNA sequences was confirmed by PCR analysis.

For virus production, initially, HEK293T cells were seeded as 2 x 10^6 onto 10-cm plates. After 24 hours, 2500 ng of the cloned plasmid with the correct sequence of gRNA was mixed with packaging vectors 225 ng of VSV-G (Addgene, 8454) and 2250 ng of psPAX2 (Addgene, 12260) in 200 µl serum-free DMEM. The mixture was also mixed with 15 µl Fugene6 (Promega, E2693) and 200 µl serum-free DMEM. The final solution was added to 10-cm plates drop by drop. After 24 hours, the cell medium was replaced with a fresh medium. At the time points of 48 and 72 hours after transfection, the media was collected from the plates and filtered through 45-µm filters to remove the cell debris. PEG8000 in 10% final concentration (Sigma, P2139) was added to the samples and incubated overnight at 4°C. Then they were centrifuged at 3000 g for 30 minutes. The pellet was resuspended in 160 µl PBS and stored at -80°C.

For virus transduction, HEK293T cells were seeded as 5 x 10^4 onto a 6-well plate. After 24 hours, the cells were transduced with 30 µl virus and 8 µg/ml protamine sulfate. The next day, the cell medium was changed to a fresh medium. The cells then were treated with 250 µg/ml hygromycin. After the selection was completed, the cells were isolated and collected for further experiments to verify the gRNA cloning and determine their targeting efficiency via T7E and ChIP-qPCR assays.

Table 2.1: gRNA sequences targeting the ATP7B promoter region.

gRNA	Forward Primer	Reverse Primer
g1.1	CACCGTGAGATCCCAGTACAGT GT	aaacACACTGTACTGGGATCTC AC
g1.2	CACCGGGCTCACCCACCGCCTG CG	aaacCGCAGGCGGTGGGTGAGC CC
g2.1	CACCGCGTAGACTAGTGTTCGG CG	aaacCGCCGAACACTAGTCTAC GC
g2.2	CACCGCACTGCTGTCCCGCCCAC GG	aaacCCGTGGGCGGGACAGCAG TGC
g3.1	CACCGATTACCTTAGATTCATGA CA	aaacTGTCATGAATCTAAGGTA ATC
g3.2	CACCGAAAATTTAGCTACACTG GAC	aaacGTCCAGTGTAGCTAAATT TTC

g3.3	CACCGCAGTGAAGCAGAAGAAAACG	aaacCGTTTTCTTCTGCTTCACTGC
g3.4	CACCGAAGTTGTTGAGGTGAGCAGC	aaacGCTGCTCACCTCAACAACTTC
g4.1	CACCGTTTAAGTGACGTGTTAACAA	aaacTTGTTAACACGTCACTTAAAC
g4.2	CACCGCGTGTTAACAATGGCAGTTT	aaacAAACTGCCATTGTTAACACGC
g5.1	CACCGTACTGCTATTCAGGAAGCTA	aaacTAGCTTCCTGAATAGCAGTAC
g5.2	CACCGCCTGAACAAAAATATGTAGG	aaacCCTACATATTTTTGTTCAGGC
g6.1	CACCGTCATAAAAGCAACACTACAG	aaacCTGTAGTGTTGCTTTTATGAC
g6.2	CACCGTTGTGCTCCATGGACCATGC	aaacGCATGGTCCATGGAGCACAAC
g7.1	CACCGGCTAACTTAGACATGTAGT	aaacACTACATGTCTAAGTTAGCC
g7.2	CACCGTTAGACATGTAGTAGGAAAA	aaacTTTTCCTACTACATGTCTAAC
NT	CACCGTATTACTGATATTGGTGGG	aaacCCCACCAATATCAGTAATAC

2.4 Determining the targeting efficiency of gRNAs

2.4.1 T7E assay

HEK293T cells were seeded as 5 x 10^4 onto a 6-well plate and transduced with the gRNA viral particles and selected with hygromycin. Then gRNA expressing HEK293T cells were seeded as 5 x 10^4 onto 6-well plates transfected with pSpCas9(BB)-2A-GFP plasmid (Addgene, 48138) which expresses a functional Cas9. Transfection protocol includes the mixing of 6 µL Pei with the 2 µg of the plasmid and 100 µL serum-free DMEM. The transfection mix was incubated at room temperature for 15 minutes and then transferred to the plate drop by drop. After 48 hours, the cells were collected by centrifugation and their genomic DNA was isolated Macherey-Nagel NucleoSpin Tissue kit (MN, 740952.50). 250 ng of genomic DNA from each sample was amplified by PCR using the Phusion enzyme (NEB, M0530) and the primer sequences designed to amplify the 1000

bp around the targeted regions on the ATP7B promoter (Table *2. 2*). The amplified products were digested with T7E endonuclease I enzyme (NEB, M0302) for 1 hour at 37°C. The cut samples were run on 1% agarose gel at 90 V for 40 minutes and imaged by Gel Doc XR+ Imaging System (Biorad, 1708195).

Table 2. 2: T7E primer sequences targeting the seven regions on the ATP7B promoter.

T7E	Forward Primer	Reverse Primer
Region 1	GAGAAAACGTCTGTGAGCCCA	CCCTTCATTTGGGACCGG
Region 2	GACGTGTTAACAATGGCAGT	GGTCCCAAAGGAAGCAACC
Region 3	TTATTAGTGGAGGGCAAGGC	CACGCCGAACACTAGTCTAC
Region 4	GCAACACTACAGAGGACAGT	CTTCTGTAGGGGTACTTGCC
Region 5	CTTCTCTGATGCTAGACCACA	CTGCCATTGTTAACACGTCAC
Region 6	CCTCCAGATATTGCCAAATGC	GGTTCTTCCCTGTCATACGT
Region 7	GGTTGAGAACCAGTGGTTTAC	GGTTCTTCCCTGTCATACGT

2.4.2 Chromatin Immunoprecipitation

HEK293T-CASPEX cells were crosslinked with 1% formaldehyde (Sigma Aldrich, 818708) for 10 minutes at room temperature. Then 125 mM glycine was added to the cells and centrifuged at 1000 g for 5 minutes at 4°C. The cell pellet was washed with cold PBS twice and resuspended in ChIP Lysis Buffer (10 mM Tris; 1 mM EDTA; 140 mM NaCl; 1% Triton X-100; 0.1% Na-deoxycholate; 1% SDS; 1 mM PMSF; Protease Inhibitor Cocktail) and incubated on ice for 15 minutes. Then the samples were sonicated with a Bioruptor Plus sonication device (Diagenode) at 45 seconds on/15 seconds of conditions at a power setting high. They were centrifuged at 10.000 g for 10 minutes at 4°C. The supernatant containing the sonicated chromatin was stored at -80°C.

Dynabeads® (Thermo Fisher protein A and G magnetic beads, 10001D-10004D) were washed with 0.5 mL PBST and 0.5 mL TE twice. Then the sonicated samples were incubated with the magnetic beads for 30 minutes at 4°C to clear the lysate and prevent nonspecific binding. FLAG (Sigma, F1804) and mouse IgG (Santa Cruz, sc-2025) antibodies were also incubated with magnetic beads and 100 µL PBST for 1 hour at room temperature. Then the antibody-bead complex was washed with 0.5 mL PBST and 0.5

mL ChIP lysis buffer. The pre-cleared lysate was then added to the antibody-bead complex and incubated overnight at 4°C.

The next day, the samples were washed twice with the buffers which are given as ChIP lysis buffer, low-salt buffer (0.1% SDS, 1% Triton-X 100, 2 mM EDTA, 20 mM Tris-HCl, 140 mM NaCl), high salt buffer (low-salt buffer, 500 mM NaCl), LiCl buffer (0.25 M LiCl, 1% IGEPAL-CA 630, 1% deoxycholic acid, 1 mM EDTA, 10 mM Tris) and Tris-EDTA. DNA was eluted with the addition of a buffer containing 1% SDS and 0.1 M $NaHCO_3$ and incubation for 15 minutes at room temperature. Then the samples were treated with RNase A (0.3 mg/ml) (Thermo Fisher Scientific, 12091021) and 5M NaCl for 30 min at 37°C. Proteinase K (0.3 mg/ml) (Thermo Fisher Scientific, EO0491) was added and samples were incubated for 1 hour at 65°C. ChIP DNA was cleaned up with the use of the ChIP DNA Clean & Concentrator kit (Zymo Research, D5205).

For qPCR quantification, primer sequences designed to target the seven regions on the ATP7B promoter were listed in Table *2.3*. The samples were run on the Roche LightCycler 480 device.

Table 2.3: ChIP primer sequences targeting the seven regions on the ATP7B promoter.

ATP7B-ChIP	Forward Primer	Reverse Primer
g1.2	CTTCCTTTGGGACCCACGG	CGCAGACTCAGCTCCCAG
g2.2	GTAGACTAGTGTTCGGCGTGG	CTGTCAATCACAGGCCACG
g3.4	GACGGGCAAGTACCCCTACA	GAAAGGAGCTGGTGCCTGTG
g4.2	AGCAGAGGATTCAACATAAGCT	GAAACCGGATCTTCCTTCTCATC
g5.1	GCCTGAACTTTTGAAAGAATTAGG	CACCTACATATTTTTGTTCAGGCTG
g6.1	CAGAGTCTGACAAAAGTGGTAAG	GTCCTGAGAAAGCAAACTGTC
g7.1	CTGTTTCTGCATTCAATCTAGTG	GTGGTCTAGCATCAGAGAAG

2.4.3 qRT-PCR

RNA was isolated from the samples using Zymo RNA Isolation Kit (Zymo, R1051). 500 ng RNA from each sample was converted to cDNA using M-MLV Reverse Transcriptase

(Thermo Fisher Scientific, 28025013). Then, 10 ng cDNA was loaded onto qPCR plates and mixed with LightCycler 480 SYBR Green I Master mix (Roche Diagnostics, 04707516001) and 0.15 μM of qPCR primers. The primer sequences designed to amplify a gene of interest are listed in Table *2.4*. The samples were incubated at 95°C for 5 minutes, followed by 40 cycles of 95°C for 10 seconds, 60°C for 30 seconds, and 72°C for 1 second. The samples were run on Roche LightCycler 480 device. Fold change values were calculated using the $2^{(-\Delta\Delta CT)}$ method.

Table 2.4: Primer sequences targeting the gene of interest for qRT-PCR analysis.

Gene	Forward Primer	Reverse Primer
GAPDH	AGCCACATCGCTCAGACAC	GCCCAATACGACCAAATCC
ATP7B	GTGGGCAATGACACCACTTT	TGGGTGCCTTTGACATCTGA
MTF1	GGGGAAAAGCCATTTCGGTG	GGGGCAGAAGAAGGGTCTTT
PINX1	GGACTCGGAGCTACCATCAA	TTGTCCGAGGAATCTGTGGT
POU3F2	GAAAAGGATGACCCCTCCCG	TGTGGTGGAGTGTCCCTACT
PRDM16	GAACCACGTCTATGGGGAACG	GCTTTTCTACCCTGCTGTAGAT
MEN1	TGGCCGACCTGTCTATCATC	TCGGAGACCTTCTTCACCAG
TP53	GCAGTCAGATCCTAGCGTCG	CGTTGTTTTCAGGAAGTAGTTTCCA

2.5 Proximity Labeling of ATP7B promoter region.

2.5.1 Biotinylation and pulldown with streptavidin

HEK293T-CASPEX-gRNA cells were treated with 2 μg/ml doxycycline for 48 hours. Then, biotin tyramide phenol (Sigma, SML2135) dissolved in DMSO was added to the cell medium to reach a final concentration of 500 μM. They were incubated for 30 minutes at 37°C and H_2O_2 diluted in serum-free DMEM was added to the medium to reach a final concentration of 1 mM. The medium was removed quickly after 60 seconds and the cells were washed three times with cold PBS containing 100 mM Sodium azide, 100 mM Sodium ascorbate, and 50 mM TROLOX to detoxify the medium. They were washed with cold PBS for additional two times and then the cells were trypsinized. They were centrifuged at 400 g for 4 minutes and the cell pellet was stored at -80°C.

When the pellets were thawed, they were lysed with hypotonic extraction buffer (20 mM Tris-HCl, pH 7.4, 10 mM NaCl, 3 mM MgCl2) and incubated for 30 minutes at 4°C. 10% NP-40 was added to the cells and vortexed for 10 seconds at the highest speed. They were centrifuged for 30 minutes at 3000 rpm and the supernatant which contains the cytoplasmic content was stored at -80°C. The remaining pellet was resuspended with RIPA lysis buffer and incubated for 30 minutes at 4°C. Then, the DNA was sonicated with a Bioruptor Plus sonication device (Diagenode) at 45 seconds on/15 seconds of conditions at the power setting high. They were centrifuged for 30 minutes at 14,000×g and the nuclear protein contents were transferred into a new tube. Their protein contents were measured by BCA assay (Thermo Fischer Scientific, 23225). 5 mg protein from each sample was loaded onto Streptavidin-coated magnetic beads (Thermo Fischer Scientific, 88816) and were incubated overnight at 4 °C. Remaining protein samples were stored for western blot analysis. The next day, the pulldown samples were isolated with a magnetic rack, and the samples were washed with RIPA buffer, 1 M KCl, and 0.1 M Na_2CO_3 solutions respectively.

2.5.2 Mass Spectrometry

They were washed with 2 M urea in 10 mM Tris-HCl and with 50 mM Tris at pH 7.4. 20 mM DTT was added to the samples and then 100 µl of 55 mM iodoacetamide prepared in 100 mM ammonium bicarbonate was added. They were incubated for 1 hour. Then, they were treated with the trypsin solution (Pierce, 90058) and incubated overnight at 37°C. The next day, formic acid was added to the samples at a final concentration of 5% and centrifuged for 30 minutes at 14,000 g. The supernatant was collected and analyzed in the Orbitrap Mass Spectrometer (Thermo Scientific, QExactive Orbitrap).

2.5.3 Proteomics Analysis

Data analysis was conducted with MaxQuant software (J. Cox & Mann, 2008). The protein group files then were examined with Cassiopeia (Varnavides et al., 2022) program for quality control and normalization steps for the label free-quantification (LFQ). Enrichment analysis was applied to the proteins detected in the ATP7B promoter region compared to the non-targeting control. Depending on their enrichment scores and their

association with cancer prognosis before, several proteins were chosen as target transcriptional regulators of ATP7B.

2.6 PINX1 relationship with ATP7B expression.

2.6.1 Generation of stable cell line overexpressing PINX1.

pLJC2-GPT2-3xFLAG (Addgene, 163447) plasmid was digested with PacI (NEB, R0547) and NotI enzymes (NEB, R189) and dephosphorylated with Antarctic Phosphatase enzyme (NEB, 0289). Primer sequences targeting the first and last twenty bases of the PINX1 cDNA sequence were designed to generate the overexpression (OX) constructs (Table *2.5*). Primers were also digested with PacI and NotI enzymes and ligated into the cut backbone by T4 Ligase (NEB, M0202). Then, the samples were transformed into competent bacteria and streaked onto LB-agar plates containing ampicillin. Upon the formation of bacterial colonies, plasmid DNA was isolated, and the cloning of correct gRNA sequences was confirmed by PCR analysis.

For virus production, initially, HEK293T cells were seeded as 2 x 10^6 onto 10-cm plates. After 24 hours, 2500 ng of the cloned plasmid with the correct sequence of gRNA was mixed with packaging vectors 225 ng of VSV-G (Addgene, 8454) and 2250 ng of psPAX2 (Addgene, 12260) in 200 µl serum-free DMEM. The mixture was also mixed with 15 µl Fugene6 (Promega, E2693) and 200 µl serum-free DMEM. The final solution was added to 10-cm plates drop by drop. After 24 hours, the cell medium was replaced with a fresh medium. At the time points of 48 and 72 hours after transfection, the media was collected from the plates and filtered through 45-µm filters to remove the cell debris. PEG8000 in 10% final concentration (Sigma, P2139) was added to the samples and incubated overnight at 4°C. Then they were centrifuged at 3000 g for 30 minutes. The pellet was resuspended in 160 µl PBS and stored at -80°C.

For virus transduction, HEK293T cells were seeded as 5x10^4 onto a 6-well plate. After 24 hours, the cells were transduced with 30 µl virus and 8 µg/ml protamine sulfate. The next day, the cell medium was changed to a fresh medium. The cells then were treated with 2 µg/ml puromycin. After the selection was completed, the cells were isolated and collected for further experiments.

2.6.2 Generation of CRISP2-Cas9 knockout of target genes.

Lenti-guide-CRISPR (Addgene, 52961) plasmid was digested with BsmBI enzyme (NEB, R0739) and dephosphorylated with Antarctic Phosphatase enzyme (NEB, 0289). Primer sequences targeting the exons of the target genes were designed to generate the knock-out (KO) constructs (Table *2.5*). Oligos were annealed with T4 PNK enzyme (NEB, M0201) and ligated into the cut backbone by T4 Ligase (NEB, M0202). Then, the samples were transformed into competent bacteria and streaked onto LB-agar plates containing ampicillin. Upon the formation of bacterial colonies, plasmid DNA was isolated, and the cloning of correct gRNA sequences was confirmed by PCR analysis.

For virus production, initially, HEK293T cells were seeded as 2 x 10^6 onto 10-cm plates. After 24 hours, 2500 ng of the cloned plasmid with the correct sequence of gRNA was mixed with packaging vectors 225 ng of VSV-G (Addgene, 8454) and 2250 ng of psPAX2 (Addgene, 12260) in 200 µl serum-free DMEM. The mixture was also mixed with 15 µl Fugene6 (Promega, E2693) and 200 µl serum-free DMEM. The final solution was added to 10-cm plates drop by drop. After 24 hours, the cell medium was replaced with a fresh medium. At the time points of 48 and 72 hours after transfection, the media was collected from the plates and filtered through 45-µm filters to remove the cell debris. PEG8000 in 10% final concentration (Sigma, P2139) was added to the samples and incubated overnight at 4°C. Then they were centrifuged at 3000 g for 30 minutes. The pellet was resuspended in 160 µl PBS and stored at -80°C.

For virus transduction, HEK293T cells were seeded as 5 x 10^4 onto a 6-well plate. After 24 hours, the cells were transduced with 30 µl virus and 8 µg/ml protamine sulfate. The next day, the cell medium was changed to a fresh medium. The cells then were treated with 2 µg/ml puromycin. After the selection was completed, the cells were isolated and collected for further experiments.

Table 2.5: Primer sequences targeting the PINX1, PRDM16, POU3F2, and MEN1 genes.

Target Gene	Forward Primer	Reverse Primer
PINX1 OX	ATATATTTAATTAAATGT CTATGCTGGCTGAACG	ATATATGCGGCCGCTTTGGAATC TTTCTTCTTCTTCTTTTTC

PINX1 KO	CACCGACGATTCCAAGTTTGGCCAG	aaacCTGGCCAAACTTGGAATCGTC
PRDM16 OX	ATATATTTAATTAAATGCGATCCAAGGCGAGGG	ATATATGCGGCCGCGAGGTGGTTGATGGGGTGAAATG
POU3F2 OX	ATATATGCTAGCATGGCGACCGCAGCGTCTAAC	ATATATGGATCCCTGGACGGGCGTCTGCACC
POU3F2 KO	CACCGCAAACTGGGATTTACCCAAG	CACCGCCAAGCAGTTCAAGCAGCGG
MEN1 OX	ATATATGCTAGCATGGGGCTGAAGGCCGCCCA	ATATATGCGGCCGCGAGGCCTTTGCGCTGCCGCT
MEN1 KO	AAACTCTTGCGGTCACAGCGCATGC	CACCGCATGCGCTGTGACCGCAAGA

2.6.3 Generation of stable cell lines overexpressing the target genes

Cell lines stably overexpressing PRDM16, POU3F2, and MEN1 were generated using the same protocol described in Chapter 2.6.1 and primer sequences written in Table 2.3. To overexpress TP53, pLenti6/V5-p53_wt (Addgene, 22945) plasmid was transformed into competent bacteria, plasmid DNA was isolated, and viral particles were generated using the same protocol described in Chapter 2.6.1.

2.6.4 Western Blot

The PINX1 protein level was quantified using the same protocol as described in Chapter 2.2.4.

2.6.5 RT-qPCR

The PINX1 expression level was quantified using the same protocol as described in Chapter 2.4.3.

2.6.6 Generating the ATP7B promoter constructs

HEK29T cells were lysed, and their genomic DNA was isolated using a Macherey-Nagel NucleoSpin Tissue kit (MN, 740952.50). ATP7B promoter constructs were amplified

from the genomic DNA by using the Phusion enzyme (NEB, M0530) and primers designed to amplify the desired length products of the ATP7B sequence (Table *2.6*). The amplified products and pMDR1-1202 (Addgene, 37627) plasmid were both digested with SmaI (NEB, R0141) and BglII (R0144) enzymes. The constructs were ligated, and their viral particles were generated and transduced into HEK293T cells using the same protocol as described in Chapter 2.6.

Table 2.6: Primer sequences designed to amplify different lengths of the ATP7B promoter.

ATP7B construct	Forward Primer	Reverse Primer
200 bp	ATATATCCCGGGAGAACACTGTGGCACC	ATATATAGATCTAACCGCCCCTTCATTTGGGA
500 bp	ATATATCCCGGGGGTGCGGAGTTCACTCTT	ATATATAGATCTAACCGCCCCTTCATTTGGGA
1000 bp	ATATATCCCGGGAAAACGTCTGTGAGC	ATATATAGATCTAACCGCCCCTTCATTTGGGA
2000 bp	ATATATCCCGGGGTCCTTTAAGTCTGG	ATATATAGATCTAACCGCCCCTTCATTTGGGA
3000 bp	ATATATCCCGGGGCGAAGGGCAAAAATC	ATATATAGATCTAACCGCCCCTTCATTTGGGA

2.6.7 Measuring luciferase activity

HEK293T, HEK-PINX1 OX, and HEK-PRDM16 OX cells were seeded as 1×10^5 onto 96-well plates and after 24 hours, they were transfected with the mini-ATP7B promoter constructs using Lipofectamine 3000 reagent (Thermo, L3000001). The transfection protocol includes the mixing of 6 µL Lipo3000 reagent with 2 µg of the plasmid and 100 µL serum-free DMEM. The transfection mix was incubated at room temperature for 30 minutes and then transferred to the plate drop by drop. After 48 hours, the cells were treated with 6 mg/ml luciferin, and the luciferase activity was measured with the microplate reader (Synergy H1 Hybrid reader, BioTek).

2.6.8 ChIP-qPCR

The PINX1 enrichment at the ATP7B promoter was quantified using the same protocol as described in Chapter 2.4.2.

2.6.9 Drug treatment

HEK293T and HEK293T-PINX1 OX cells were seeded as 1×10^5 onto 6-well plates and treated with increasing doses of cisplatin and copper for 72 hours.

2.6.10 Sulforhodamine B (SRB) Cell Viability Assay

Cells were seeded as 4×10^3 on 96-well plates and treated with cisplatin and copper after 24 hours. They were treated with several doses of cisplatin for 72 hours and then fixed with 50% (w/v) TCA (Sigma, T6399) for 1 hour at 4°C. They were washed with deionized water. After the plates are dried, the samples were treated with 0.4% (w/v) SRB (Santa Cruz, sc-253615) for 30 min at room temperature. They were washed with 1% acetic acid and then treated with 10 mM Trizma base (Sigma, T1503) for resolution. Their absorbances at 564 nm were measured with the microplate reader (Synergy H1 Hybrid reader, BioTek).

2.6.11 Colony Formation Assay

Cells were seeded as 1×10^3 on 12-well plates and after 24 hours, they were treated with cisplatin. After 72 hours, the medium was replaced with fresh medium. After 10 days, when microscopically observable colonies started to grow, the plates were fixed with cold methanol for 10 minutes. Then they were treated with 0.5% (w/v) crystal violet and washed with dH_2O. The results were quantified by using ImageJ (Schneider, Rasband, & Eliceiri, 2012).

2.7 Generation of CRISPR-Cas9 KO of MTF1

HEK293T-MTF1 KO cell lines were generated using the same protocol as described in Chapter 2.6.

Table 2.7: Primer sequences targeting the ATP7B and MTF1 genes.

Gene	Forward Primer	Reverse Primer
MTF1	CACCGAAATTTAGGTGCGA TCACGA	AAACTCGTGATCGCACCTAAATT TC

2.8 HDAC inhibitor activity increases ATP7B expression

2.8.1 Drug treatment

HEK293T cells were seeded as 1×10^5 onto 6-well plates and treated with 10 uM of selected drugs of BET and HDAC inhibitors for 72 hours.

2.8.2 RT-qPCR

The ATP7B expression level was quantified using the same protocol as described in Chapter 2.4.3.

2.8.3 SRB Cell viability assay

HEK293T cells were seeded as 1×10^5 onto 6-well plates and treated with increasing doses of N-acetyl-L-cysteine (NAC) for 72 hours. Cell viability was quantified using the same protocol as described in Chapter 2.6.9.

2.8.4 Reactive Oxygen Species (ROS) quantification

HEK293T cells were seeded as 1×10^5 onto 6-well plates. The next day, they were treated with 5 mM NAC, 10 μM epi-drugs, 10 μM cisplatin, and H_2O_2. After 48 hours, the cells were centrifuged for 5 minutes at 400 g. Reactive oxygen quantification was performed with Muse Oxidative Stress Kit (Luminex, MCH100111). Initially, the pellet was resuspended with 1:100 diluted 1X Assay buffer. Then, it was diluted again with 1X Assay buffer at a 1:80 ratio. 150 μL of the final solution was added onto 50 μL cell suspension and they were incubated for 30 minutes at 37°C. The samples were analyzed with Muse Cell Analyzer (Merck Millipore) and the percentage of ROS-positive cells in the population was calculated.

2.9 Statistical Analysis

Data were analyzed using GraphPad Prism version 9.0. Significant analyses were performed with student's t-test and a value of $p < 0.05$ was considered statistically significant.

Chapter 3:
RESULTS

3.1 Generation of HEK293T-CASPEX cells

Generating a stable cell line expressing CASPEX protein only in the presence of doxycycline is essential for the proximity labeling assay. To achieve this aim, the HEK293T cell line was chosen for its high transfection efficiency and high expression of ATP7B compared to other cell lines. qPCR analysis showed that among many normal and cancer cell lines, endogenous ATP7B levels were the highest in HEK293T cells (Figure *3.1*).

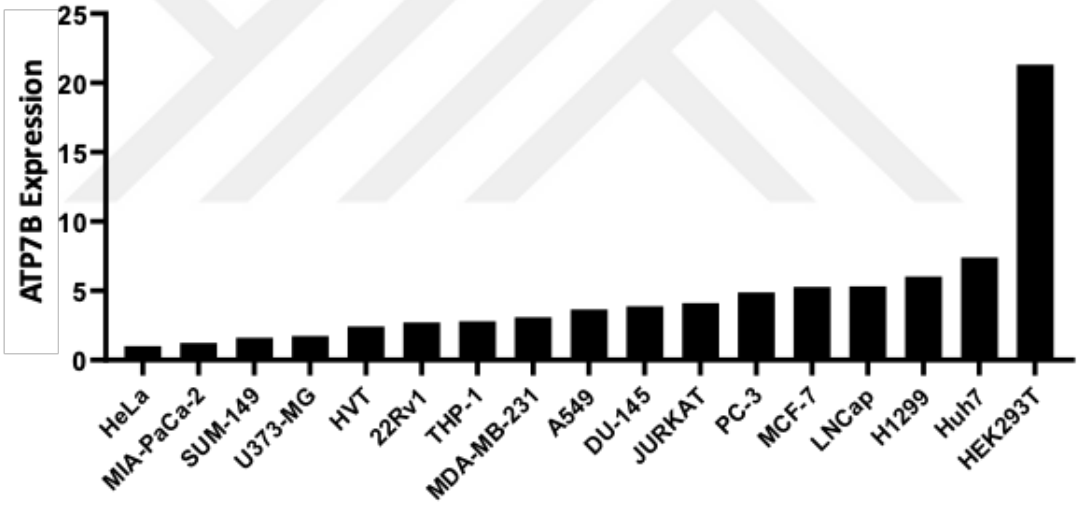

Figure 3.1: HEK293T cells have the highest endogenous expression of ATP7B.

qPCR analysis showing ATP7B expression in different cell lines. The figure was generated by Ph.D. Student Barıs Sergi.

Firstly, HEK293T cells were transfected with dCas9-APEX2 plasmid and Piggy-Bac Transposase as explained in the previous section. Transposase enables the integration of the plasmid into the genome through 'TTAA' sites (Zhao et al., 2016). After puromycin selection was completed for the cells, they were treated with doxycycline and after 24 hours the cells were analyzed with flow cytometry. For the first polyclonal cell collection,

GFP-positive cell lines were 96.12% (Figure *3.2A*). Then, the cells were sorted with the cell sorter, and the single colonies were grown. Selected colonies were again treated with doxycycline and analyzed with flow cytometry. The results showed that this cell population grown from a single cell had 99.74% GFP-positive cells (Figure *3.2B*).

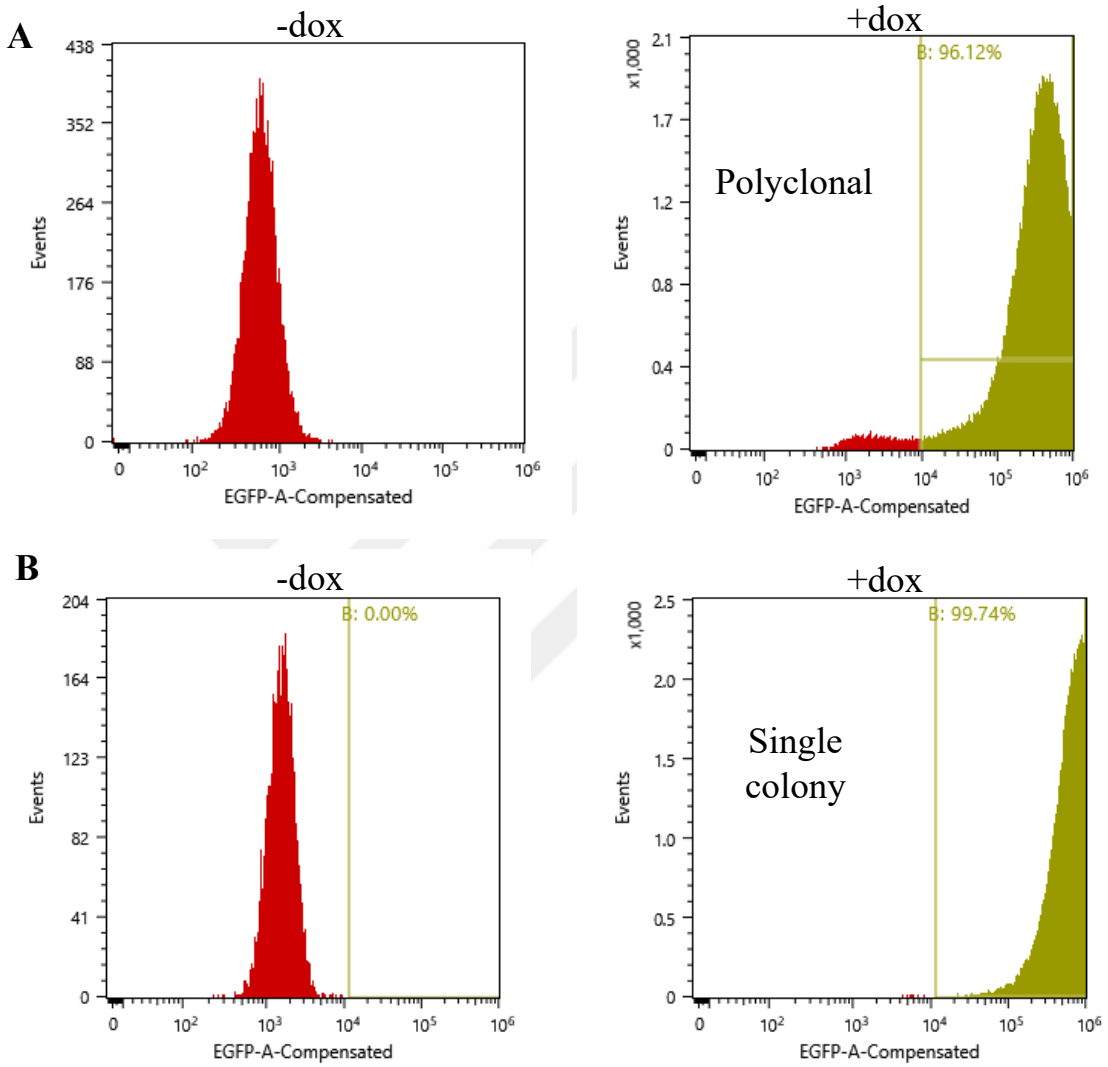

Figure 3.2: Flow cytometry analysis to sort GFP-positive HEK293T-CASPEX colonies.

The figure was generated with Batuhan Altay. (A) Flow cytometry results for polyclonal HEK293T-CASPEX cells, showing GFP-positive cell ratios -/+ doxycycline conditions (B) Flow cytometry results for HEK293T-CASPEX cells after sorting and obtaining a single colony, showing GFP-positive cell ratios -/+ doxycycline conditions.

Immunofluorescence and immunoprecipitation experiments further supported the confirmation of CASPEX protein expression in the presence of doxycycline. Initially, HEK293T-CASPEX cells were stained with an anti-V5 antibody since the dCas9-APEX2

plasmid has both V5 and FLAG tags. The location of dCas9-APEX2 protein in the nucleus was confirmed by DAPI staining (blue) which stains DNA, GFP staining (green), and V5 staining (red) patterns (Figure *3.3A*). When the cells were treated with dox, CASPEX protein is expressed and a green GFP signal could be seen. However, when there is no dox treatment, the GFP signal could not be observed. The red signal also could be seen from the cells which express V5 tagged-CASPEX protein in the presence of doxycycline. Imaging results demonstrate that CASPEX protein is expressed in the cells only in the presence of doxycycline.

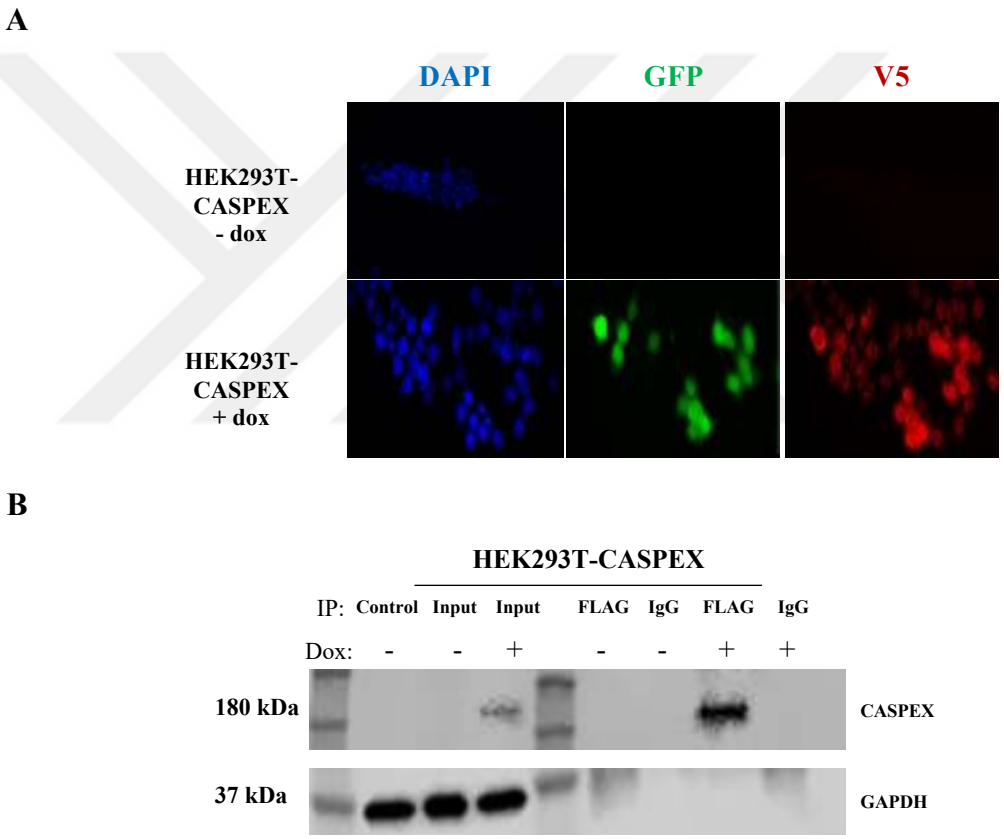

Figure 3.3: Confirmation of CASPEX protein expression in HEK293T-CASPEX cells

The figure was generated with Batuhan Altay. (A) Immunofluorescence assay of HEK293T-CASPEX cells performed with anti-V5 antibody to examine the location of CASPEX protein. (B) Immunoprecipitation assay of HEK293T-CASPEX cells performed with anti-FLAG antibody to verify the expression of CASPEX protein.

Immunoprecipitation assay of HEK293T-CASPEX cell lysates with anti-FLAG antibody also verified the doxycycline-inducible system of the cell line. Mouse IgG antibody was

used as a negative control and as expected, there was no band at the size of CASPEX protein. On the other hand, the protein lysates obtained from doxycycline-treated HEK293T-CASPEX cells resulted in a band at the 180 kDa size indicating the presence of CASPEX expression (Figure *3.3B*). Taken together, these experiments support the generation of a stable HEK293T-CASPEX cell line expressing the dCas9-APEX2 protein in a doxycycline-inducible system.

3.2 Cloning of gRNAs targeting ATP7B promoter region into HEK293T cells

The putative ATP7B promoter region resided between TSS (+1) to -3000 bp region and was targeted with 15 different gRNAs. *In silico* analysis conducted on TRANSFAC and PROMO databases showed the presence of many transcription-binding motifs in the 3000 bp region (Wingender, Dietze, Karas, & Knüppel, 1996)(Messeguer et al., 2002). 22 factors were found from both databases, which were associated with tumor progression before (Figure *3.4*). So, the 3000 bp area was divided into seven regions regarding the biotinylation capacity of the APEX2 enzyme which is 20 nm (Tan et al., 2020), and two gRNAs were designed for each region (Table *2.1*).

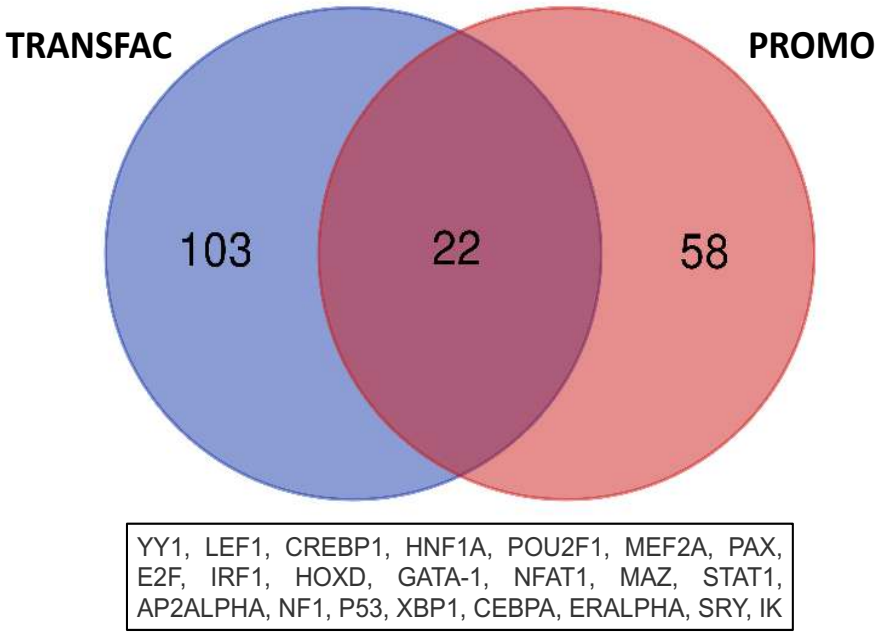

Figure 3.4: Transcription factor binding analysis of ATP7B promoter.

The figure was generated by Dr. Selahattin Can Ozcan and Ph.D. Student Barıs Sergi.

These gRNAs were cloned into Lenti-guide hygro backbone and plasmids were transformed into competent bacteria. After the plasmid DNA isolation, the cloning of gRNAs was confirmed with PCR amplification and gel electrophoresis. The presence of bands at 200 bp size verified the cloning, and the viral particles for each plasmid were generated (Figure *3.5*). Both HEK293T and HEK293T-CASPEX cells were transduced with these viral particles and selected against hygromycin treatment.

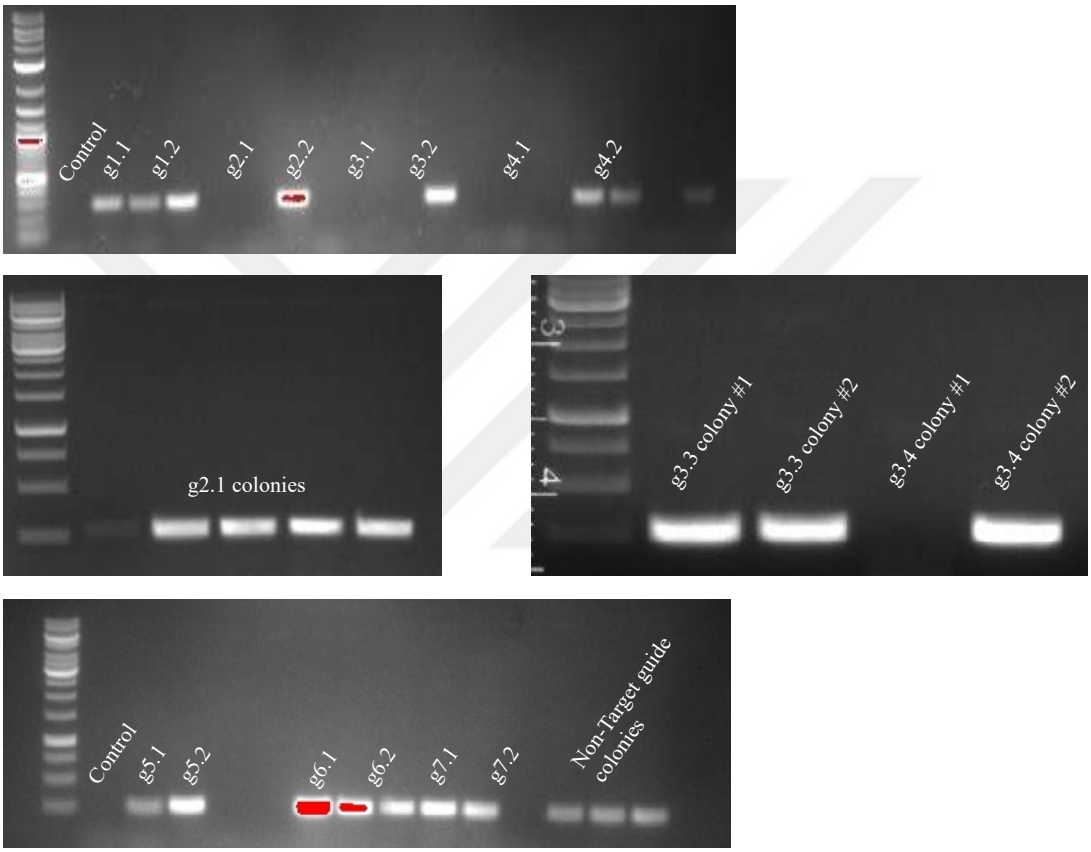

Figure 3.5: PCR confirmation for cloned gRNAs into LentiGuide-hygro vector and transformed into bacteria.

3.3 Determining the targeting efficiency of gRNAs

The targeting efficiency of the gRNAs is very essential to the proximity labeling assay since lower targeting efficiency could lead to false-negative results after the mass spectrometry analysis. Thus, gRNAs targeting the correct sequences on the ATP7B promoter region were verified with two molecular techniques called T7E and ChIP assays, and for each region, one gRNA with the higher targeting efficiency was selected.

3.3.1 Confirmation of gRNA efficiency with T7E assay

HEK293T cells were treated with gRNAs spanning the 3000 bp on the ATP7B promoter region. These cells were then transfected with pSpCas9(BB)-2A-GFP plasmid (Addgene, 48138), which expresses a functional Cas9 and results in the cleavage of the targeted regions on the promoter. The cleavage efficiency of the gRNAs was then quantified with the T7E method. In this technique, an enzyme called T7 Endonuclease is used to recognize and digest the structural deformities on DNA (Mashal, Koontz, & Sklar, 1995). After the targeted CRISPR/Cas9 activity, the non-homologous end-joining (NHEJ) repair mechanism could result in mutations in the cut area and the T7E enzyme cuts the DNA mismatches (Guschin et al., 2010). The separation of the samples by agarose-gel electrophoresis resulted in both full-length and cut products which confirms the endonuclease activity in the targeted region (Figure *3.6A*).

Gene editing efficiency for each gRNA was quantified using the formula of (% gene modification = 100 x (1 – (1- cut fragment)$^{1/2}$)) (Guschin et al., 2010). Several gRNAs showed high targeting efficiency such as g1.2, g2.2, and g6.1 (Figure *3.6B*). For each region, one gRNA with better editing efficiency was selected to continue to further confirm its efficiency with ChIP-qPCR assay.

A

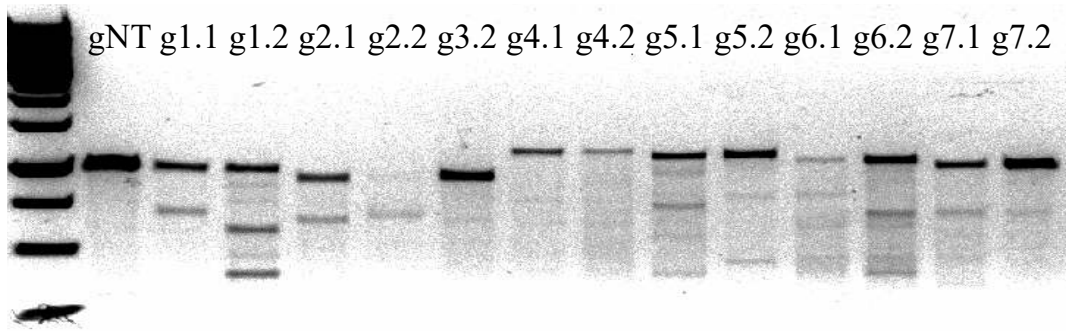

B

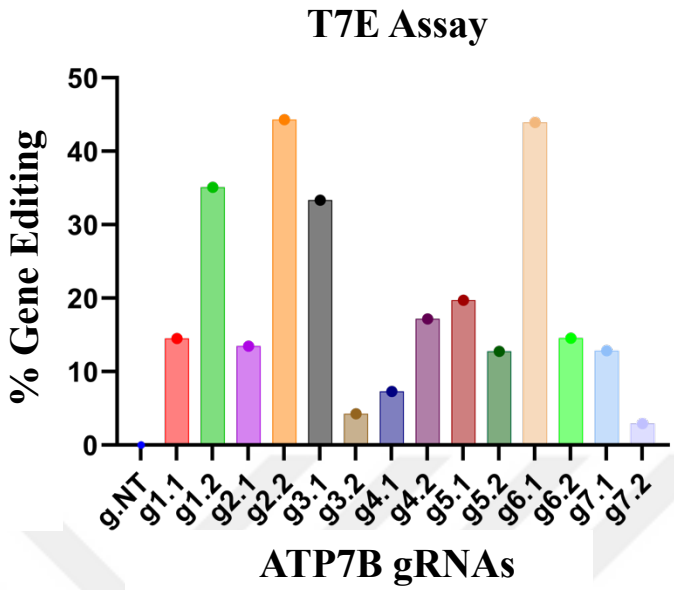

Figure 3.6: T7E assay.

(A) Gel electrophoresis image of T7E analysis of 15 gRNAs spanning a region of 3000 bp at ATP7B promoter to determine their targeting efficiency. (B) Gene editing efficiency of gRNAs was calculated using the formula of (% gene modification = 100 x (1 – (1- cut fragment)$^{1/2}$)) (Guschin et al., 2010). The figure was generated with Batuhan Altay.

3.3.2 Confirmation of gRNA binding to ATP7B promoter region

The targeting efficiency of gRNAs was further confirmed with ChIP-qPCR experiments. HEK293T-CASPEX cells cloned with the gRNAs which were selected after the T7E assay based on their gene-editing scores were fixed and sonicated for 50 cycles. The sonicated DNA was imaged on agarose gel that is sized below 250 bp and further ChIP experiments were performed with this protocol (Figure *3.7A*). Compared to the negative control mouse IgG and non-targeting gRNA, the enrichment scores of the gRNAs were calculated according to the %input formula (%input = 100*2^ (Adjusted input-Ct (IP)) (Solomon, Caldwell, & Allan, 2021). Except for the gRNAs targeting region 3, all gRNAs showed enrichment compared to the IgG compartment (Figure *3.7B*). It was concluded that these gRNAs get localized to the promoter region when induced with doxycycline.

A

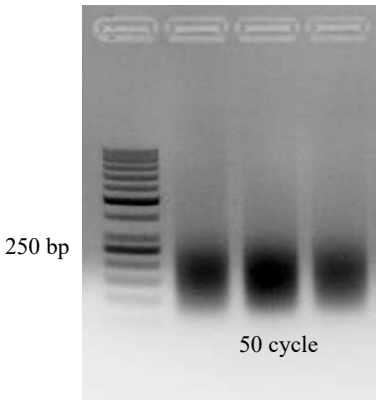
250 bp
50 cycle

B

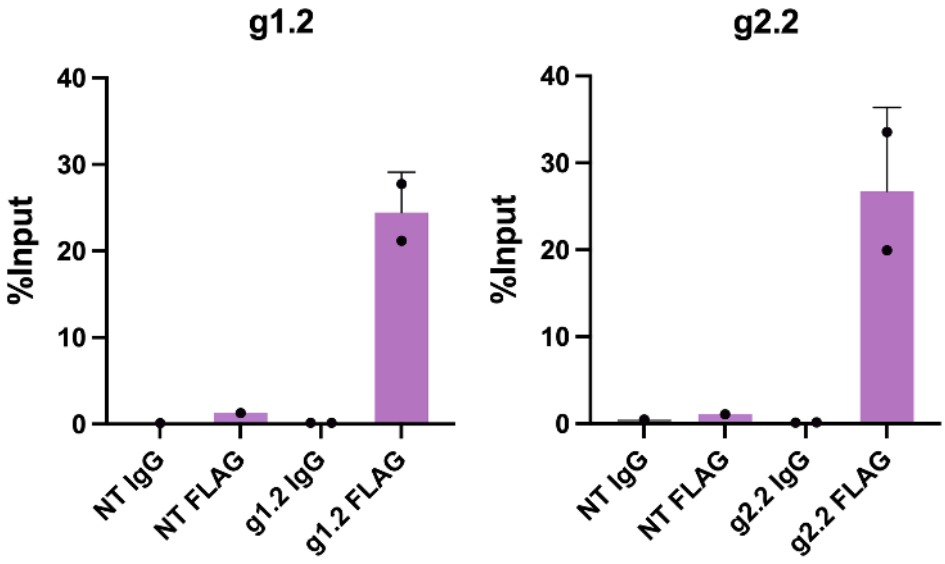
g1.2
%Input
40
30
20
10
0
NT IgG
NT FLAG
g1.2 IgG
g1.2 FLAG
g2.2
%Input
40
30
20
10
0
NT IgG
NT FLAG
g2.2 IgG
g2.2 FLAG

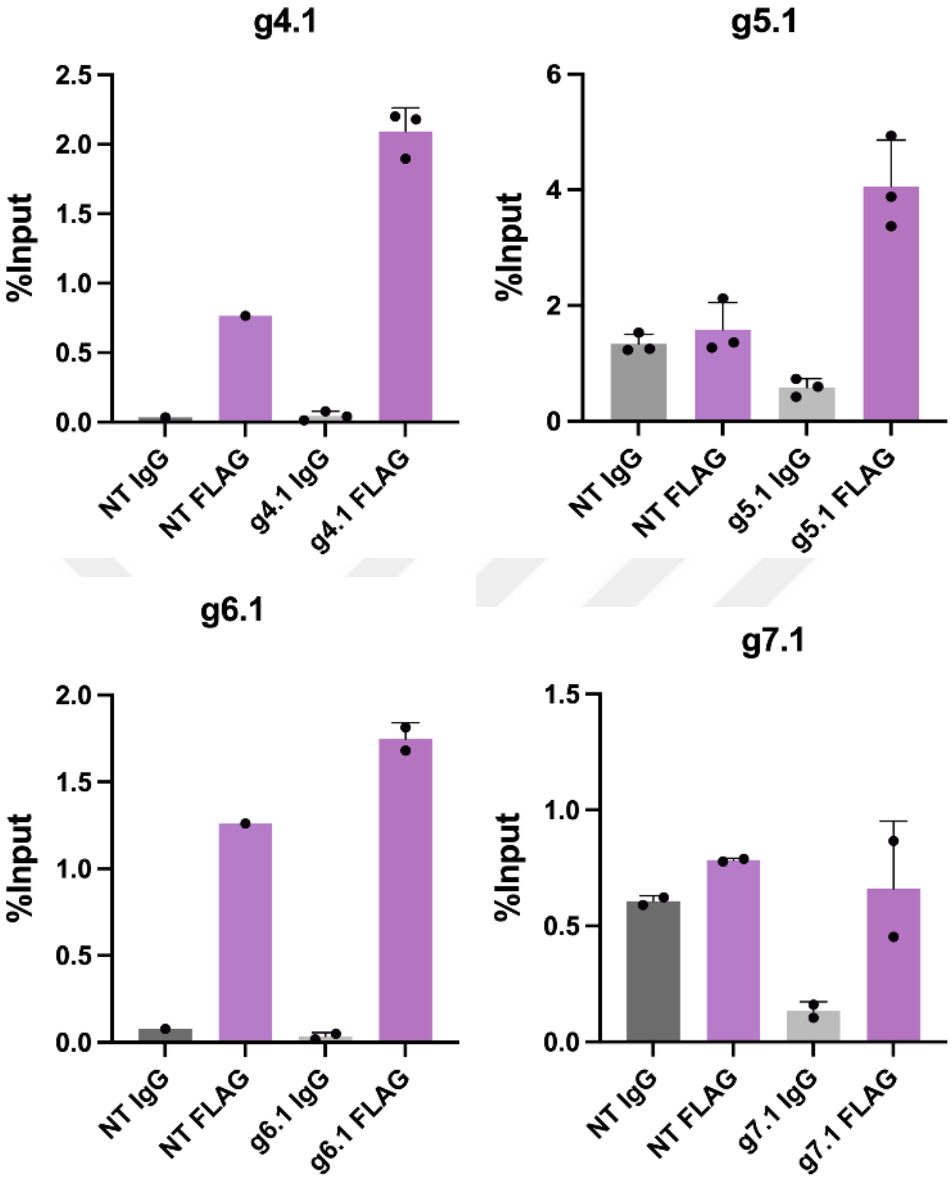
g4.1
%Input
2.5
2.0
1.5
1.0
0.5
0.0
NT IgG
NT FLAG
g4.1 IgG
g4.1 FLAG
g5.1
%Input
6
4
2
0
NT IgG
NT FLAG
g5.1 IgG
g5.1 FLAG
g6.1
%Input
2.0
1.5
1.0
0.5
0.0
NT IgG
NT FLAG
g6.1 IgG
g6.1 FLAG
g7.1
%Input
1.5
1.0
0.5
0.0
NT IgG
NT FLAG
g7.1 IgG
g7.1 FLAG

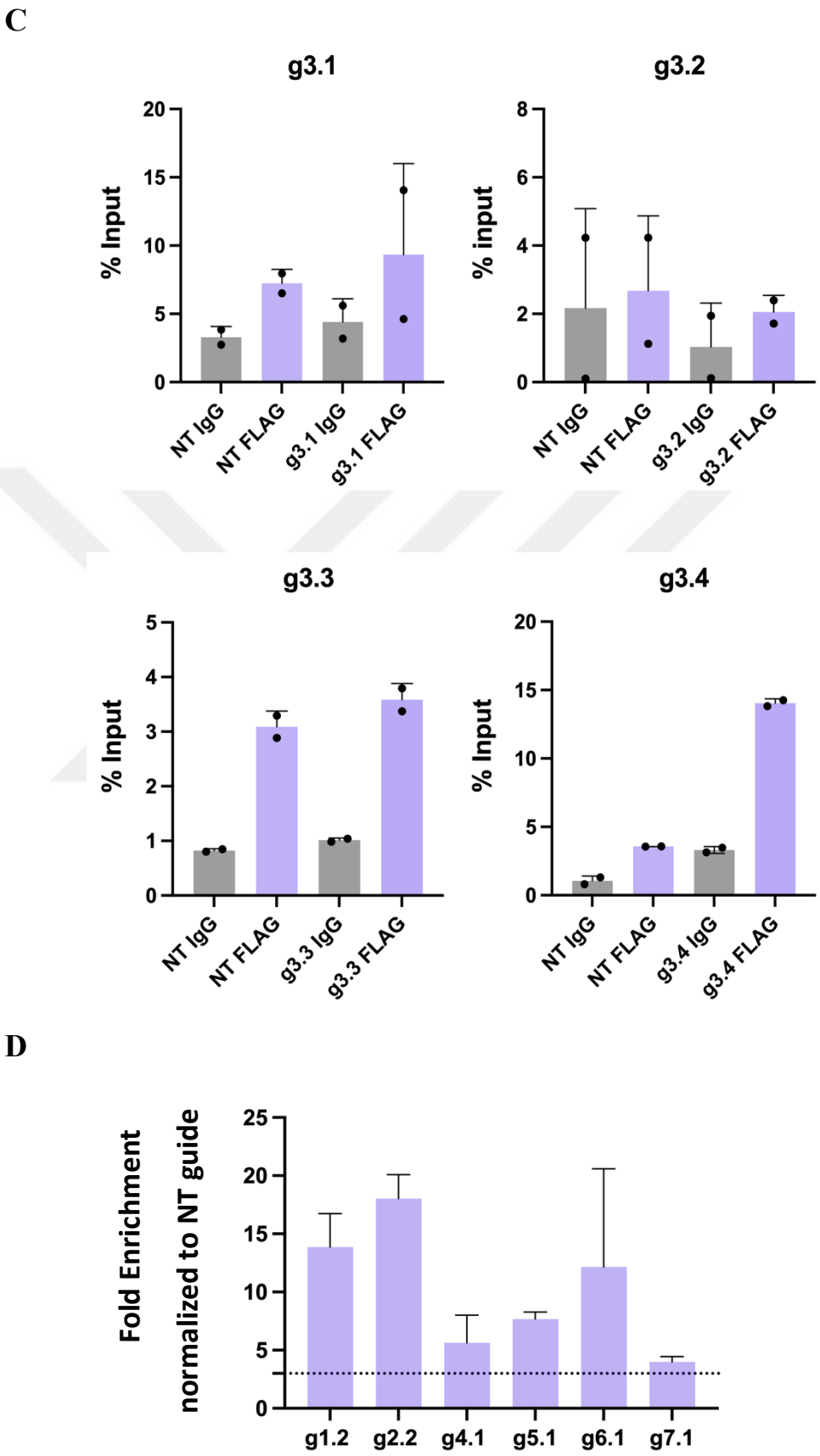

Figure 3.7: ChIP-qPCR experiment to determine the targeting efficiency of gRNAs

The figure was generated with Batuhan Altay. (A) Sonication assay was performed with HEK293T cells on BioRuptor Sonicator for 50 cycles with 45 sec on/15 sec off conditions. (B) ChIP-qPCR assay for HEK293T-CASPEX cells expressing different gRNAs which target the seven regions on ATP7B promoter. The enrichment scores for each gRNA were calculated as %input normalized to negative control mouse IgG. (C) For Region 3, four different gRNAs were designed, and their targeting efficiency was quantified with ChIP-qPCR assay. g3.4 was selected due to its higher enrichment at the targeted region on the ATP7B promoter. (D) Fold enrichment values for each gRNA were normalized to non-targeting guide RNA control, confirming the binding of the gRNAs to the target regions using the formula of (Fold Enrichment = 2^(gRNA IgG – gRNA FLAG) / 2^(NT IgG – NT FLAG)).

For Region 3, initially designed gRNAs did not show an enrichment after ChIP-qPCR analysis. This result could stem from the fact that the targeted region was AT-rich and the designed qPCR primers were not optimal for the experiment protocol. Thus, additional gRNAs were designed and labeled as g3.3 and g3.4 (Table *2.1*). After generating the stable cell lines expressing these gRNAs, they were sonicated and precipitated with anti-FLAG antibody. %input calculation demonstrated that HEK293T-CASPEX-g3.4 cells showed an enrichment of the binding of gRNA on region 3 of the promoter sequence (Figure *3.7C*). Also, double normalization with non-targeting gRNA results was calculated and further confirmed the binding of the selected gRNAs to the targeted regions on the ATP7B promoter (Figure *3.7D*).

3.4 Proximity Labeling of ATP7B Promoter Region

3.4.1 Biotinylation confirmation of HEK293T-CASPEX cells

HEK293T-CASPEX cells expressing the gRNAs with the higher targeting efficiency were treated with biotin phenol and H_2O_2. At the targeted regions on the ATP7B promoter, the proteins near the gRNA binding region were biotinylated. The biotinylation of proteins was confirmed with a western blot assay using Streptavidin-HRP (Figure *3.8*). Initially, the cytosolic fraction and nuclear fraction of the HEK293T-CASPEX-NT and HEK293T-CASPEX-g1.2 samples were analyzed with streptavidin-HRP blot. Only in the presence of doxycycline, biotin, and H_2O_2, the proteins were biotinylated which is indicated by the pattern of proteins on the membrane (Figure *3.8A*). The biotinylation pattern also demonstrates the efficiency of the additional nuclear-isolation step in the protocol to yield more purified nuclear proteins. This isolation step removed the non-

specific biotinylation products before the mass spectrometry analysis. Next, the HEK293T-CASPEX-g2.2 and HEK293T-CASPEX-g3.4 samples were biotinylated and imaged by the Streptavidin-HRP blot resulting in a protein pattern similar to the previous blot (Figure *3.8B*).

A

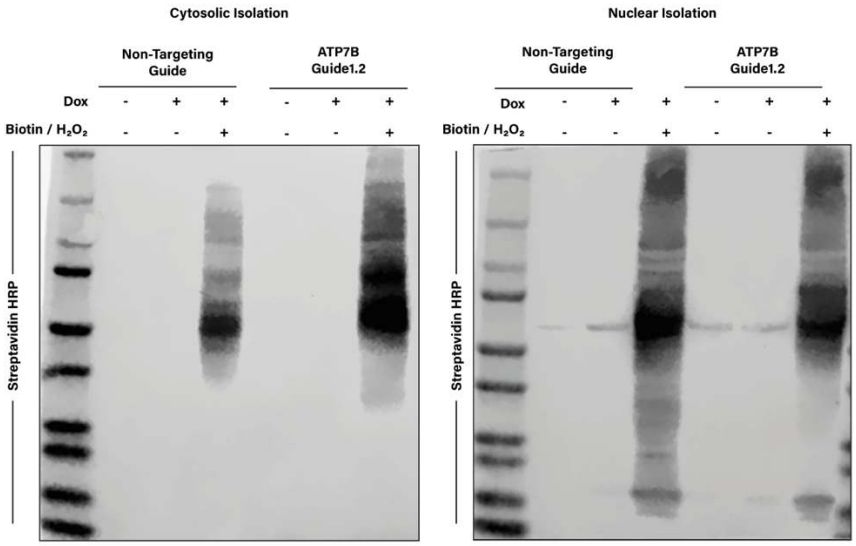

B

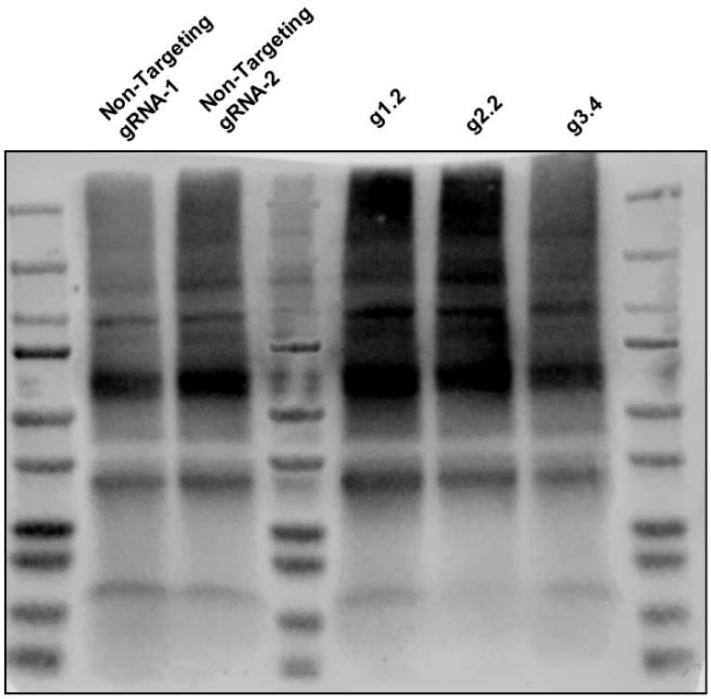

C

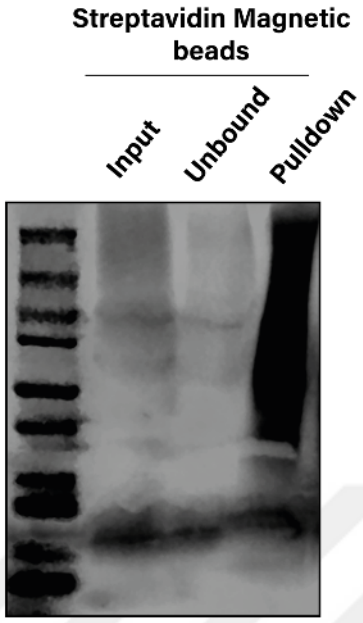

Figure 3.8: Western blot confirmation of biotinylated HEK293T-CASPEX samples

(A) Streptavidin-HRP blot of cytosolic protein and nuclear protein fragments isolated from HEK293T-CASPEX-NT and HEK293T-CASPEX-g1.2 samples. (B) Biotinylation confirmation of HEK293T-CASPEX cells expressing NT guide, g1.2, g.2.2, and g3.4 with Streptavidin-HRP blot. (C) Pulldown assay for biotinylated HEK293T-CASPEX-g1.2 cells using streptavidin-coated magnetic beads, confirming the pulldown efficiency. The figure was generated with Batuhan Altay.

When dCas9-APEX2 is expressed and adds a biotin tag to the proteins at the targeted region, the next step requires the pulldown of those tagged proteins. Streptavidin binds very strongly to the biotin via noncovalent interactions, thus the protein of interest could be isolated from a sample by adding a biotin tag to the protein and performing a pulldown with streptavidin-coated beads (Chivers, Koner, Lowe, & Howarth, 2011)(Santos-Barriopedro, van Mierlo, & Vermeulen, 2021). The HEK293T-CASPEX-g1.2 cells treated with biotin phenol and H_2O_2 were incubated with streptavidin-coated magnetic beads overnight. The next day, the samples were put on a magnetic rack to isolate the protein-bead complexes from the flowthrough. Then, the flowthrough solution and the protein samples dissociated from the streptavidin beads were imaged by the streptavidin-HRP blot (Figure *3.8C*). The pulldown efficiency was verified since there were not any biotinylated proteins remaining in the flowthrough solution, indicating the majority of the biotinylated proteins were pulled down with the magnetic beads. The whole sample

groups were then biotinylated, pulled down with the indicated protocol, and sent to the mass spectrometry analysis to identify the proteins resided at the ATP7B promoter region.

3.4.2 Mass Spectrometry Analysis

Mass spectrometry analysis was performed on the Orbitrap Mass Spectrometer (Thermo Scientific, QExactive Orbitrap). The data was analyzed on MaxQuant software (J. Cox & Mann, 2008) and Cassiopeia (Varnavides et al., 2022) program for quality control and normalization steps for the label free-quantification (LFQ) analysis. The proteins detected at the ATP7B promoter were identified and their enrichment scores were calculated. MA plots were generated based on the average expression and logFC enrichment values of the proteins (Figure *3.9*). MA plots are a visualization of biological data comparing two measurements between the experiment groups (Gatto, Breckels, Naake, & Gibb, 2015).

ATP7B Promoter Region 1

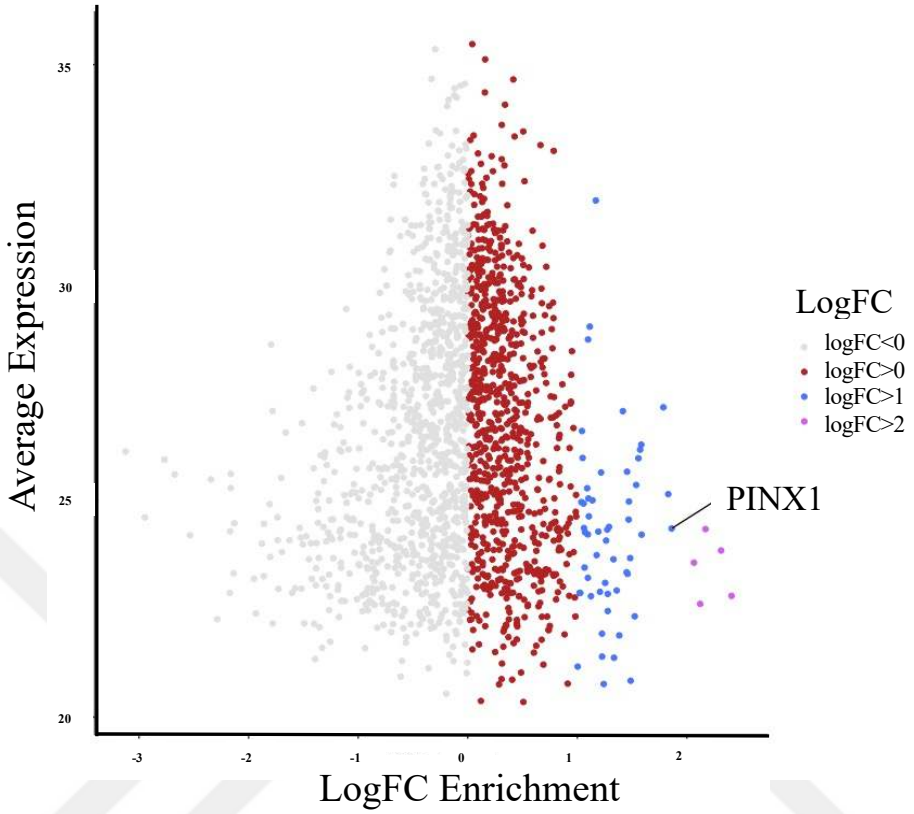

ATP7B Promoter Region 2

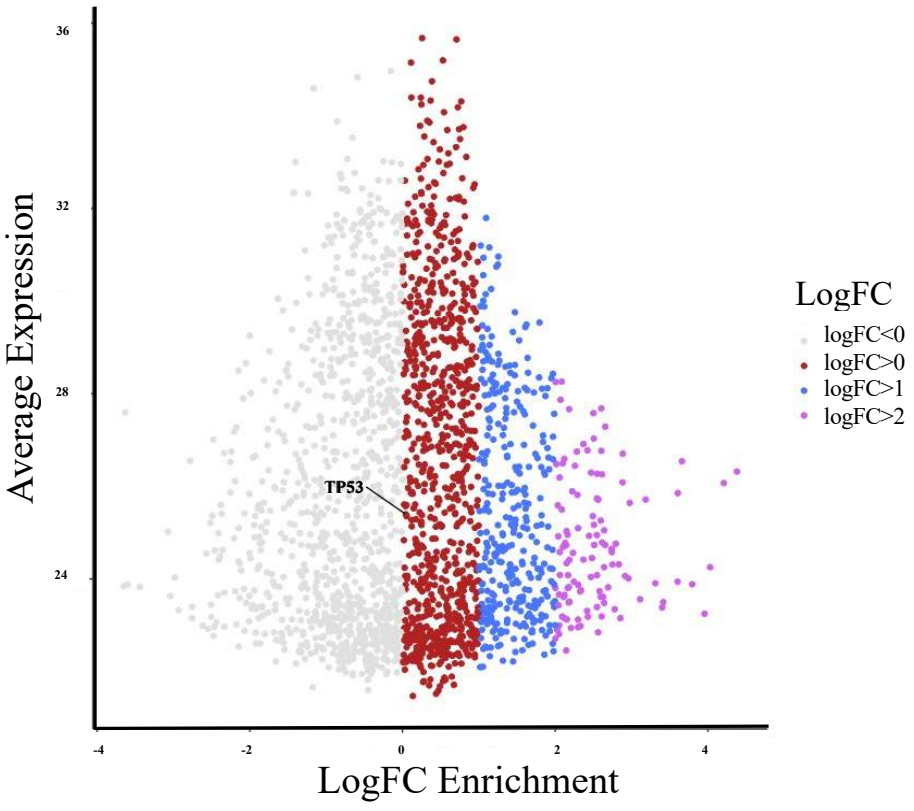

ATP7B Promoter Region 3

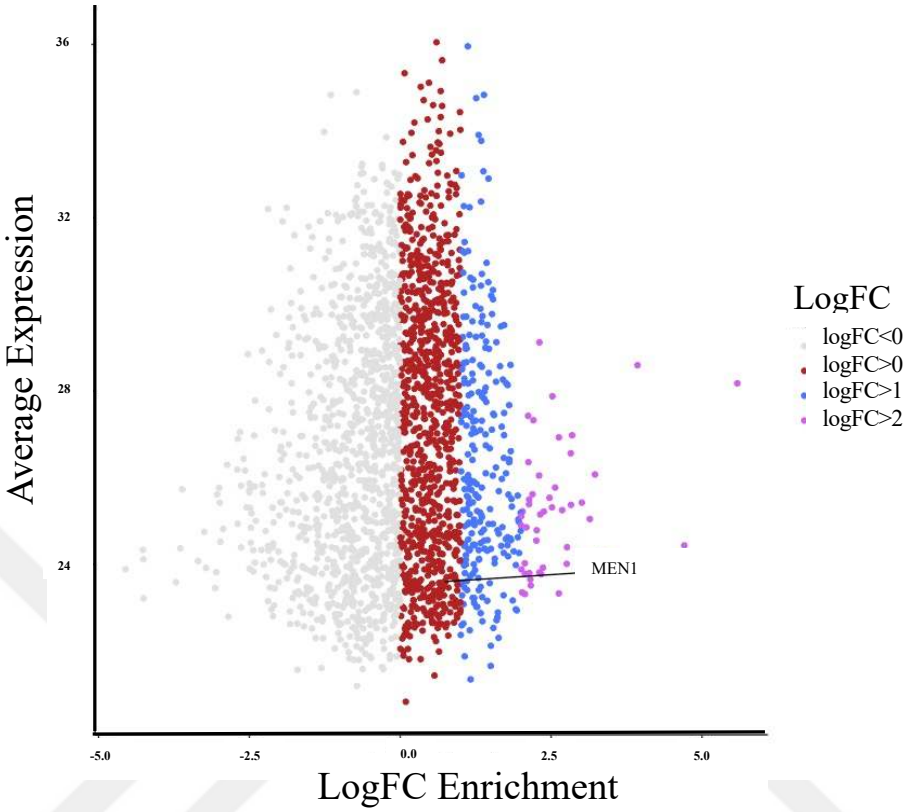

ATP7B Promoter Region 4

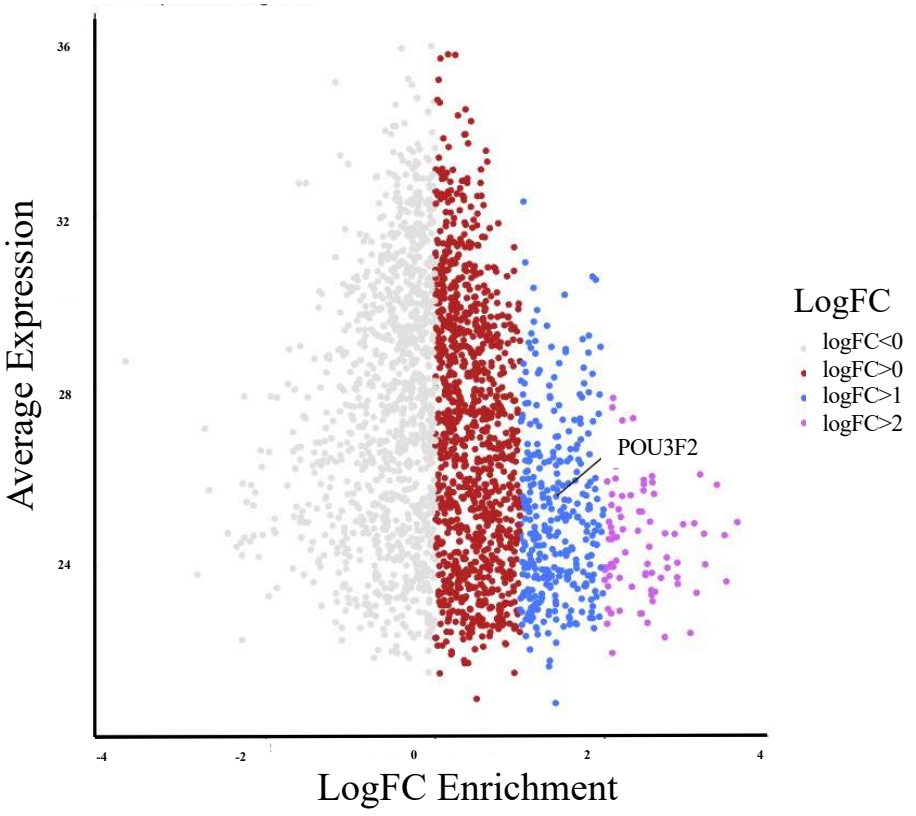

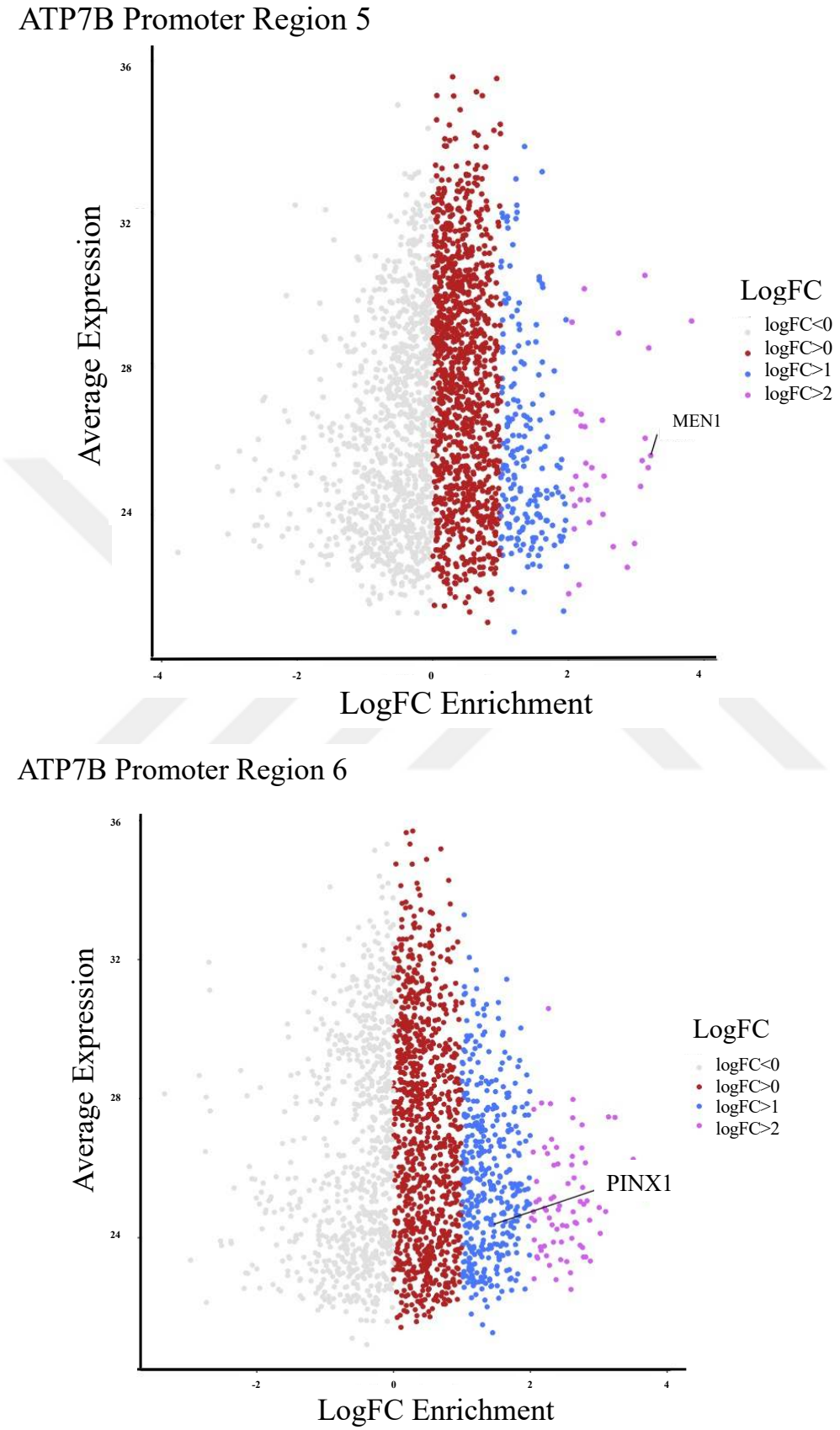

Figure 3.9: MA plots for the targeted regions on the ATP7B promoter.

The figure was generated with Dr. Selahattin Can Ozcan. Mass spectrometry analysis was conducted for the targeted regions on the ATP7B promoter sequence. The proteins with logFC values higher than 2 were depicted as pink, and higher than 1 were depicted as blue. The proteins with a logFC value between 0 and 1 were depicted as red and the others as grey. The target proteins TP53, MEN1, POU3F2, and PINX1 were enriched compared to the NT control.

3.5 Potential Regulators of ATP7B

Mass spectrometry analysis identified many proteins residing at the ATP7B promoter. Based on their enrichment scores and their association with cancer progression and chemotherapeutic drug resistance, several proteins were selected. Among these proteins, a telomerase inhibitor, PINX1, a tumor suppressor, MEN1, and several transcription factors TP53, POU3F2, and PRDM16 were selected to investigate their role in ATP7B regulation. The relationship between these target proteins and the ATP7B expression was investigated. Firstly, the correlation between ATP7B expression and the target proteins in different cancer types was analyzed using the TIMER2.0 database (T. Li et al., 2020). In most of the cancer cell lines, the target proteins' expression was correlated with ATP7B expression (Figure *3.10*). Next, changes in the expression of target proteins were examined to understand their impact on ATP7B expression.

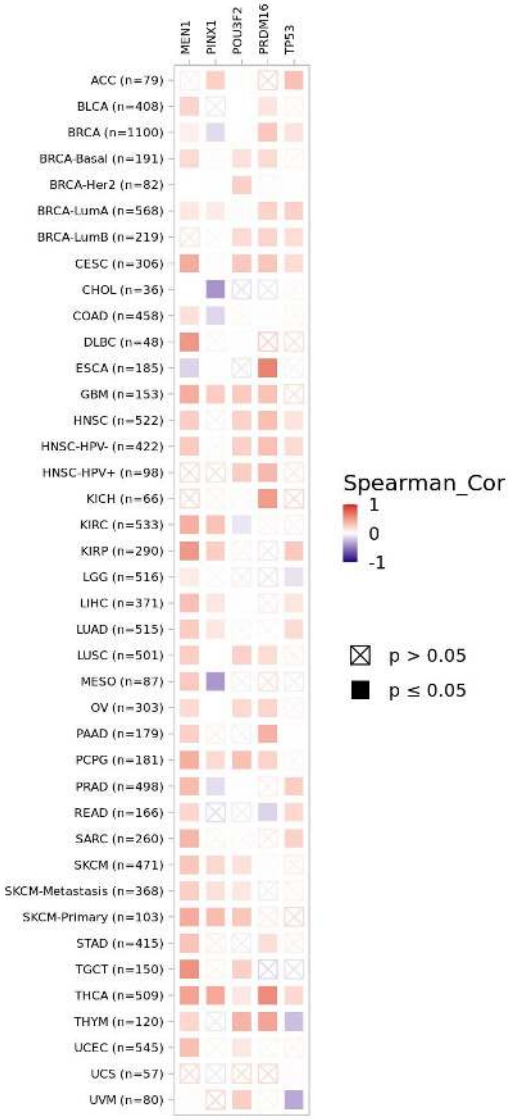

Figure 3.10: Correlation between ATP7B and the target proteins in cancers.

3.5.1 TP53

Tumor protein (TP53) is a tumor suppressor gene whose activity was lost in many human cancers (Aubrey, Strasser, & Kelly, 2016). The transcription factor analysis conducted on TRANSFAC/PROMO databases demonstrated that the targeted region on the ATP7B promoter had a binding motif for TP53 (Figure *3.4*). TP53 protein was also identified in mass spectrometry analysis and its overexpression in the hepatocellular carcinoma cell line was generated. TP53 overexpression resulted in an increase in ATP7B expression both in protein and RNA levels in the Huh7 cells (Figure *3.11*).

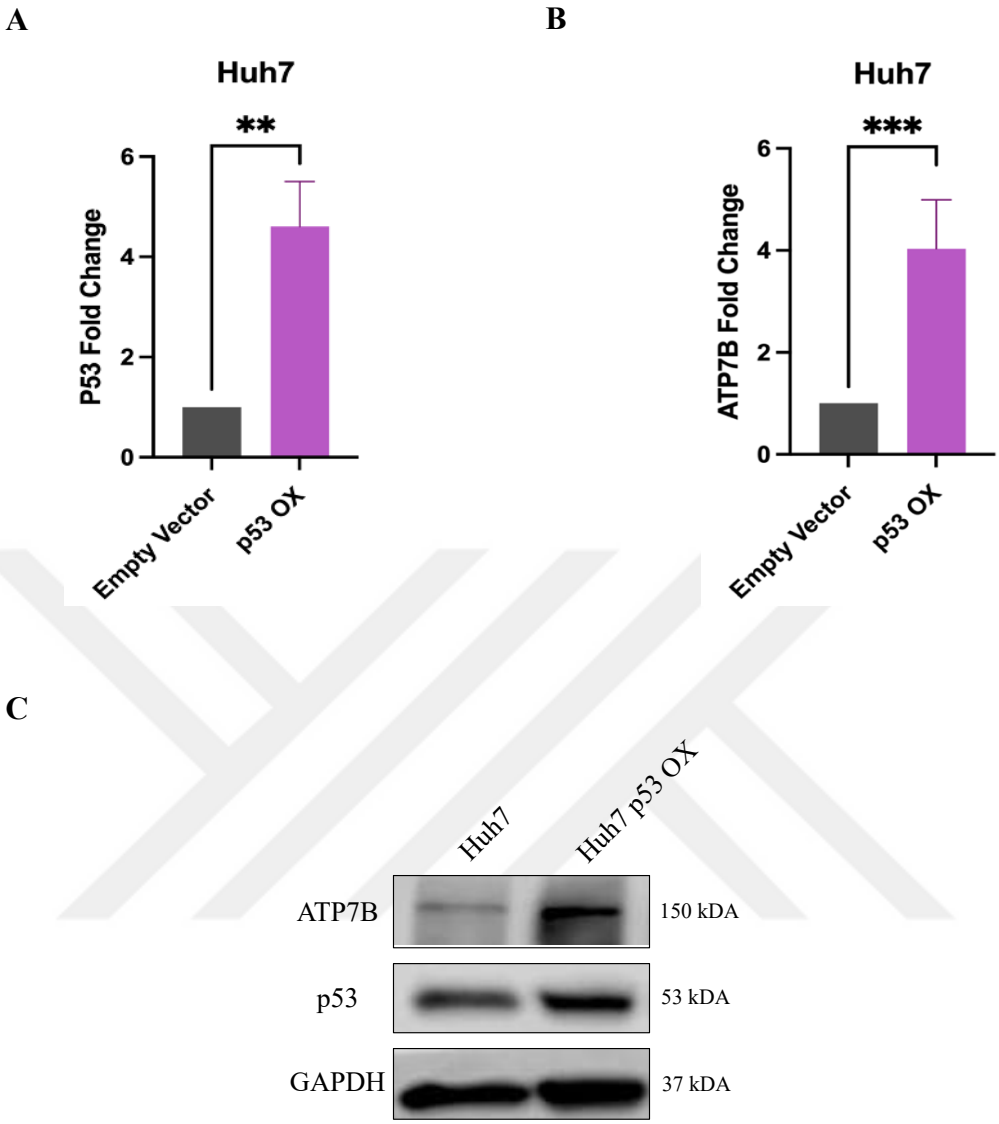

Figure 3.11: TP53 overexpression increases the ATP7B expression in Huh7 cells.

Huh7-P53 OX cells were lysed and the P53 expression (A) and ATP7B expression (B) levels were quantified with qPCR analysis. (C) The same lysates were blotted against anti-ATP7B antibody, anti-p53, and anti-GAPDH antibodies.

3.5.2 MEN1

Menin 1 (MEN1) was also found to be enriched in region 5 on the ATP7B promoter (Figure *3.9*). MEN1 gene is a tumor suppressor, and its levels are found to be reduced in melanoma cancer cells. These cells also show insufficient DNA-repair activity after double-strand breaks (Fang et al., 2013). Thus, it was proposed that MEN1 could regulate the ATP7B expression and to investigate its relationship with ATP7B activity, both its

overexpression and knock-out constructs were generated and treated to HEK293T and Huh7 cells.

MEN1 cDNA was amplified and cloned into the pLJC2-GPT2-3xFLAG (Addgene, 163447) backbone, and its viral particles were transduced into both HEK293T and Huh7 cells. After the selection ended, the cells were lysed, protein samples were blotted with an anti-FLAG antibody, and the protein's overexpression was confirmed (Figure *3.12*). In HEK-MEN1 OX cells, ATP7B expression levels were decreased by qPCR analysis however at the protein level, there was an increase in ATP7B expression (Figure *3.12A*).

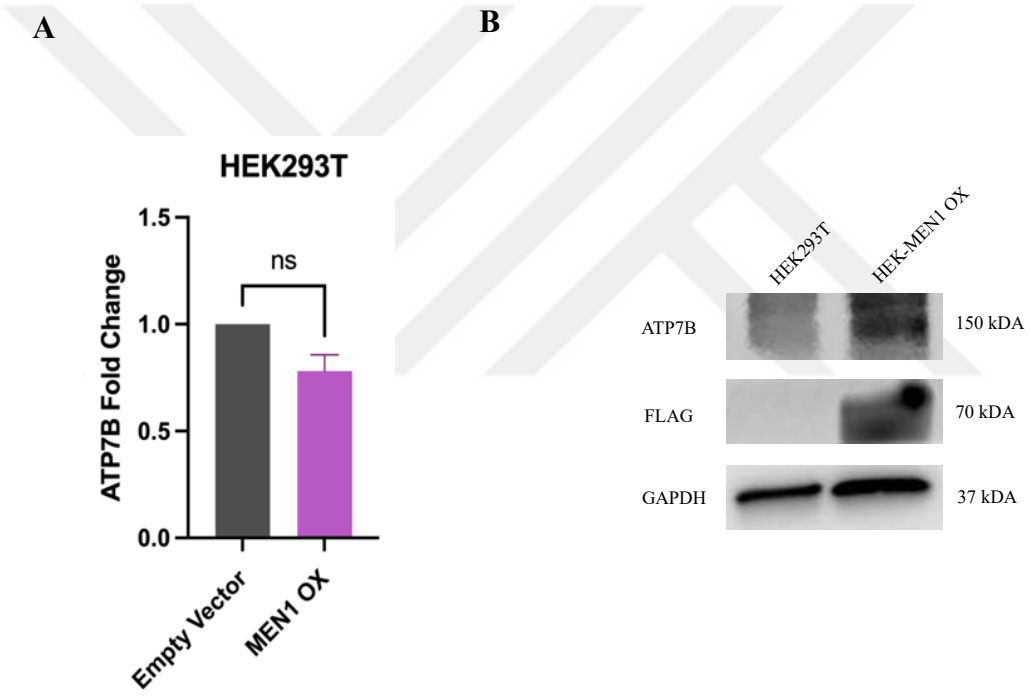

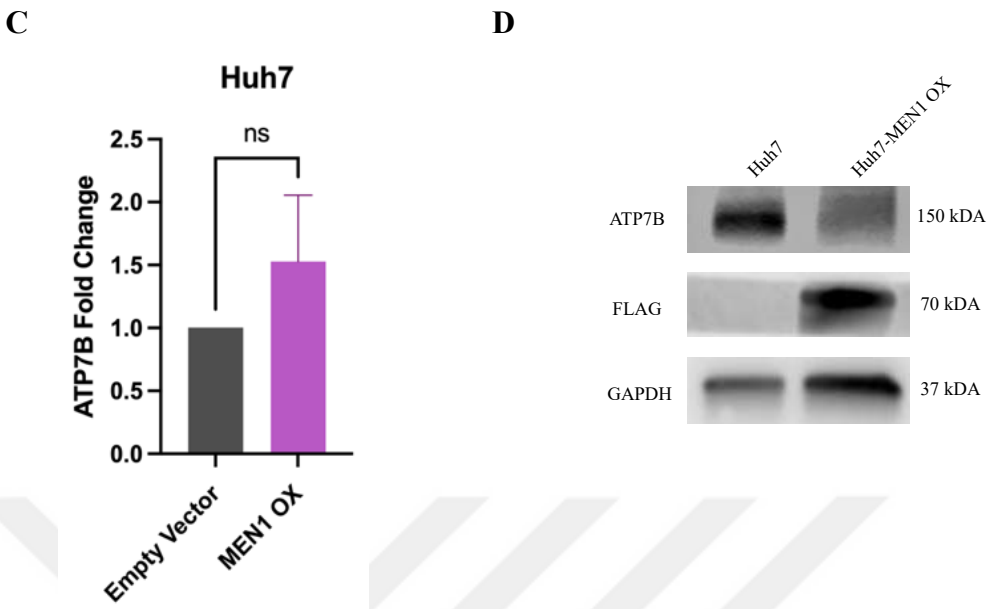

Figure 3.12: Generation of HEK-MEN1 OX and Huh7-MEN1 OX cell lines.

MEN1 overexpressing HEK293T (A-B) and Huh7 (C-D) cells were analyzed with both qPCR and Western blot assays to determine the effect of MEN1 OX on ATP7B levels.

A similar controversy was observed in Huh7-MEN1 OX cells. ATP7B fold change was increased according to the qPCR analysis, however at the protein level, ATP7B levels were diminished in the cells. This difference might be the result of some post-transcriptional modifications which balance the levels of ATP7B to prevent any disturbances in the copper metabolism in the cells.

To investigate the outcome of diminished MEN1 activity on the ATP7B expression, CRISPR-mediated knock-out of the MEN1 construct was generated and its viral particles were transduced into the cells. Due to a lack of antibodies against the target proteins, we examined the mRNA levels of MEN1 and the other proteins to validate the targeting efficiency. While CRISPR technology does not affect the transcription of genes, it can cause changes in mRNA stability due to insertion-deletion (INDEL) mutations introduced by the NHEJ mechanism, leading to a decrease in the expression of the target gene (Tuladhar et al., 2019). Thus, the decrease in MEN1 expression was verified with qPCR (Figure *3.13*). The knockout of MEN1 did not lead to significant changes in ATP7B expression levels in either HEK293T or Huh7 cells, suggesting that MEN1 is likely not functioning as a transcriptional regulator of ATP7B.

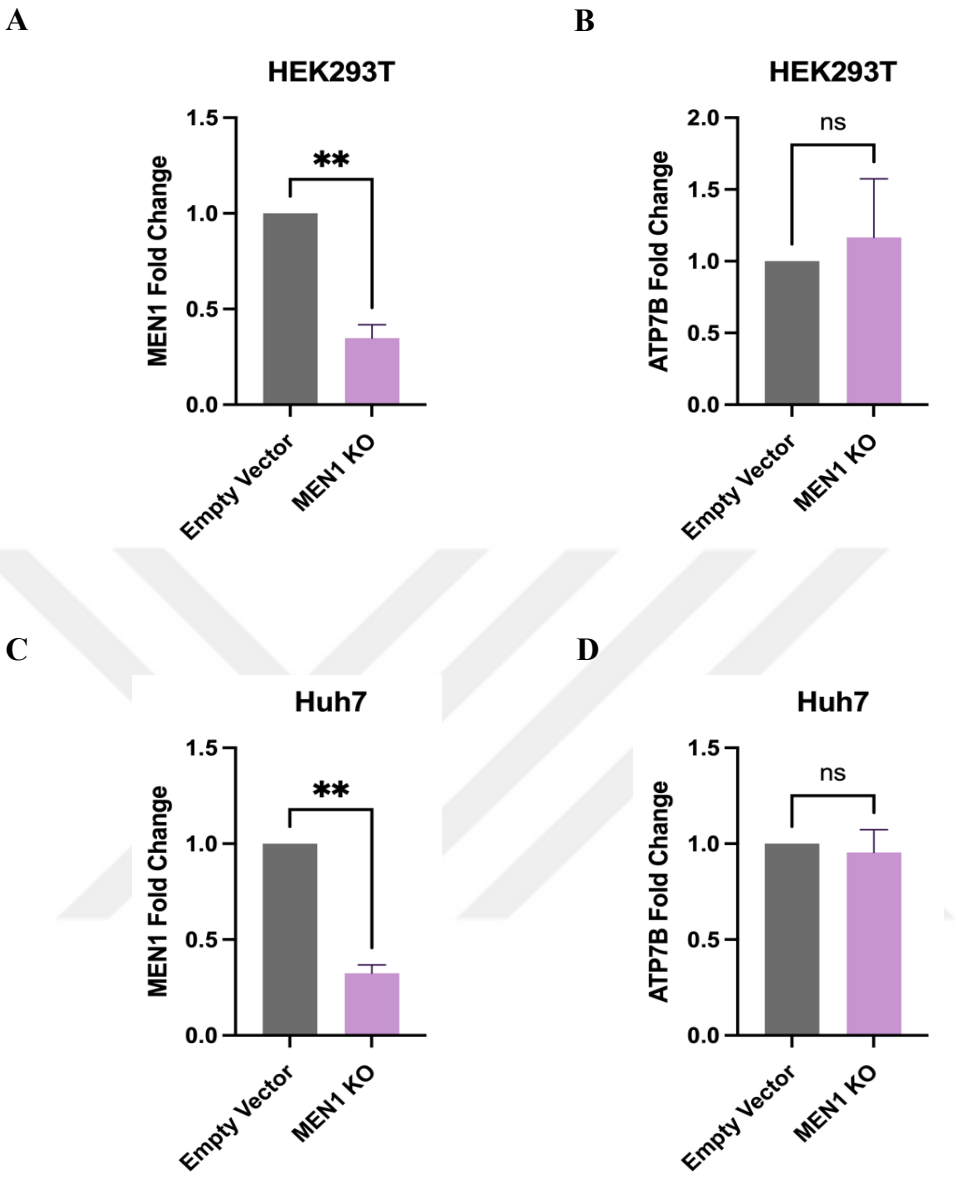

Figure 3.13: Generation of HEK-MEN1 KO and Huh7-MEN1 KO cell lines.

MEN1 expression was diminished in HEK293T and Huh7 cells with CRISPR-mediated knockout and confirmed by the quantification of MEN1 expression in the cells with qPCR. ATP7B expression was also quantified with qPCR in the HEK-MEN1 KO and Huh7-MEN1 KO cells.

The cells were treated with cisplatin and the cell viabilities were quantified with SRB assay to investigate whether the alterations of ATP7B expression in MEN1 OX cells also affect the cells' response to cisplatin. MEN1 overexpression increased the cell viability at certain doses of cisplatin whereas MEN1 knockout did not change the cell viability in HEK293T cells (Figure *3.14A*). However, the increase in cell viability could not be a result of ATP7B activity since both qPCR and Western assays did not yield any

significant results. Also, in Huh7 cells, both MEN1 OX and MEN1 KO phenotypes did not change cell viability compared to the control cell lines (Figure *3.14B*).

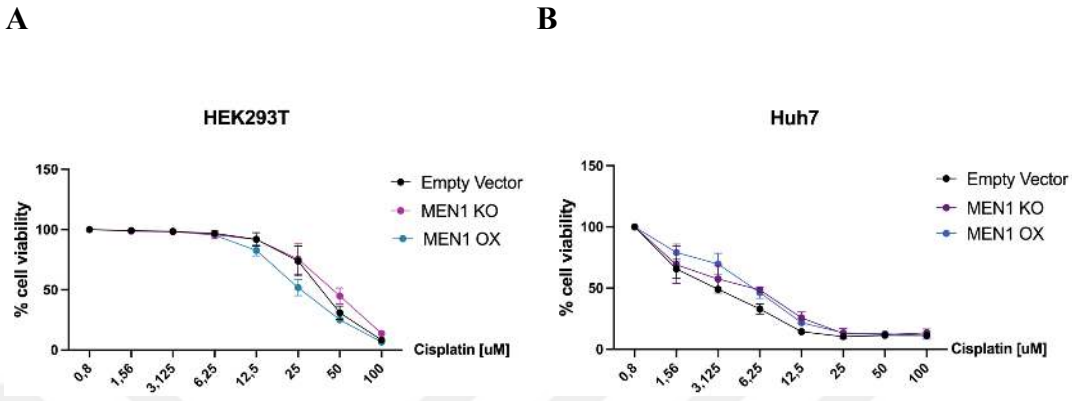

Figure 3.14: SRB cell viability assays for cisplatin-treated HEK293T-MEN1 OX/MEN1 KO and Huh7-MEN1 OX/MEN1 KO cells.

Both MEN1 OX and MEN1 KO cell lines were treated with cisplatin and the cell viability was measured with SRB assay.

3.5.3 POU3F2

The POU Class 3 Homeobox 2 protein (POU3F2) is a member of the class of proteins with a POU-domain and is usually expressed in the developmental and neuronal differentiation processes (He et al., 1989). POU3F2 is a transcription factor and its expression was found to be increased in breast cancer cells that could induce radioresistance (Zhang et al., 2023). POU3F2 was also enriched during the biotinylation process of the ATP7B promoter regions 1, 4, and 5, thus it was hypothesized that this protein may regulate ATP7B expression (Figure *3.9*).

To test this hypothesis, overexpression of POU3F2 was generated in HEK293T and Huh7 cells. In HEK-POU3F2 OX cells, ATP7B expression did not change significantly compared to the control cell lines (Figure *3.15B*). However, in Huh7-POU3F2 OX cells, ATP7B levels were decreased both at RNA and protein levels (Figure *3.16*). This decrease could propose a potential regulatory mechanism of ATP7B by POU3F2 in liver cancer cells by directly binding POU3F2 to the ATP7B promoter region or by recruiting additional proteins to alter the gene's expression.

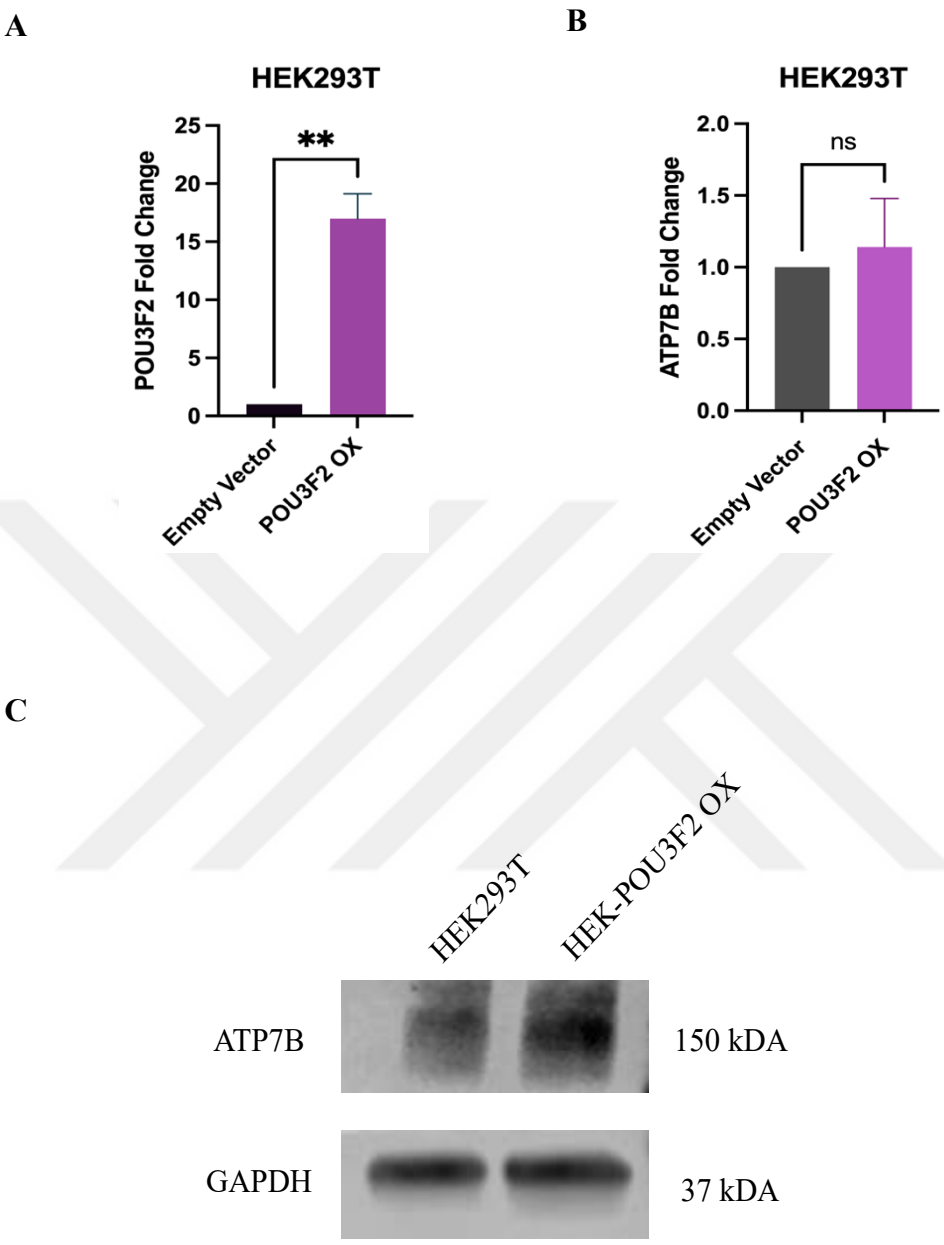

Figure 3.15: Generation of HEK-POU3F2 OX cell lines.

POU3F2 overexpressing HEK293T cells were analyzed with both qPCR and Western blot assays to determine the effect of POU3F2 OX on ATP7B levels.

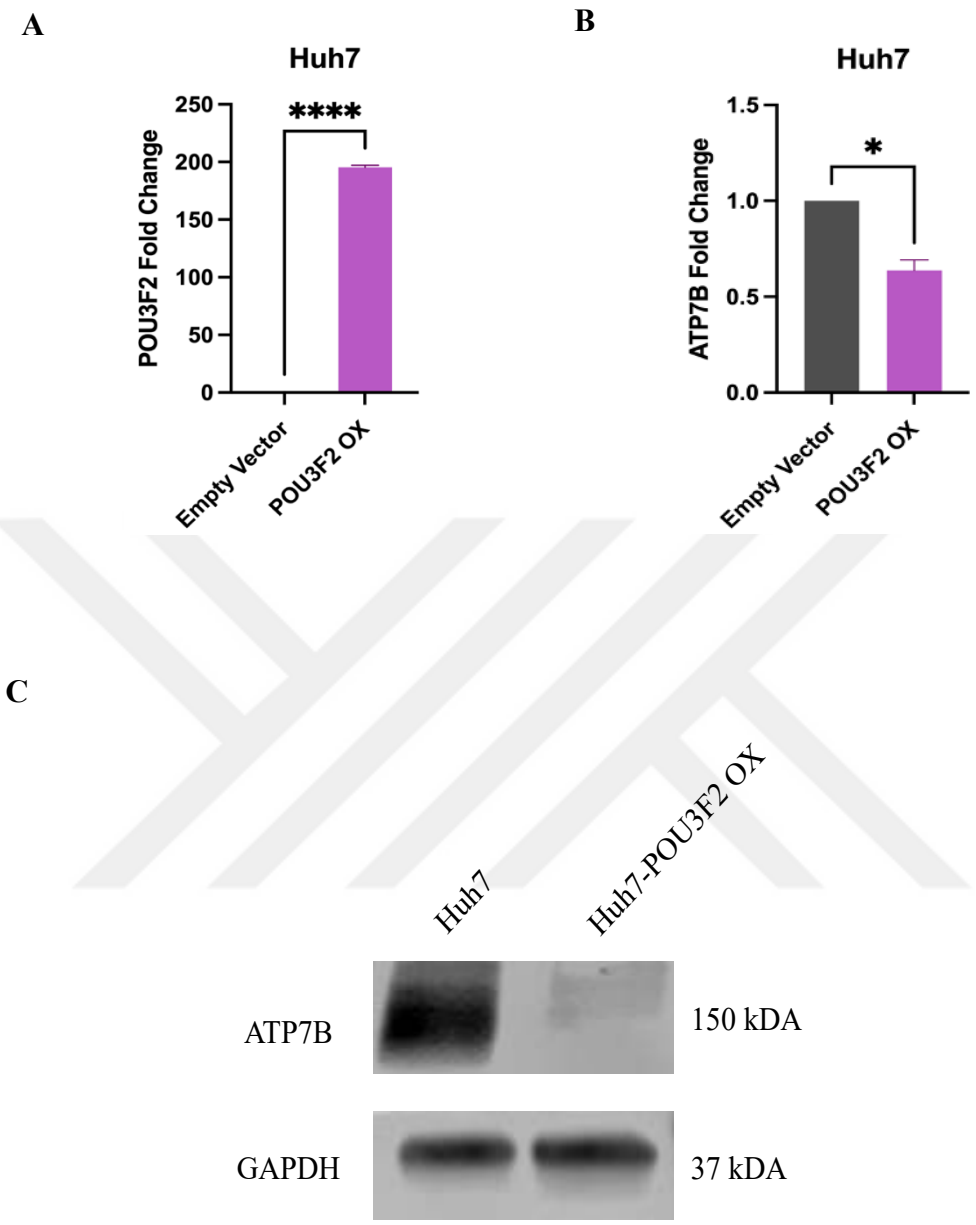

Figure 3.16: Generation of Huh7-POU3F2 OX cell lines.

POU3F2 overexpressing Huh7 cells were analyzed with both qPCR and Western blot assays to determine the effect of POU3F2 OX on ATP7B levels.

To investigate the reverse effect, POU3F2 activity was decreased in the cells by the CRISPR-mediated knock-out model. The decrease in POU3F2 expression was verified with qPCR (Figure *3.17A*). In HEK293T cells, POU3F2 KO increased the ATP7B expression however, in Huh7 cells, the knock-out of POU3F2 did not significantly alter the ATP7B expression (Figure *3.17D).*

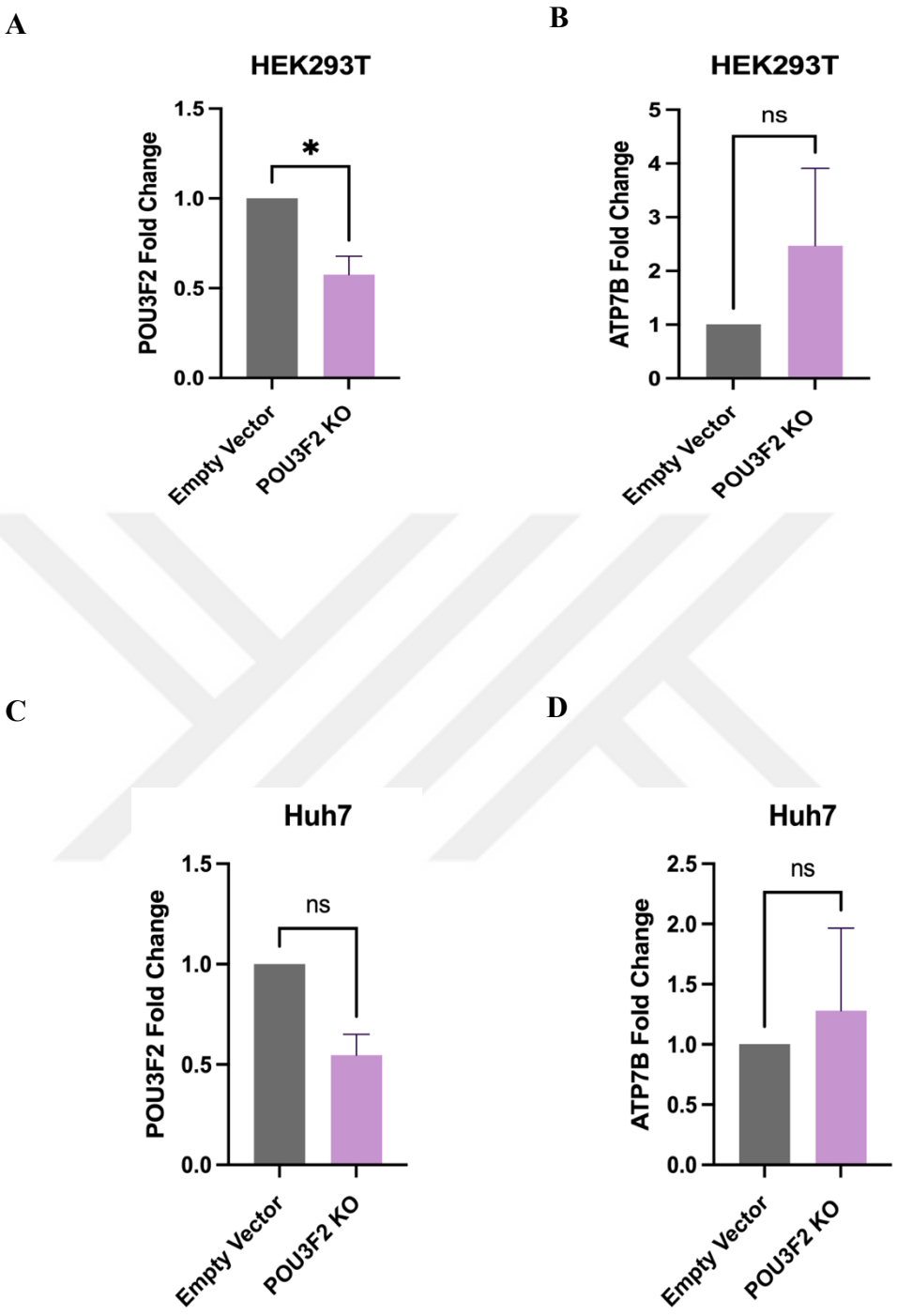

Figure 3.17: Generation of HEK-POU3F2 KO and Huh7-POU3F2 KO cell lines

POU3F2 expression was diminished in HEK293T and Huh7 cells with CRISPR-mediated knockout and confirmed by the quantification of POU3F2 expression in the cells with qPCR. ATP7B expression was also quantified with qPCR in the HEK-POU3F2 KO and Huh7-POU3F2 KO cells.

The response of HEK and Huh7 POU3F2 OX cells to the cisplatin treatment was also studied with SRB assay. There was no change in the cell viability between the normal and overexpression cell line (Figure *3.18*). The effect of POU3F2 overexpression on ATP7B activity may not also influence the cisplatin or copper efflux in the cells, so there was no change in cell viability upon drug treatment.

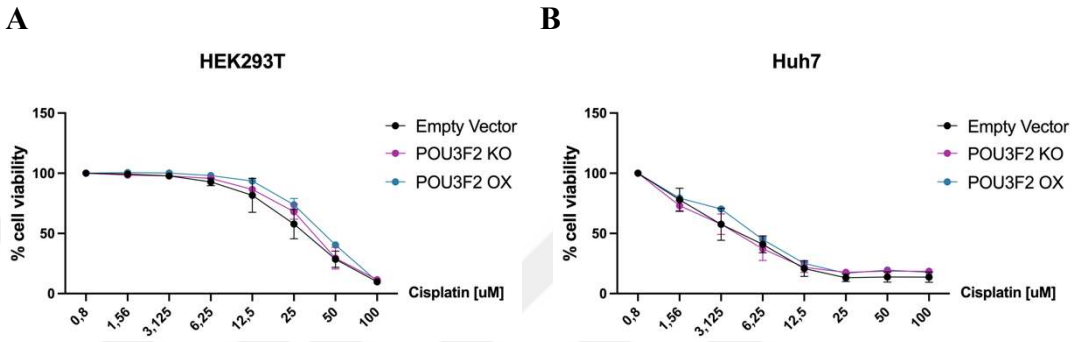

Figure 3.18: SRB cell viability assays for cisplatin-treated HEK293T POU3F2 OX/POU3F2 KO and Huh7-POU3F2 OX/POU3F2 KO cells.

Both POU3F2 OX and POU3F2 KO cell lines were treated with cisplatin and the cell viability was measured with SRB assay.

3.5.4 PRDM16

According to the mass spectrometry analysis, the PR domain containing 16 (PRDM16) was one of the enriched proteins at the ATP7B promoter of HEK293T cells. It is a transcription factor that is involved in the development of brown adipose tissue (Seale et al., 2008). In both lung adenocarcinoma and thyroid cancer, PRDM16 is proposed as a tumor suppressor since its overexpression in cancers resulted in the suppression of proteins associated with epithelial-to-mesenchymal transition (EMT) (Fei et al., 2019) (W. L. Liu et al., 2021). These findings about the relationship between PRDM16 and cancer development raised the possibility of the role of PRDM16 in cisplatin resistance through the transcriptional regulation of ATP7B. To investigate this proposed regulation, PRDM16 expression was overexpressed in both HEK293T and Huh7 cells and the change of ATP7B levels in these cells was examined with qPCR and Western blot assays. In HEK293T cells, PRDM16 OX did not result in a significant change in ATP7B levels both

at RNA and protein levels (Figure *3.19A, B*). In Huh7 cells, PRDM16 overexpression did not alter the ATP7B in the protein level however it increased the ATP7B fold change by twofold at the RNA level (Figure *3.19C, D*). Thus, PRDM16 could alter ATP7B expression either by direct binding or recruiting other proteins to the promoter site.

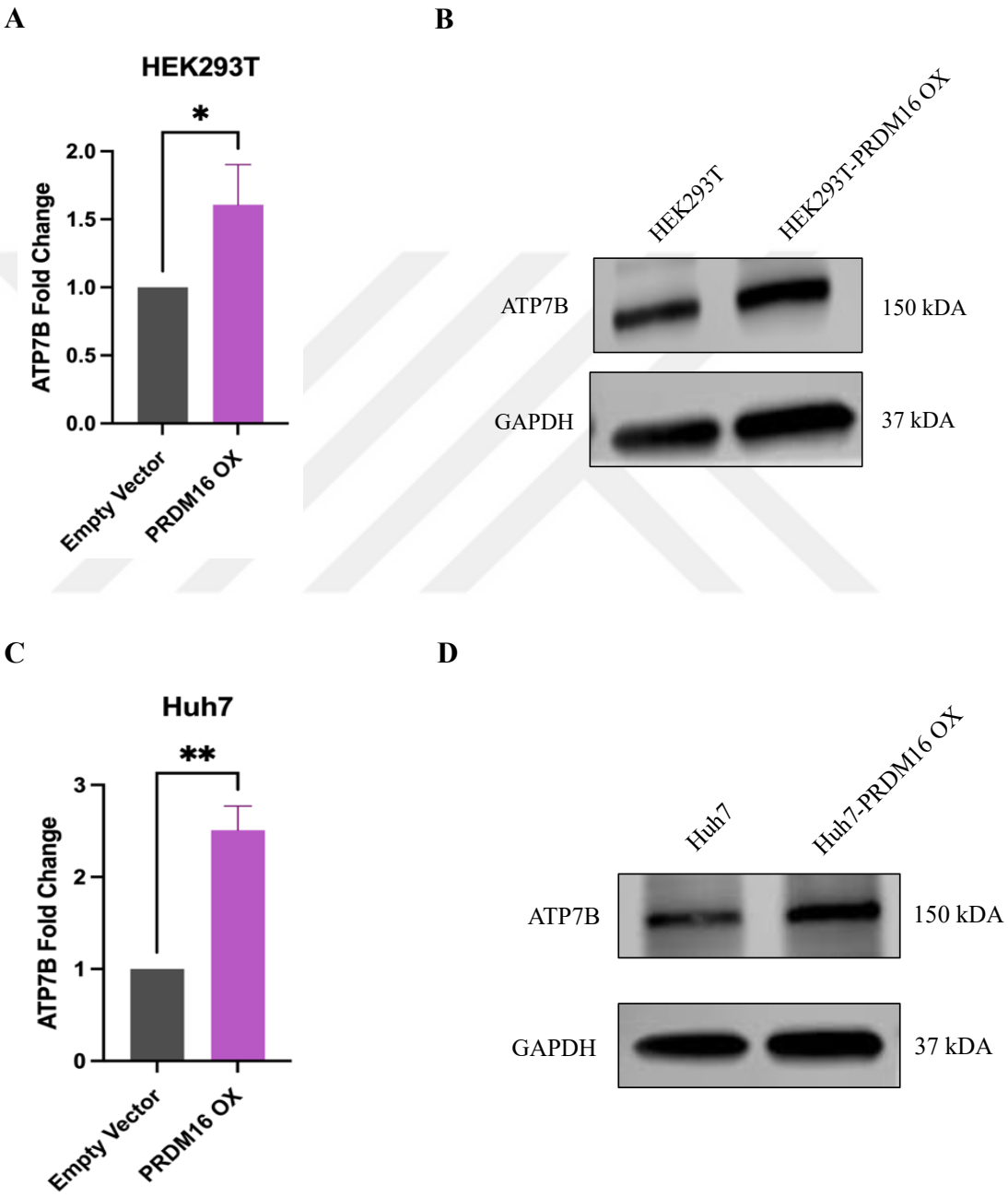

Figure 3.19: Generation of HEK-PRDM16 OX and Huh7-PRDM16 OX cell lines.

PRDM16 overexpressing HEK293T and Huh7 cells were analyzed with both (A-B) qPCR and (C-D) Western blot assays to determine the effect of PRDM16 OX on ATP7B levels.

PRDM16 overexpression altered the cells' response to cisplatin treatment in HEK293T cells at certain doses however it did not affect their response against copper (Figure *3.20*).

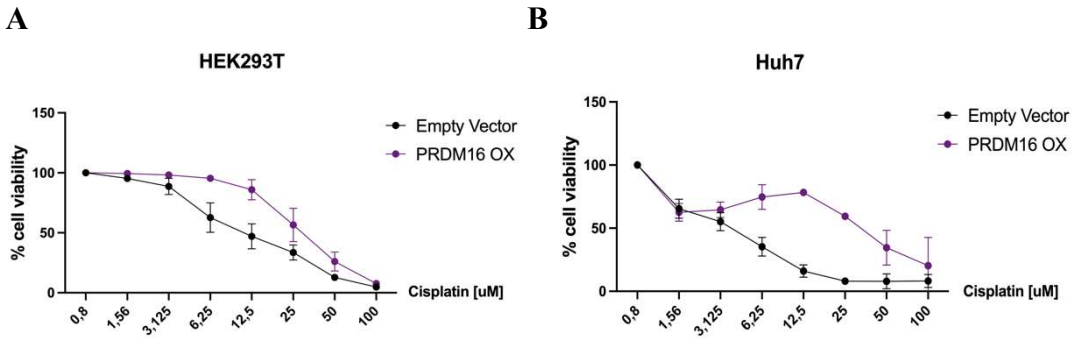

Figure 3.20: SRB cell viability assays for cisplatin and copper-treated HEK293T-PRDM16 OX cells.

Both PRDM16 OX and PRDM16 KO cell lines were treated with cisplatin and the cell viability was measured with SRB assay.

The effect of PRDM16 overexpression on ATP7B activity was also examined via luciferase reporter assay. Reporter assays are techniques used to determine the regulatory potential of a target promoter by cloning the sequence into a detectable reporter protein such as luciferase (Cheng et al., 2010). Initially, the putative ATPB promoter sequence was cloned in a luciferase-gene backbone, and different lengths of fragments were transfected into HEK293T-PRDM16 OX cells, and the relative luciferase signals were measured (Figure *3.21A*). However, the luciferase reporter assay with the ATP7B constructs of various size did not significantly change ATP7B promoter activity in HEK293T-PRDM16 OX cells (Figure *3.21*B). PRDM16 could be involved in the recruitment of additional proteins that alter the cells' response against cisplatin or could regulate other transcription factors which directly bind to the ATP7B promoter region.

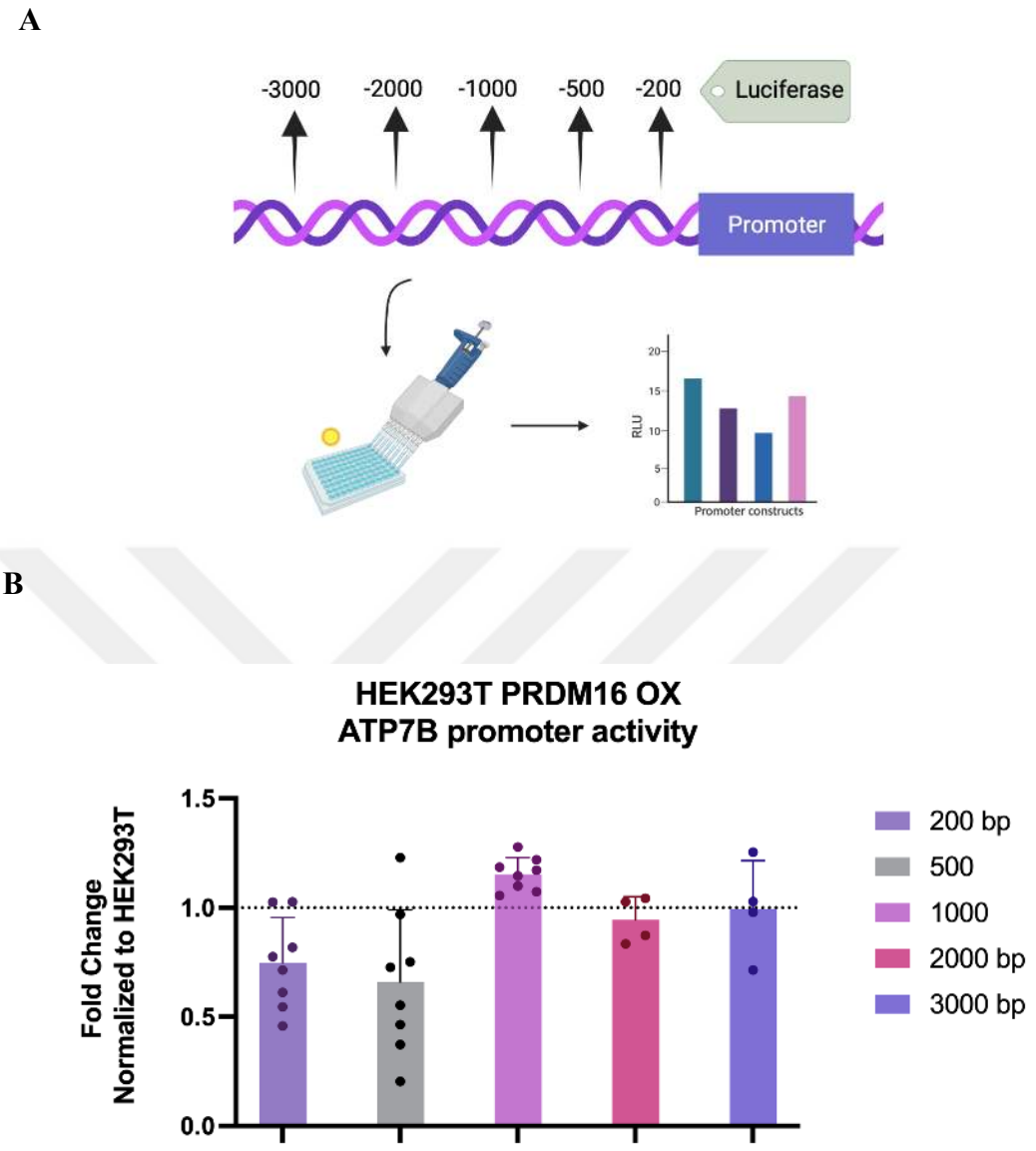

Figure 3.21: Promoter Activity of ATP7B in HEK293T-PRDM16 OX cell lines.

A) Generation of ATP7B promoter constructs. (B) ATP7B promoter activity of HEK293T-PRDM16 OX cells normalized to untransfected HEK293T cells.

3.6 PINX1 relationship with ATP7B expression

The analysis was conducted for the seven regions, and, for Region 1, region 4, and region 6, PINX1 was found to be enriched compared to the non-targeting control (Figure *3.9*). PINX1 is a telomerase inhibitor protein that binds to hTERT and decreases its activity (Zhou & Lu, 2001). In several cancer types, PINX1 overexpression also affects the cell's

destiny against chemotherapeutic drugs. Thus, the protein was selected to investigate its potential role in the regulation of ATP7B.

3.6.1 Alterations in PINX1 expression affect ATP7B expression.

To assess if the altered levels of PINX1 expression affect the ATP7B levels, both overexpression and knock-out of PINX1 constructs were generated. PINX1 cDNA was amplified and cloned into the pLJC2-GPT2-3xFLAG (Addgene, 163447) backbone. Then, its viral particles were generated and transduced into both HEK293T and Huh7 cells to generate cell lines that stably overexpressed PINX1. Huh7 cells were also chosen since they have a higher endogenous expression of ATP7B after HEK293T cells (*Figure 3.1*). Comparing the results between the two cell lines could also provide novel information about the regulation of the gene in a different cellular background. To verify the PINX1 overexpression, the cells were analyzed with a western blot assay using an anti-FLAG antibody, and the overexpression of the protein was confirmed (Figure *3.22*). The fold change of ATP7B in these cells was studied with qPCR assay and the results indicated that there was an increase in ATP7B expression (Figure *3.22A*). However, at the protein level, PINX1 OX slightly decreased the ATP7B expression (Figure *3.22B*). The decrease might stem from a potential activation of some post-transcriptional modification triggered by PINX1 OX which also affects ATP7B levels.

In Huh7 cells, PINX1 overexpression resulted in an increase in ATP7B expression both in RNA and protein levels (Figure *3.22*). These findings support the hypothesis of the potential role of PINX1 as a regulator of ATP7B activity, thus additional molecular assays were performed to study the function of the target protein.

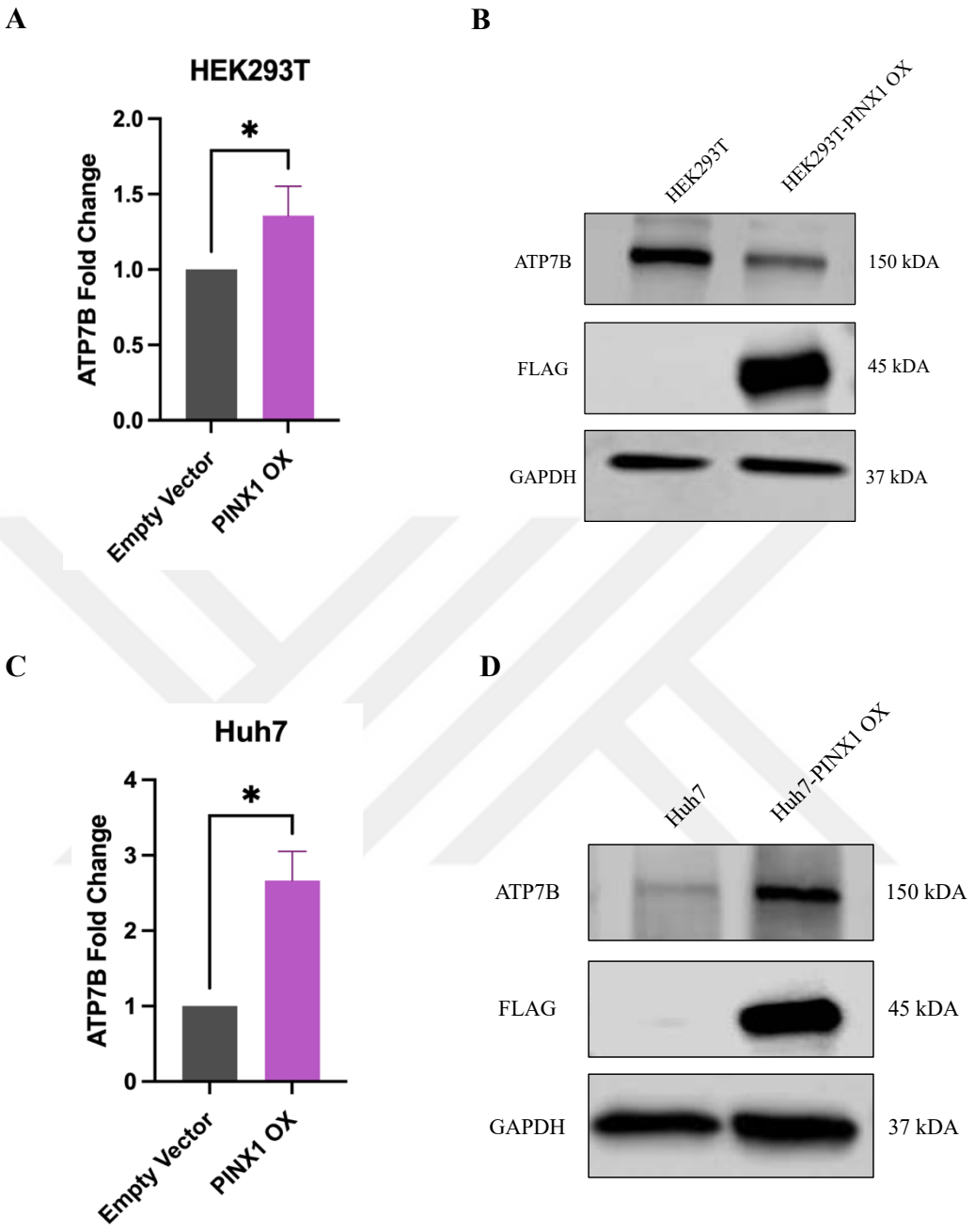

Figure 3.22: Generation of HEK-PINX1 OX and Huh7-PINX1 OX cell lines

PINX1 overexpressing HEK293T and Huh7 cells were analyzed with both qPCR and Western blot assays to determine the effect of PINX1 OX on ATP7B levels.

To examine the reverse effect, PINX1 expression was silenced in both HEK293T and Huh7 cells by designing specific gRNAs that target the exons of PINX1 and then ligating into Lenti-guide-CRISPR (Addgene, 52961) backbone. The decreased PINX1 expression in these cells was verified with qPCR analysis (Figure *3.23*). In HEK-PINX1 KO cells, ATP7B expression was initially decreased, however, the results were not reproducible in

the second biological replica, suggesting the first result showing a decrease in ATP7B expression might be incorrect. Alternatively, this might be the result of a mechanism in the cells that restores the ATP7B levels in the cells after a while to maintain copper homeostasis in the cell. In Huh7-PINX1 OX cells, ATP7B expression was also decreased suggesting a relationship with PINX1 and ATP7B in a transcriptional manner.

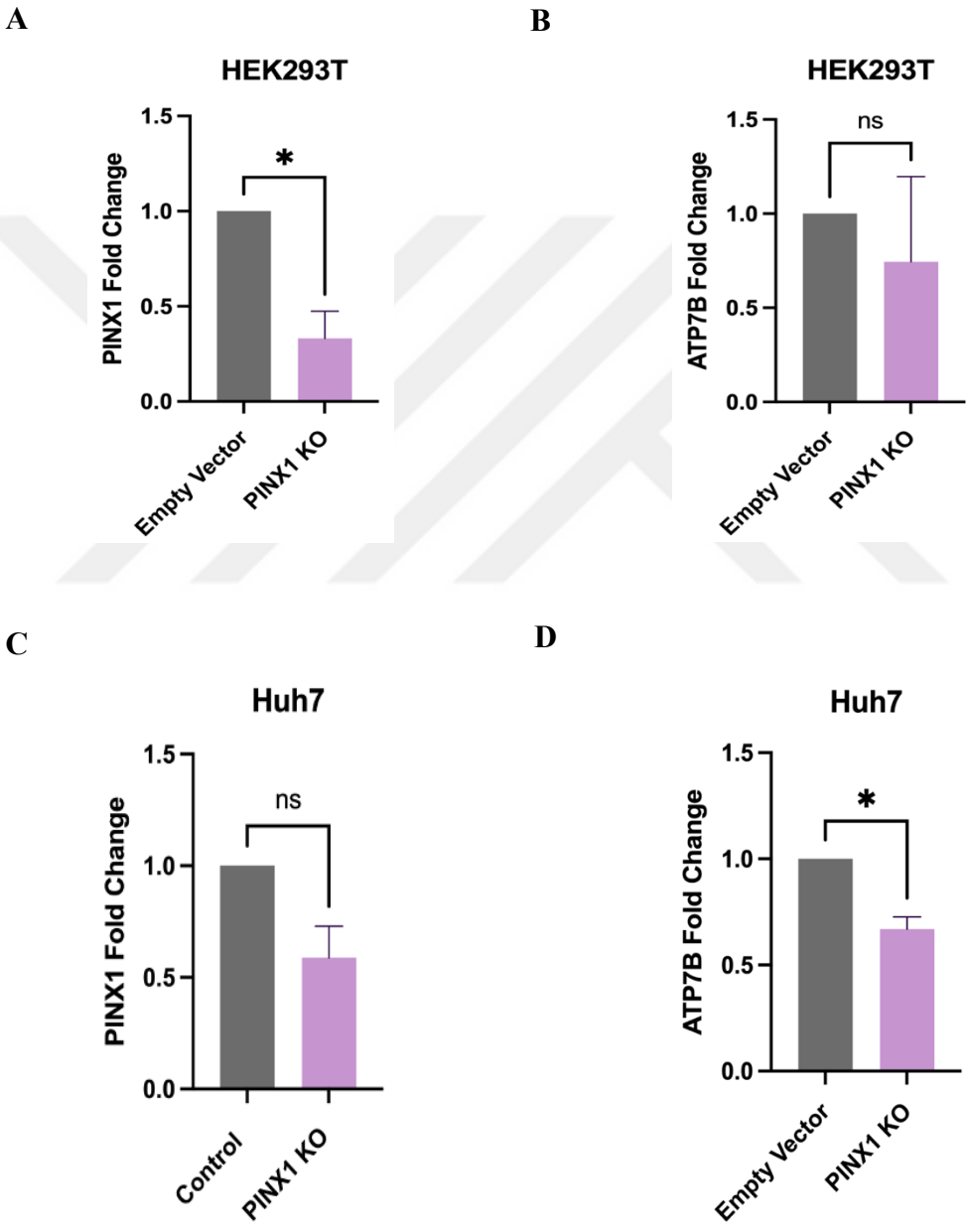

Figure 3.23: Generation of HEK-PINX1 KO and Huh7-PINX1 KO cell lines.

PINX1 expression was diminished in HEK293T and Huh7 cells with CRISPR-mediated knockout and confirmed by the quantification of PINX1 expression in the cells with qPCR. ATP7B expression was also quantified with qPCR in the HEK-PINX1 KO and Huh7-PINX1 KO cells.

The effect of PINX1 overexpression on ATP7B activity was also examined via luciferase reporter assay. The luciferase signal in HEK293T-PINX1 OX cells transfected with exogenous ATP7B promoter constructs with various sizes was increased compared to the untransfected HEK293T cells (Figure *3.24*). The increase in ATP7B promoter activity decreases in 2000 bp, suggesting a potential repressor activity in that region.

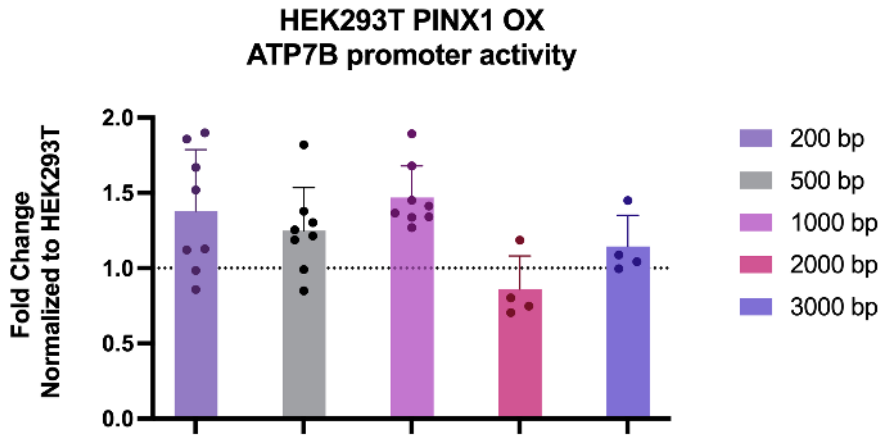

Figure 3.24: Promoter Activity of ATP7B in HEK293T-PINX1 OX cell lines.

ATP7B promoter activity of HEK293T-PINX1 OX cells normalized to untransfected HEK293T cells.

3.6.2 PINX1 binds to the ATP7B promoter.

To verify the results of the presence of PINX1 at the ATP7B promoter region, ChIP-qPCR analysis was performed. Both HEK293T-PINX1 OX and Huh7-PINX1 OX cells were fixed, sonicated, and pulled down with an anti-FLAG antibody. The enrichment of PINX1 at the determined seven regions on the ATP7B promoter was quantified by the %input method. Gene desert (GD) primer was used as a negative control since gene desert region do not contain protein-coding genes (Ovcharenko et al., 2005). In HEK293T cells, PINX1 was mostly enriched in region 1 on the ATP7B promoter and in Huh7 cells, PINX1 was mostly enriched in region 2 (Figure *3.25*).

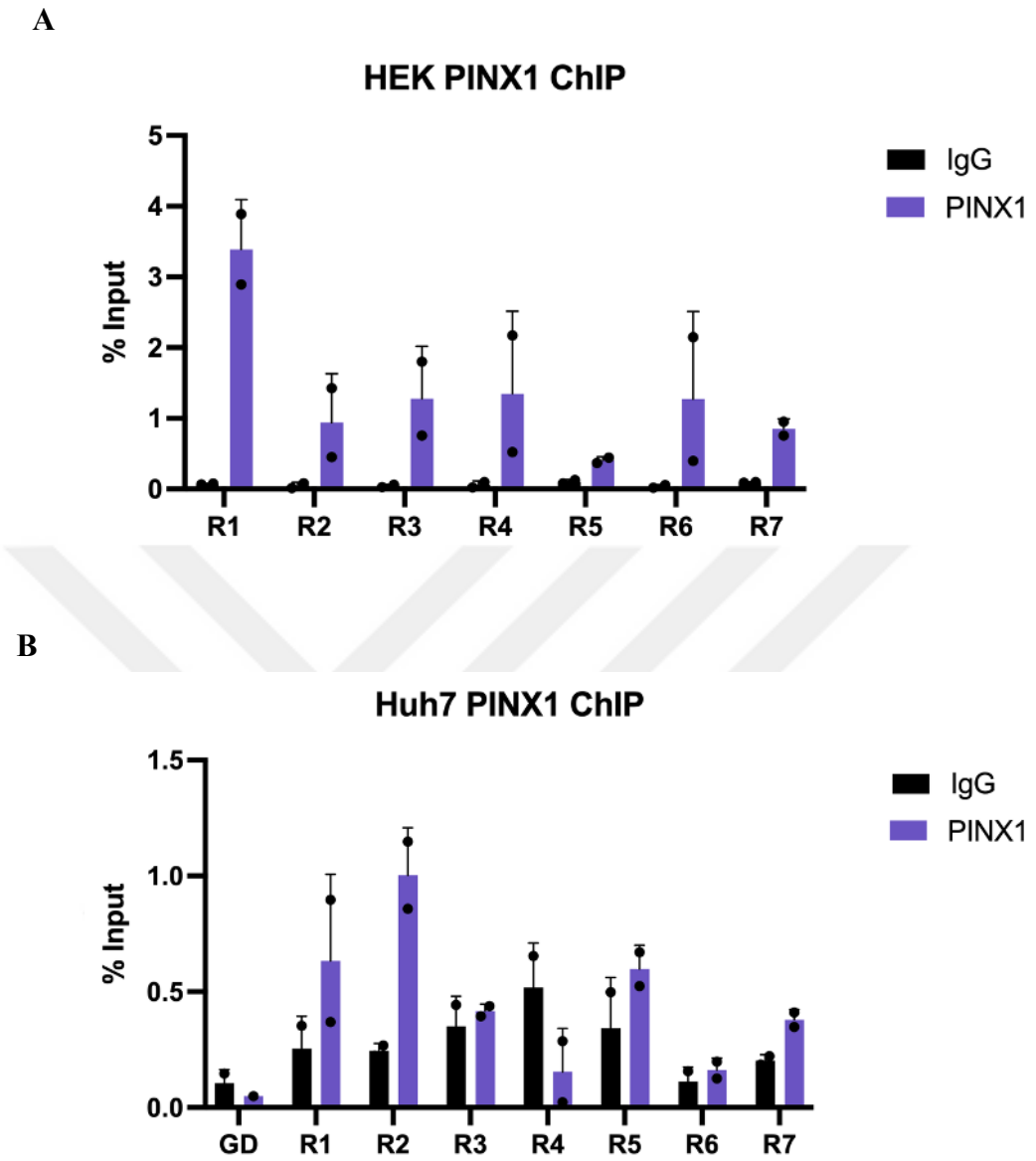

Figure 3.25: ChIP-qPCR analysis for investigating PINX1 occupancy at ATP7B promoter region.

ChIP-qPCR analysis was performed in (A) HEK293T-PINX1 OX and (B) Huh7-PINX1 OX cells using an anti-FLAG antibody and determining the PINX1 occupancy at the seven regions on the ATP7B promoter, results were calculated by the %input method.

ChIP-qPCR and luciferase-reporter assays resulted in a significant enrichment in the ATP7B promoter at the -1000 bp region in HEK293T-PINX1 OX cells. Both experiments confirm the presence of PINX1 at the targeted region on the ATP7B promoter and its effect on the enhancement of ATP7B gene activity.

3.6.3 Alterations in PINX1 expression affect the cells' response to cisplatin.

The effect of PINX1 overexpression and PINX1 knock-out on the colony-forming ability of HEK293T and Huh7 cells were analyzed with colony formation assay. HEK293T cells were treated with 0.5 uM cisplatin for 72 hours and the colony numbers after the drug treatment were quantified. Changes in PINX1 expression did not affect the colony formation capabilities of HEK293T cells, as seen in Figure *3.26A*.

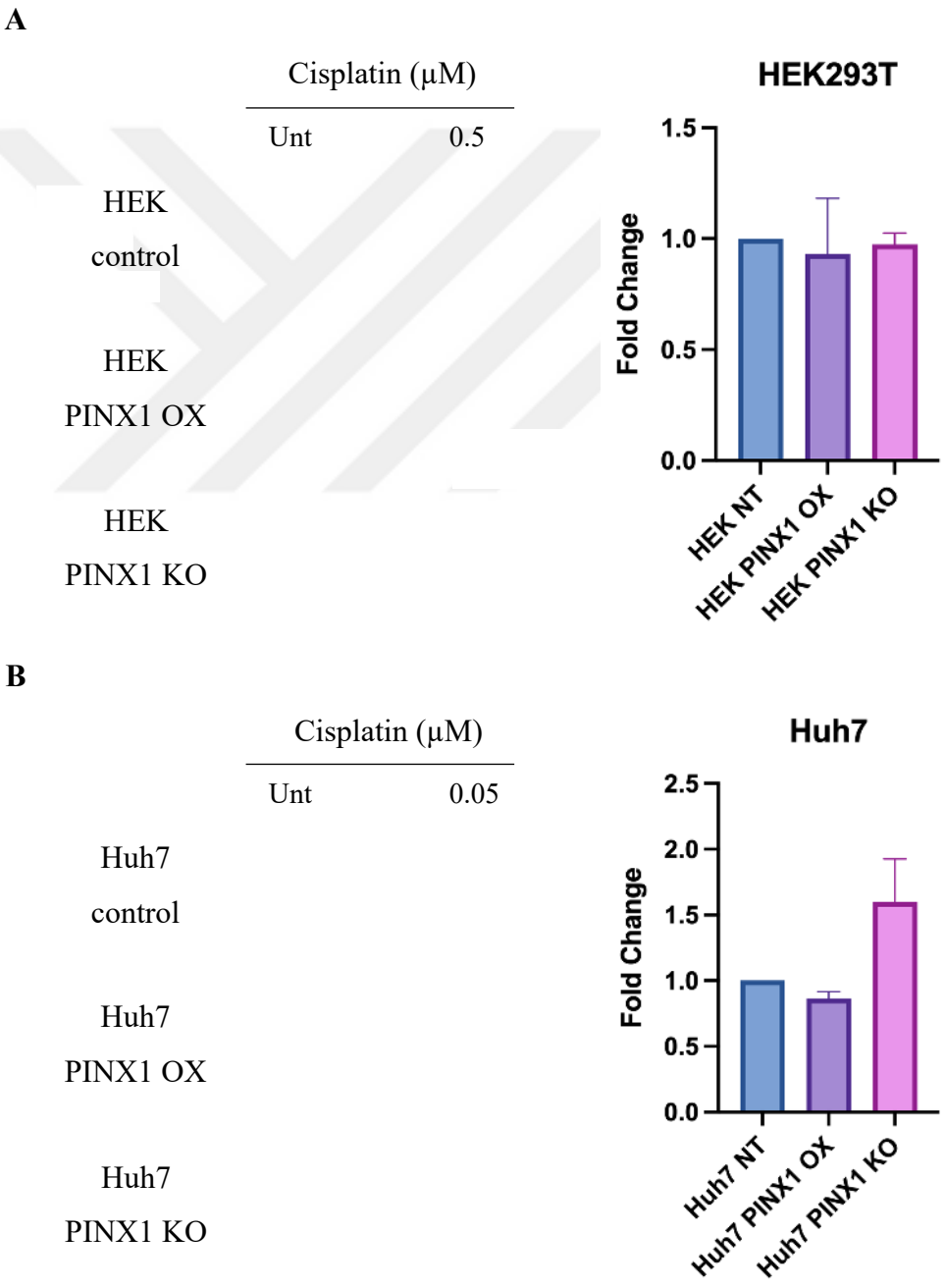

Figure 3.26: Colony formation assay for cisplatin-treated PINX1 OX and PINX1 KO cells

Clonogenic images and their quantifications for cisplatin-treated (A) HEK-PINX1 OX and HEK-PINX1 KO, (B) Huh7-PINX1 OX and Huh7-PINX1 KO cells.

After the cisplatin treatment, the number of colonies formed did not change for Huh7-PINX1 OX cells. However, in Huh7-PINX1 OX cells, an increase in colony formation ability was observed. This alteration could result from an increase in the copper pump activity in the cell, which is a reverse effect compared to the qPCR analysis (Figure *3.26*).

We speculated that an increase in PINX1 overexpression might influence the response of cells to cisplatin treatment, potentially impacting ATP7B expression levels as well. To test this hypothesis, HEK293T and HEK-PINX1 OX cells were treated with increasing doses of cisplatin and the cell viability was measured with sulforhodamine B (SRB) viability assay. SRB assay measures the total protein content of the cell population and could yield a result for the cell viability after treatment of the cells with a chemical (Vichai & Kirtikara, 2006). Compared to the nontreated HEK293T cells, PINX1 overexpression resulted in resistance against the cisplatin treatment. On the other hand, when HEK-PINX1 KO cells were treated with cisplatin, there was not any change in the cell viability compared to the nontreated control cells (Figure *3.27A*).

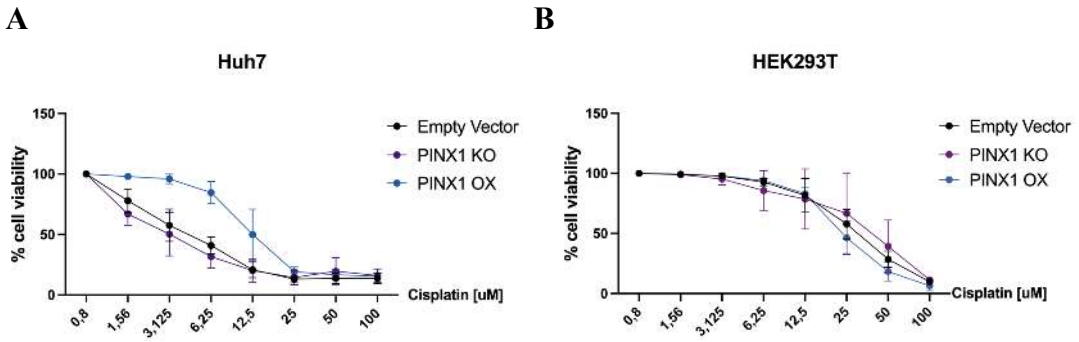

Figure 3.27: SRB viability assay for cisplatin-treated HEK293T-POU3F2 OX/POU3F2 KO and Huh7-POU3F2 OX/POU3F2 KO cells.

Both PINX1 OX and PINX1 KO cell lines were treated with cisplatin and the cell viability was measured with SRB assay.

Also, in hepatocellular carcinoma cell lines, the overexpression of PINX1 slightly increased the cell viability against cisplatin. However, the reverse effect was not observed in Huh7-PINX1 KO cells, the cell viability did not change compared to the control cell line (Figure *3.27B*). PINX1 overexpression thus increases ATP7B expression which in turn could increase the efflux of cisplatin from the cells and block the drug's activity and result in an increase in the cell viability.

3.6.4 Gene expression correlation between ATP7B and PINX1

As one of the enriched proteins in the ATP7B promoter region, *PINX1* (Pin2/TRF1-Interacting Protein) was selected and further studied as a potential regulator of ATP7B activity. First, the correlation between PINX1 and ATP7B in cancers was investigated. In glioblastoma, PINX1 expression is positively correlated with ATP7B expression (Figure *3.28A*). Analysis was conducted using RNA-seq data from the TIMER2.0 public database (T. Li et al., 2020). Also, in thyroid carcinoma (THCA) and liver hepatocellular carcinoma (LIHC), PINX1 expression was found to be positively correlated with ATP7B expression (Figure *3.28B, C*).

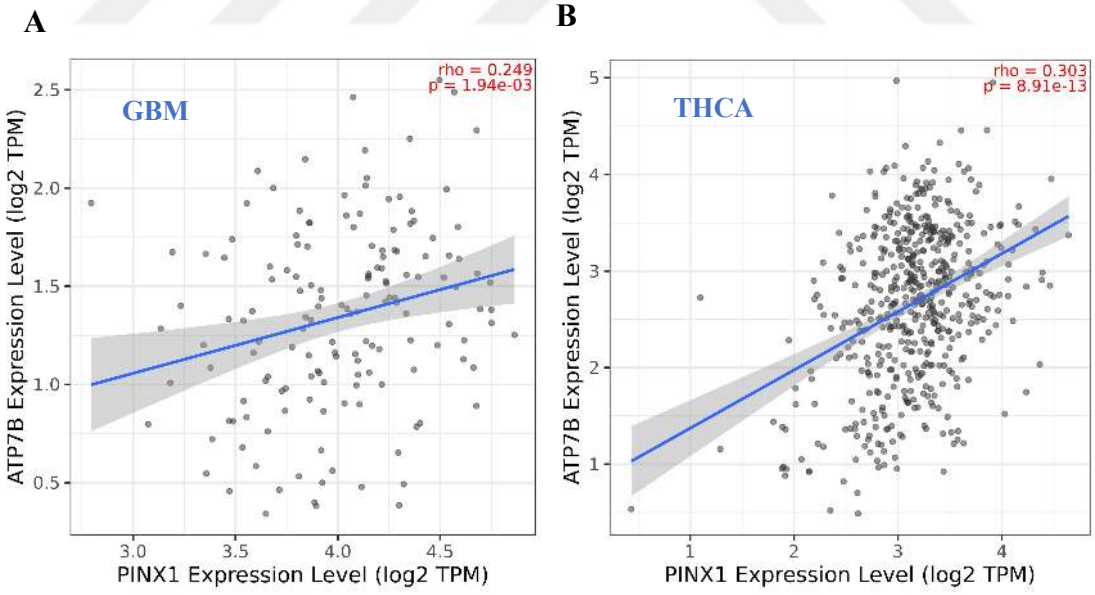

C

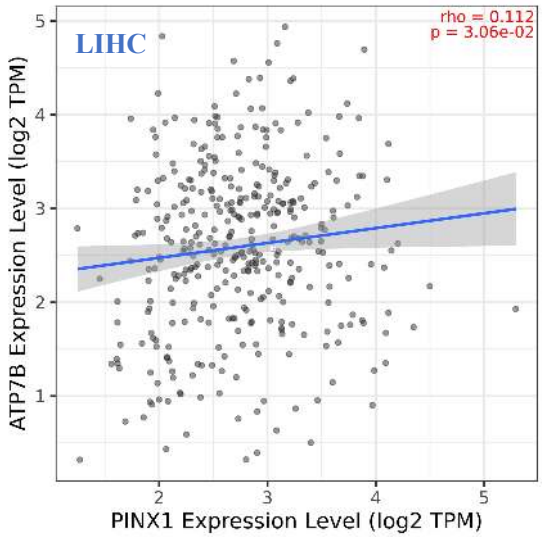

Figure 3.28: Correlation between ATP7B and PINX1 expression in cancer types.

Correlation between ATP7B and PINX1 expression was analyzed in (A) GBM, (B) THCA, and (C) LIHC using TIMER2.0 software. The data was obtained from 153 GBM, 509 THCA, and 371 LIHC samples.

3.7 HDAC inhibitor activity increases ATP7B expression

3.7.1 The activity of BET inhibitors and HDAC inhibitors on ATP7B expression

Epigenetic drug library screening performed by Ph.D. Student Barıs Sergi revealed that many drugs which affect histone modifications and epigenetic marks are also involved in the change of ATP7B expression. Some of these drugs were selected and their effect on ATP7B expression in HEK293T cells was investigated by qPCR analysis (Figure *3.29*).

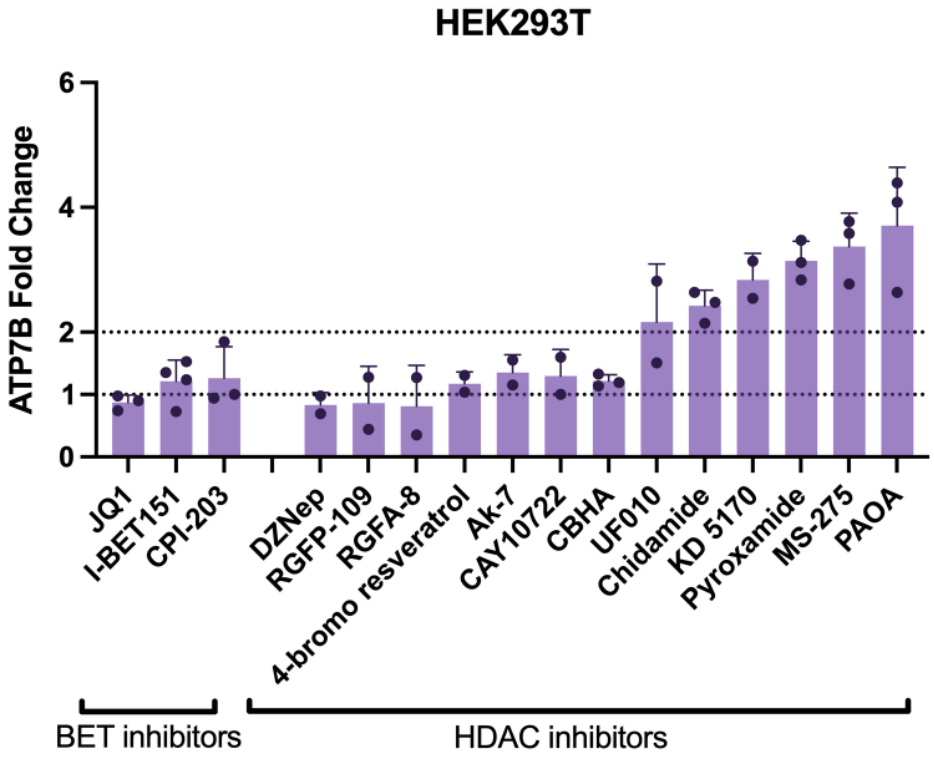

Figure 3.29: The effect of epidrugs on ATP7B expression in HEK293T cells.

BET inhibitors could disrupt the interaction of bromodomains and acetylation marks, and block the recruitment of transcription factors (Pérez-Salvia & Esteller, 2017). Thus, their effect on gene expression got us to contemplate their potential impact on ATP7B expression. The three BET inhibitors (JQ1, I-BET151, CPI-203) did not change the ATP7B expression in HEK293T cells whereas several HDAC inhibitors (Chidamide, KD5170, Pyroxamide, MS-275, PAOA) increased the ATP7B expression more than twofold. Further experiments were performed with these selected HDAC inhibitor drugs.

HDACs remove the acetyl group from histones and are mostly connected with reduced gene expression. As expected, inhibitors of HDAC activity make DNA more accessible to several proteins by hindering deacetylase activity and could increase gene expression at target regions (Z. Wang et al., 2009). The drugs found to increase ATP7B expression in HEK293T cells were also given to prostate and liver cancer cell lines (Figure *3.30*).

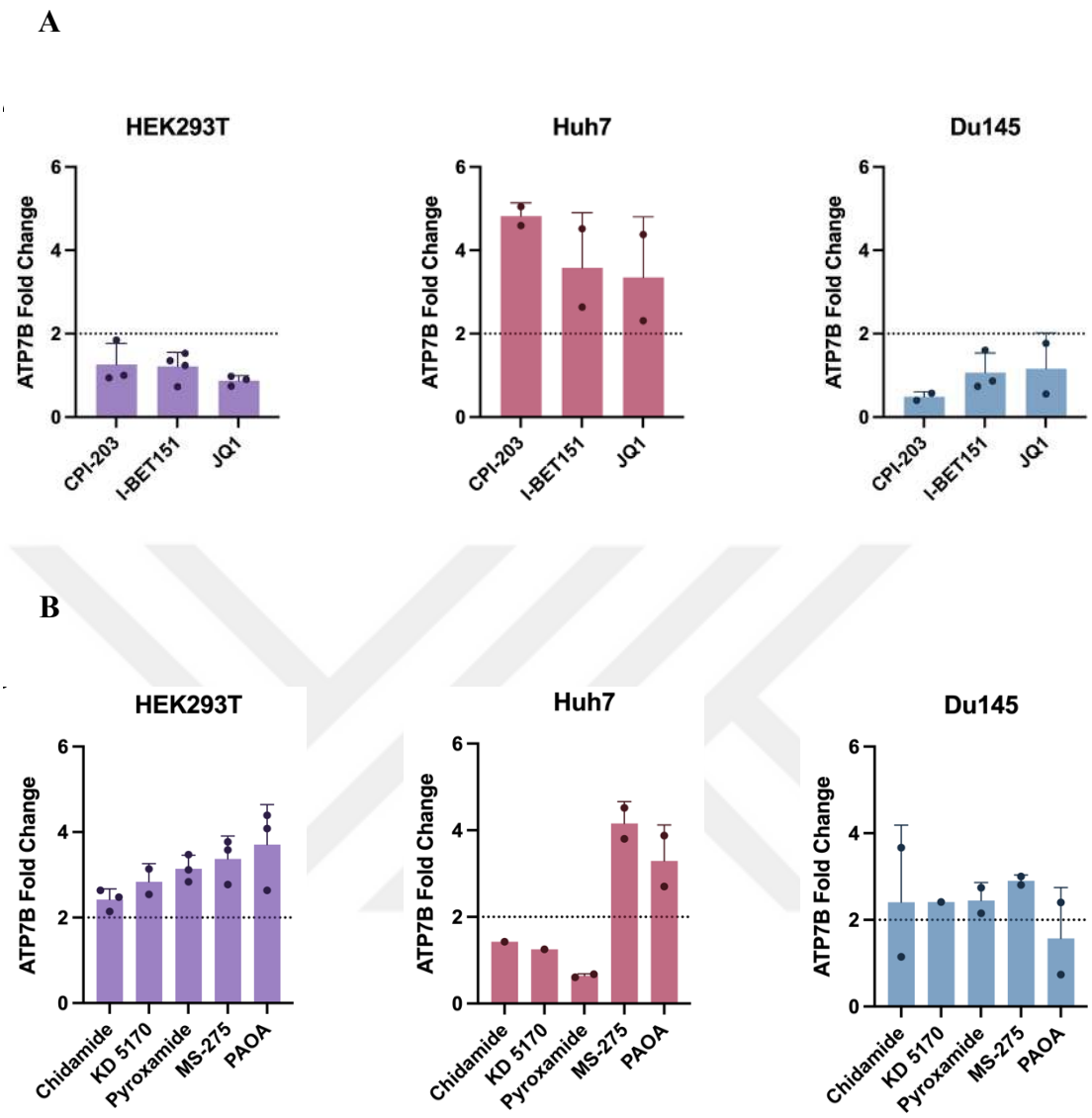

Figure 3.30: Effect of drugs on ATP7B expression in different cell lines.

(A) HEK293T, Huh7, and Du145 cells were treated with BET inhibitors CPI-203, I-BET-151, JQ1, and their effects on ATP7B expression were analyzed with qPCR assay. (B) HEK293T, Huh7, and Du145 cells were treated with HDAC inhibitors Chidamide, KD5170, Pyroxamide, MS-275, PAOA, and their effects on ATP7B expression were analyzed with qPCR assay.

BET inhibitors that did not change ATP7B expression in HEK293T cells did also not change the expression in Du145 cells. In the hepatocellular carcinoma cell line, however, these three drugs increased the ATP7B expression (Figure *3.30A*). Hepatocellular carcinoma and prostate cancer lines were treated with HDAC inhibitors which increased ATP7B expression twofold in HEK293T cells. Chidamide, KD5170, Pyroxamide, and PAOA did not result in a significant change in ATP7B expression in these cancer cell

lines, although MS-275 increased ATP7B expression approximately fourfold in Huh7 cells and twofold in Du145 cells (Figure *3.30B*).

The HDAC inhibitors that increase the ATP7B expression were also given to HEK-MTF1 KO cells. HEK293T-MTF1 KO cells were analyzed with qPCR to verify the knock-out of MTF1 expression and it was shown that MTF1 fold change decreased significantly compared to the control sample, confirming the knock-out generation (Figure *3.31A*). The same cells were also analyzed with qPCR assay, and it was found that upon the generation of the MTF1-KO model, ATP7B expression also decreased significantly (Figure *3.31B*). As a transcriptional regulator of ATP7B, deficient MTF1 expression in the cells resulted in a decline in ATP7B expression.

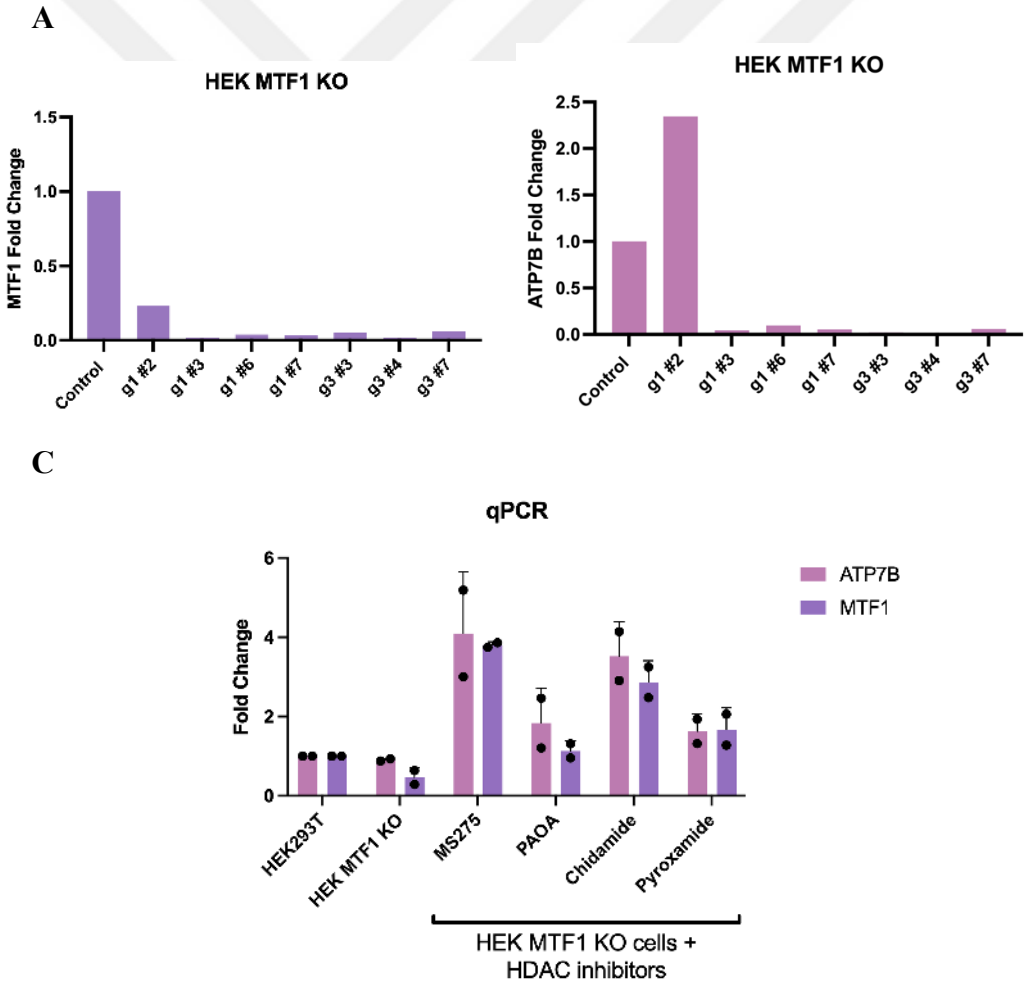

Figure 3.31: Generation of HEK293T-MTF1 KO cells.

(A) qPCR analysis of HEK293T-MTF1 KO cells to confirm the knock-out of the gene expression. (B) The same colonies were also analyzed with qPCR to examine the change in ATP7B expression. Target gene expression was normalized to GAPDH expression, and relative expression was calculated with the $2^{(-\Delta\Delta CT)}$ method. (C) HEK-MTF1 KO cells were treated with HDAC inhibitors MS-275, PAOA, Chidamide, and Pyroxamide, and their effects on ATP7B expression were analyzed with qPCR assay.

The treatment of MS275, PAOA, Chidamide, and Pyroxamide to the HEK-MTF1 KO cells did not only revert the expression of ATP7B and MTF1 to normal levels but also, they were increased more than twofold (Figure *3.31C)*. To investigate the reverse effect, a stable cell line of MTF1 overexpressing HEK293T cells was generated, and the overexpression was confirmed by qPCR assay (Figure *3.32*). The copper treatment further increased the MTF1 overexpression indicating the copper induces the MTF1 activity in the cells to further activate the expression of genes associated with copper homeostasis.

A

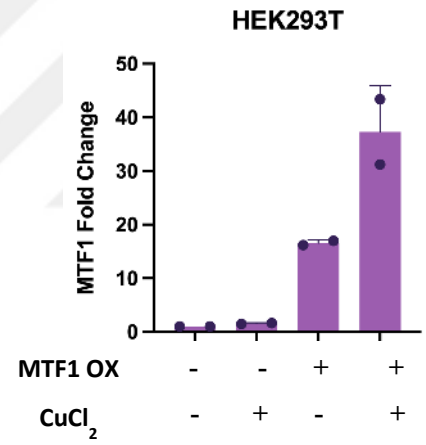

B

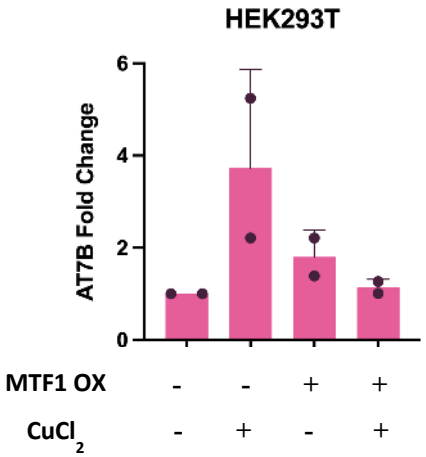

C

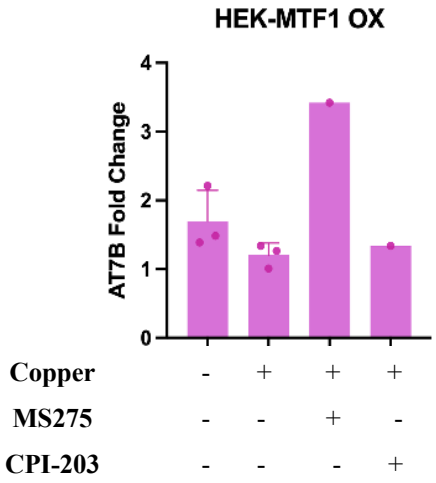

Figure 3.32: HDAC inhibitors increase MTF1 and ATP7B activity.

(A) HEK-MTF1 OX cells were generated and the overexpression of MTF1 expression was verified with qPCR. (B) HEK-MTF1 OX cells were treated with copper and the change in ATP7B expression was quantified by qPCR. (C) HEK-MTF1 OX cells were treated with HDAC inhibitor MS-275, and bromodomain inhibitor CPI-203, and their effects on ATP7B expression were analyzed with qPCR assay.

HEK-MTF1 OX cells were then treated with MS275 and ATP7B expression increased significantly compared to the copper-treated cells (Figure *3.32C*). When the same cells were treated with bromodomain inhibitor CPI-203 however ATP7B expression did not change compared to the non-treated HEK-MTF1 OX cells (Figure *3.32C*). The HDAC inhibition results in a more open chromatin state and leads to an increase in not only ATP7B activity but also the transcription factor MTF1 which plays a vital role in maintaining copper balance in the cells.

3.7.2 The increase in ATP7B activity by HDAC inhibitors does not depend on oxidative stress generated by the drugs.

HDACs have been found to regulate oxidative stress levels in the cell through several pathways such as inhibition of SLC7A11 (L. Wang et al., 2018). We wanted to determine whether the change of ATP7B expression upon HDAC inhibitor treatment is a result of increased ROS levels in the cell. For this purpose, HEK293T cells were treated with a ROS scavenger called NAC which can enhance the glutathione levels in the cell to reduce

oxidative stress (Halasi et al., 2013). According to the viability assays, 5 mM NAC was chosen as an optimal dose for further experiments (Figure *3.33A*).

The cells were treated with selected HDAC inhibitor drugs and with NAC, and the ROS-positive cells were sorted with Muse Cell Analyzer. The drug cisplatin and H_2O_2 treatment increased the ROS-positive cells in the population however it decreased upon NAC treatment (Figure *3.33B*).

A

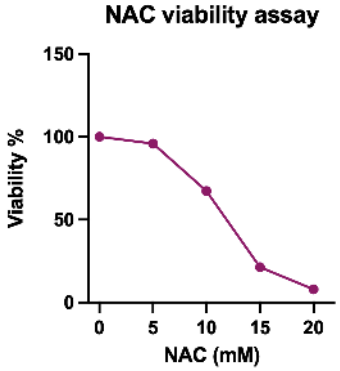

B

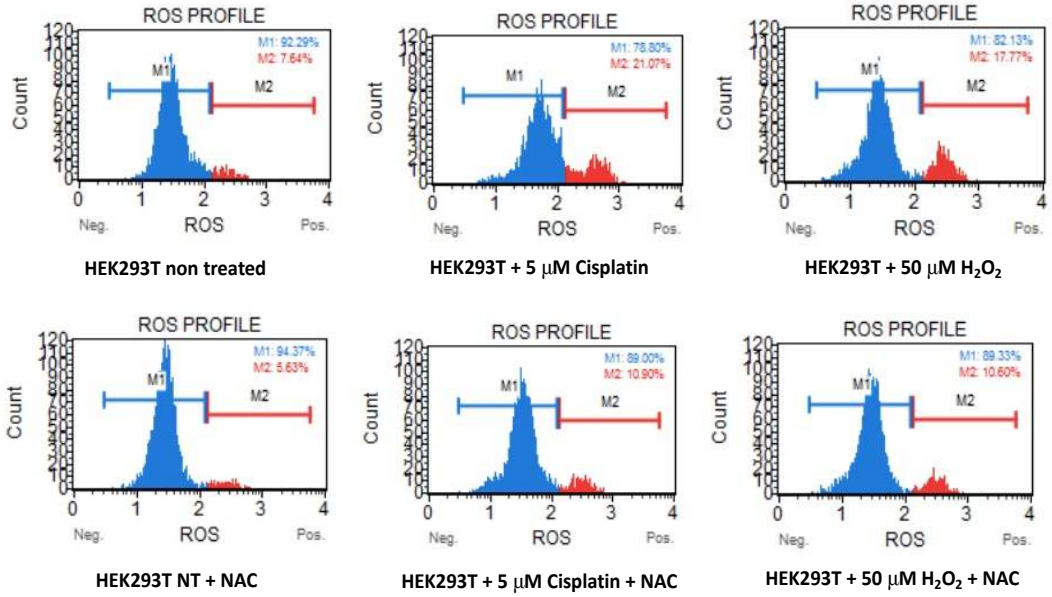

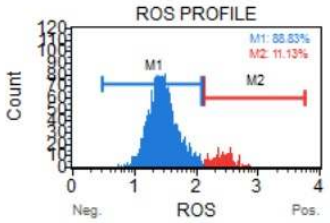

HEK293T + MS275

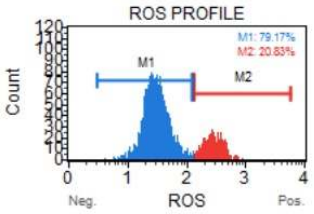

HEK293T + Chidamide

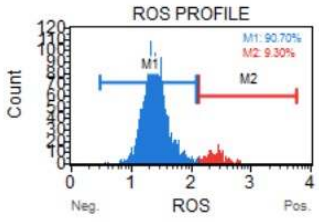

HEK293T + MS275 + NAC

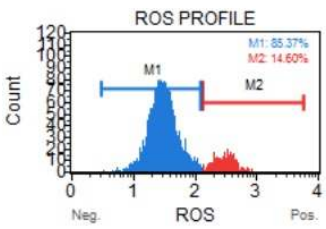

HEK293T + Chidamide +NAC

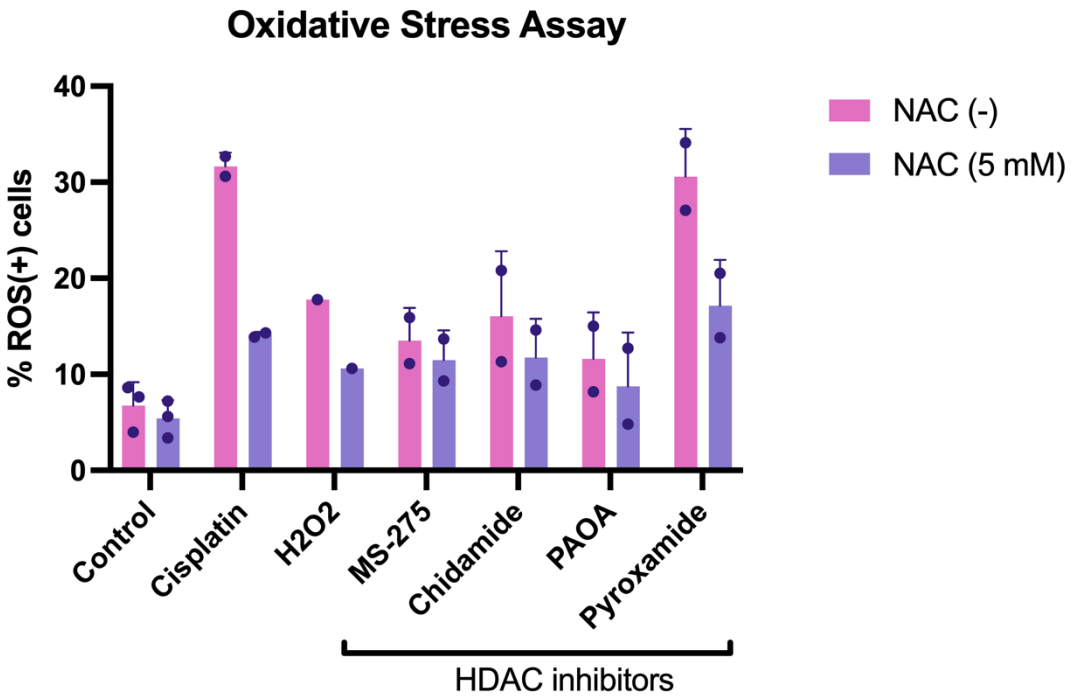

C

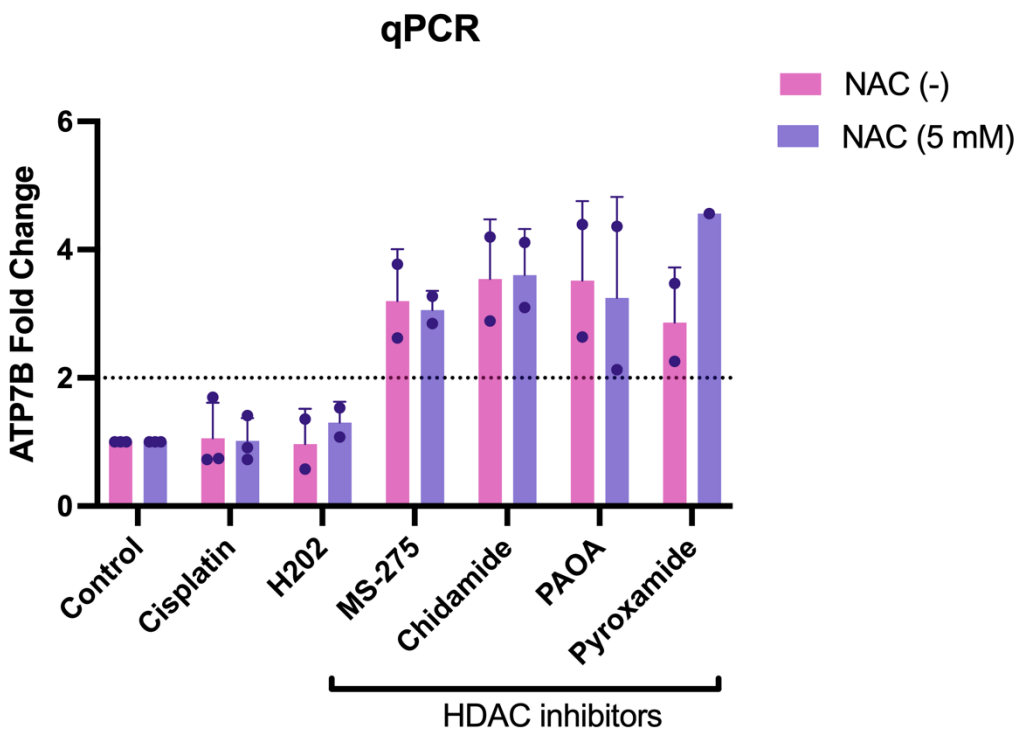

Figure 3.33: ATP7B expression does not increase due to the oxidative stress resulting from drug treatment.

(A) SRB viability assay was performed, and the optimal dose of NAC was selected as 5 mM. (B) HEK293T cells were treated with cisplatin and H_2O_2, which are both to known to induce oxidative stress, NAC, a ROS scavenger, and selected HDAC inhibitors. The percent of ROS-positive cells in the population was calculated with Muse Cell Analyzer. (C) qPCR analysis to investigate the change in ATP7B expression in drug-treated cells, indicating the increase in ATP7B expression is not connected with the oxidative stress induced by the drug treatment.

The same cells were lysed and their ATP7B expression was analyzed with qPCR. The treatment of the cells with the selected drugs increases the ATP7B expression, as depicted in Figure *3.33*. Not surprisingly, upon NAC treatment and the subsequent decrease in ROS levels, the expression of the ATP7B gene did not diminish. Thus, the increase in ATP7B expression resulting from HDAC inhibitor treatment is not dependent on ROS activity.

Chapter 4:
DISCUSSION

Targeting gene regulation holds significant advantages in various areas, ranging from gaining insights into molecular and genetic changes driving disease progression to developing novel therapies for those diseases. The activity of the ATP7B gene is intricately controlled within cells through precise regulations. This control mechanism can be likened to a delicate weighing scale, and any deviation from the balance can lead to physiological disorders, either due to metal accumulation or the expulsion of chemical drugs from the cells.

A deficiency in ATP7B activity results in the harmful accumulation of excess copper, which becomes toxic to the cells. Conversely, overexpression of this gene in cancers leads to the expulsion of platinum-based drugs from the cells before they can target and attack the intended sites. Understanding the transcriptional and epigenetic regulation of ATP7B could shed light on how dysregulations in gene activity contribute to disease progression.

4.1 Identifying PINX1 as a regulator of ATP7B

In this thesis, the Genomic Locus Proteomics approach was used to explore the regulators of ATP7B gene activity. The ATP7B promoter region was analyzed using public databases and several transcription-factor binding sites were discovered (Figure *3.4*). gRNAs spanning the region from +1 (TSS) to the -3000 bp region were designed and cloned into the HEK293T-CASPEX cells. Mass spectrometry analysis and the subsequently performed ChIP-qPCR assays demonstrated that PINX1 binds to the ATP7B promoter region both in HEK293T and Huh7 cells. The direct binding of PINX1 to this region proposes a mechanism of gene regulation between the two genes. Not surprisingly, *in-vitro* experiments that asses both the RNA expression and protein levels displayed that PINX1 affect the ATP7B activity.

Telomeres are repeated sequences of DNA located on the end of chromosomes which get shortened after each cell division cycle. Eventually, this shortage leads to a critical loss of genomic locus and the cell enters senescence (Zhou & Lu, 2001). To avoid this

destiny, the telomerase enzyme adds telomere repeats to the ends to protect the telomere length however usually most somatic cells do not have active telomerase activity. Telomerase activity is maintained by the catalytic unit of telomerase reverse transcriptase (TERT) and its RNA component (Jafri, Ansari, Alqahtani, & Shay, 2016). Several telomere-binding proteins such as TRF1 and TRF2 mainly function in the preservation of chromosome ends and the telomere length (H. L. Li et al., 2016). Telomerase activity is regulated in the cells by various controlling mechanisms however transformed cells and usually in cancer cells, telomerase activity is restored providing the cells an escape from senescence and they could continue to divide indefinitely (Zhou & Lu, 2001).

PINX1 gene encodes a 45 kDA-protein which affects telomerase activity (Zhou & Lu, 2001). PINX1 protein binds to the human TERT (hTERT) via its TID domain (telomerase inhibitory domain), which is stationed at its C-terminal region. The binding of PINX1 to the catalytic unit of hTERT inhibits its activity, leads to telomere shortening, and eventually gives rise to crisis (Zhou & Lu, 2001). Unsurprisingly, PINX1 expression and/or activity loss was observed in many cancers, such as hepatocellular carcinoma and ovarian cancer. The decrease in expression usually stems from a loss of heterozygosity (LOH) in the genomic locus of the *PINX1* coding region. This specific region was found to host many known tumor suppressor genes and LOH mutations usually occur in these sequences during tumor initiation (H. L. Li et al., 2016) Diminishing PINX1 activity results in chromosomal instability and gives rise to an increase in tumorigenicity. Thus, PINX1 is reputed as a tumor suppressor (H. L. Li et al., 2016)

PINX1 also interacts with microtubules and its function is crucial in the correct separation of chromosomes in the cell cycle process. The decrease in PINX1 activity leads to lagging chromosomes, potentially coupled with the chromosomal instability in tumor cells (Yuan et al., 2009). PINX1 activity was also suppressed in a cohort of non-small cell lung cancer (NSCLC) patients and hypothesized to be used as an indicator for the disease progression (Tian et al., 2017). Reduced PINX1 activity also results in telomerase activation in cervical cancers. A well-studied tumor suppressor p53 was revealed as a transcriptional activator of PINX1 (Wu et al., 2014). In gastric cancers, increased *PINX1* expression reduces c-Myc expression, an oncogenic transcription factor while inhibiting the protein's binding to its target *hTERT*. This increased activity of PINX1 slows cell growth by decreasing telomerase activity (H. bin Wang et al., 2010).

PINX1 expression is usually diminished as a result of loss of heterozygosity mutations (LOH) in many cancers which led to the classification of the gene as a potential tumor suppressor (Zhou et al., 2011). PINX1 expression was found to be lower in ovarian cancer tissues compared to the normal tissue (Cai et al., 2010). In another study, the single nucleotide variants (SNPs) in the PINX1 gene in ovarian cancers were associated with poor response to the platinum-based cancer therapies (Sun, Tao, Huang, Wu, & Gu, 2017).

In several cancer types, PINX1 overexpression affects the cell's destiny against chemotherapeutic drugs. Response to cisplatin and paclitaxel drugs is weakened by increased levels of PINX1 activity in cervical carcinomas, whereas reducing the protein's activity sensitizes the cells to paclitaxel (Tian et al., 2014). Our research also drew a connection between PINX1 activity and cisplatin cytotoxicity in cancer cells. It was shown that in the hepatocellular carcinoma cell line, PINX1 overexpression protects the cells against the cisplatin treatment, and they resist the higher doses of the drug compared to the normal cells (Figure *3.27*).

The reduced levels of PINX1 in cancers result in chromosomal instability in the cells, and PINX1 is referred to as a putative tumor suppressor (H. L. Li et al., 2016). However, PINX1 was not identified as a transcriptional regulator, thus its role in gene regulation should be investigated in detail. The binding of PINX1 to the ATP7B promoter was demonstrated with ChIP-qPCR assay. PINX1 levels are enriched in the first two regions which were targeted by the gRNAs spanning the 1000 bp on the ATP7B promoter (Figure *3.25*). The protein resides in the promoter region in both HEK293T and Huh7 cells.

PINX1 binds to hTERT and hinders its activity and gets localized to telomeres with its associate proteins (Zhou & Lu, 2001). PINX1 also has an RNA binding domain and similarly, yeast PINX1 is associated with RNA processing (Yoo, Oh, & Park, 2009). ChIP-qPCR analysis demonstrated the presence of PINX1 at the ATP7B promoter (Figure *3.25*). PINX1 could recruit other proteins to the ATP7B promoter which could work as a team to regulate the gene's activity. Transcription factors have been shown to contain RNA-binding domains and occupy chromatin regions (Oksuz et al., 2023). Further, the role of PINX1 in transcriptional regulation could be explored by analyzing these interacting complexes which could change the chromatin accessibility in the target region. These altered chromatin marks could be defined with experimental procedures such as ATAC-seq and the role of this team of proteins in the transcription process could

be illuminated (Ji et al., 2018). Also, performing ChIP-seq analysis could assist the illustration of the binding sites of PINX1 and its interacting proteins on DNA, preferably on the promoter sequences (Park, 2009). Identifying the binding partners of PINX1 and their relationships with ATP7B expression could be the next step of this project to illuminate the significance of gene regulation pathways in disease progression.

4.2 Potential Regulators of ATP7B

Mass spectrometry analysis resulted in many target proteins which could be potential transcriptional regulators of the ATP7B gene. The relationship between the target genes and ATP7B activity was studied in both HEK293T and Huh7 cells to investigate the effect of different cell backgrounds on the regulation process. Both cell lines have high endogenous ATP7B expression (Figure *3.1*). The modifications in the transcription factors' activity had different outcomes in the cancer cell line compared to the normal cell line. For instance, MEN1 OX resulted in resistance to cisplatin treatment in HEK293T cells however Huh7-MEN1 OX cells were more sensitive to the cisplatin treatment (Figure *3.12*). Cancer progression may alter the transcriptional regulation of certain genes, and in this case, additional factors may be involved in the ATP7B activity in cancer cell lines. Investigating the regulation mechanisms of a gene both in normal and cancer cell lines is beneficial to examine the differences in the transcription regulation process. The next step in this research could be developing a similar experimental procedure to label the proteins on the ATP7B promoter in different cancer cell lines and study the target proteins' influence on the drug resistance in these cells.

One of the target proteins was MEN1, which is a tumor suppressor and the loss of MEN1 activity leads to tumor formation (Zablewska et al., 2003). MEN1 was found to interact with other proteins to inhibit their activity. It could also recruit HDACs and other additional proteins to the telomere sequences and could be involved in the transcriptional silencing of the genes (Suphapeetiporn, Greally, Walpita, Ashley, & Bale, 2002). The presence of MEN1 at the ATP7B promoter suggests that MEN1 could also regulate the ATP7B activity. MEN1 overexpression did not result in a significant change in ATP7B expression (Figure *3.12*) and it did not alter the cell viability against cisplatin treatment (Figure *3.14*). Although MEN1 could not affect ATP7B activity in a transcriptional manner, it could recruit other additional factors to the promoter area.

POU3F2 is a transcription factor that was also enriched in the ATP7B promoter region however its overexpression did not significantly change the ATP7B activity (Figure *3.15*) or alter the cell viability after the drug treatment (Figure *3.20*). In colon cancers, through p53 activity and ROS generation, POU3F2 is regulated, and it regulates tNOX expression to determine the cell survival against oxaliplatin treatment (H. Y. Chen et al., 2018). Although the viability assays did not result in a change in HEK293T-POU3F2 OX cells against cisplatin treatment, POU3F2 may recruit and activate additional factors other than ATP7B in cancer cells to sensitize the cells to the platinum-based drug.

PRDM16 is one of the transcription factors identified after the mass spectrometry analysis. Due to its classification as a tumor suppressor and its role in metastasis as a transcriptional regulator of certain proteins (Fei et al., 2019), PRDM16 was also targeted to investigate its effect on ATP7B activity. Although HEK293T-PRDM16 OX cells resisted the cisplatin compared to normal cells (Figure *3.20*), the luciferase reporter assay did not confirm the direct effect of PRDM16 OX on the ATP7B expression (Figure *3.21*). Thus, PRDM16 might not be a regulator of ATP7B in a transcriptional manner, rather it could interact with other factors to control the gene expression.

4.3 Epigenetic Alterations Control ATP7B Expression

Epigenetic control mechanisms could also be modified in different cells such as bromodomain inhibition decreased the ATP7B activity in HEK293T cells however the same treatment increased the activity in Huh7 cells (Figure *3.30*). The same difference was observed upon HDAC activity inhibition; the treatment with the pyroxamide drug increased the fold change of ATP7B in normal cell lines but decreased the fold change of ATP7B in the cancer cell line. Moreover, the increase in gene expression was a direct result of epigenetic changes rather than a result of increased oxidative stress in the cell (Figure *3.33*). Investigating the alterations in the regulation mechanisms occurring in the cells during cancer development is crucial and may shed light on the understanding of the resistance phenotypes of cancer cells against certain drugs.

Chapter 5:
CONCLUSIONS

ATP7B plays a crucial role in maintaining copper balance in the body and can influence cell response to cancer treatments. Therefore, investigating the regulatory mechanisms controlling ATP7B expression could offer valuable insights into developing innovative cancer therapies.

In this research project, PINX1 emerged as a potential regulator of ATP7B gene expression. The upregulation of PINX1 led to an increase in ATP7B expression and subsequently resulted in resistance to cisplatin treatment. By targeting both epigenetic and transcriptional regulators of the ATP7B gene, it is possible to have significant translational effects in overcoming drug resistance in cancer therapies and developing novel treatment approaches for Wilson's disease.

BIBLIOGRAPHY

Ala, A., Walker, A. P., Ashkan, K., Dooley, J. S., & Schilsky, M. L. (2007). Wilson's disease. *Lancet*, *369*(9559), 397–408. https://doi.org/10.1016/S0140-6736(07)60196-2

Aubrey, B. J., Strasser, A., & Kelly, G. L. (2016). Tumor-Suppressor Functions of the TP53 Pathway. *Cold Spring Harbor Perspectives in Medicine*, *6*(5). https://doi.org/10.1101/CSHPERSPECT.A026062

Cai, M. Y., Zhang, B., He, W. P., Yang, G. F., Rao, H. L., Rao, Z. Y., … Xie, D. (2010). Decreased expression of PinX1 protein is correlated with tumor development and is a new independent poor prognostic factor in ovarian carcinoma. *Cancer Science*, *101*(6), 1543–1549. https://doi.org/10.1111/J.1349-7006.2010.01560.X

Casamassimi, A., & Ciccodicola, A. (2019). Transcriptional Regulation: Molecules, Involved Mechanisms, and Misregulation. *International Journal of Molecular Sciences*, *20*(6). https://doi.org/10.3390/IJMS20061281

Chen, H. I., Jagadeesh, K. A., Birgmeier, J., Wenger, A. M., Guturu, H., Schelley, S., … Bejerano, G. (2018). An MTF1 binding site disrupted by a homozygous variant in the promoter of ATP7B likely causes Wilson Disease. *European Journal of Human Genetics 2018 26:12*, *26*(12), 1810–1818. https://doi.org/10.1038/s41431-018-0221-4

Chen, H. Y., Islam, A., Yuan, T. M., Chen, S. W., Liu, P. F., & Chueh, P. J. (2018). Regulation of tNOX expression through the ROS-p53-POU3F2 axis contributes to cellular responses against oxaliplatin in human colon cancer cells. *Journal of Experimental & Clinical Cancer Research : CR*, *37*(1). https://doi.org/10.1186/S13046-018-0837-9

Cheng, Z., Garvin, D., Paguio, A., Stecha, P., Wood, K., & Fan, F. (2010). Luciferase Reporter Assay System for Deciphering GPCR Pathways. *Current Chemical Genomics*, *4*, 84. https://doi.org/10.2174/1875397301004010084

Chivers, C. E., Koner, A. L., Lowe, E. D., & Howarth, M. (2011). How the biotin–streptavidin interaction was made even stronger: investigation via crystallography and a chimaeric tetramer. *Biochemical Journal*, *435*(Pt 1), 55. https://doi.org/10.1042/BJ20101593

Chueh, A. C., Tse, J. W. T., Tögel, L., & Mariadason, J. M. (2015). Mechanisms of Histone Deacetylase Inhibitor-Regulated Gene Expression in Cancer Cells. *Antioxidants & Redox Signaling*, *23*(1), 66. https://doi.org/10.1089/ARS.2014.5863

Cochran, A. G., Conery, A. R., & Sims, R. J. (2019). Bromodomains: a new target class for drug development. *Nature Reviews Drug Discovery 2019 18:8*, *18*(8), 609–628. https://doi.org/10.1038/s41573-019-0030-7

Cohen, I., Poręba, E., Kamieniarz, K., & Schneider, R. (2011). Histone Modifiers in Cancer: Friends or Foes? *Genes & Cancer*, *2*(6), 631. https://doi.org/10.1177/1947601911417176

Cox, D. B. T., Platt, R. J., & Zhang, F. (2015). Therapeutic genome editing: prospects and challenges. *Nature Medicine 2015 21:2*, *21*(2), 121–131. https://doi.org/10.1038/nm.3793

Cox, J., & Mann, M. (2008). MaxQuant enables high peptide identification rates, individualized p.p.b.-range mass accuracies and proteome-wide protein quantification. *Nature Biotechnology 2008 26:12*, *26*(12), 1367–1372. https://doi.org/10.1038/nbt.1511

Culotta, V. C., & Hamer, D. H. (1989). Fine mapping of a mouse metallothionein gene metal response element. *Molecular and Cellular Biology*, *9*(3), 1376–1380. https://doi.org/10.1128/MCB.9.3.1376-1380.1989

Dasari, S., & Bernard Tchounwou, P. (2014). Cisplatin in cancer therapy: molecular mechanisms of action. *European Journal of Pharmacology*, *740*, 364. https://doi.org/10.1016/J.EJPHAR.2014.07.025

Doench, J. G., Fusi, N., Sullender, M., Hegde, M., Vaimberg, E. W., Donovan, K. F., …

Root, D. E. (2016). Optimized sgRNA design to maximize activity and minimize off-target effects of CRISPR-Cas9. *Nature Biotechnology*, *34*(2), 184. https://doi.org/10.1038/NBT.3437

Doudna, J. A. (2020). The promise and challenge of therapeutic genome editing. *Nature 2020 578:7794*, *578*(7794), 229–236. https://doi.org/10.1038/s41586-020-1978-5

Fang, M., Xia, F., Mahalingam, M., Virbasius, C.-M., Wajapeyee, N., & Green, M. R. (2013). MEN1 Is a Melanoma Tumor Suppressor That Preserves Genomic Integrity by Stimulating Transcription of Genes That Promote Homologous Recombination-Directed DNA Repair. *Molecular and Cellular Biology*, *33*(13), 2635. https://doi.org/10.1128/MCB.00167-13

Fei, L. R., Huang, W. J., Wang, Y., Lei, L., Li, Z. H., Zheng, Y. W., … Xu, H. T. (2019). PRDM16 functions as a suppressor of lung adenocarcinoma metastasis. *Journal of Experimental and Clinical Cancer Research*, *38*(1). https://doi.org/10.1186/s13046-019-1042-1

Fujie, T., Hara, T., & Kaji, T. (2016). Toxicology of organic-inorganic hybrid molecules: bio-organometallics and its toxicology. *The Journal of Toxicological Sciences*, *41*(Special), SP81–SP88. https://doi.org/10.2131/JTS.41.SP81

Fujisawa, C., Kodama, H., Sato, Y., Mimaki, M., Yagi, M., Awano, H., … Akasaka, Y. (2022). Early clinical signs and treatment of Menkes disease. *Molecular Genetics and Metabolism Reports*, *31*, 100849. https://doi.org/10.1016/J.YMGMR.2022.100849

Gallinari, P., Di Marco, S., Jones, P., Pallaoro, M., & Steinkühler, C. (2007). HDACs, histone deacetylation and gene transcription: from molecular biology to cancer therapeutics. *Cell Research 2007 17:3*, *17*(3), 195–211. https://doi.org/10.1038/sj.cr.7310149

Gao, J., Brackley, S., & Mann, J. P. (2018). The global prevalence of Wilson disease from next-generation sequencing data. *Genetics in Medicine 2018 21:5*, *21*(5), 1155–1163. https://doi.org/10.1038/s41436-018-0309-9

Gatto, L., Breckels, L. M., Naake, T., & Gibb, S. (2015). Visualization of proteomics data using R and Bioconductor. *Proteomics*, *15*(8), 1375. https://doi.org/10.1002/PMIC.201400392

Greig, J. A., Nordin, J. M. L., Smith, M. K., Ashley, S. N., Draper, C., Zhu, Y., … Wilson, J. M. (2019). A Gene Therapy Approach to Improve Copper Metabolism and Prevent Liver Damage in a Mouse Model of Wilson Disease. *Https://Home.Liebertpub.Com/Humc*, *30*(1), 29–39. https://doi.org/10.1089/HUMC.2018.219

Guschin, D. Y., Waite, A. J., Katibah, G. E., Miller, J. C., Holmes, M. C., & Rebar, E. J. (2010). A rapid and general assay for monitoring endogenous gene modification. *Methods in Molecular Biology (Clifton, N.J.)*, *649*, 247–256. https://doi.org/10.1007/978-1-60761-753-2_15

Halasi, M., Wang, M., Chavan, T. S., Gaponenko, V., Hay, N., & Gartel, A. L. (2013). ROS inhibitor N-acetyl-l-cysteine antagonizes the activity of proteasome inhibitors. *The Biochemical Journal*, *454*(2), 201. https://doi.org/10.1042/BJ20130282

He, X., Treacy, M. N., Simmons, D. M., Ingraham, H. A., Swanson, L. W., & Rosenfeld, M. G. (1989). Expression of a large family of POU-domain regulatory genes in mammalian brain development. *Nature 1989 340:6228*, *340*(6228), 35–42. https://doi.org/10.1038/340035a0

Hess-Stumpp, H., Bracker, T. U., Henderson, D., & Politz, O. (2007). MS-275, a potent orally available inhibitor of histone deacetylases—The development of an anticancer agent. *The International Journal of Biochemistry & Cell Biology*, *39*(7–8), 1388–1405. https://doi.org/10.1016/J.BIOCEL.2007.02.009

Höflich, C., Brieger, A., Zeuzem, S., & Plotz, G. (2021). Investigation of the Wilson gene ATP7B transcriptional start site and the effect of core promoter alterations. *Scientific Reports 2021 11:1*, *11*(1), 1–10. https://doi.org/10.1038/s41598-021-87000-9

Jaenisch, R., & Bird, A. (2003). Epigenetic regulation of gene expression: how the

genome integrates intrinsic and environmental signals. *Nature Genetics 2003 33:3*, *33*(3), 245–254. https://doi.org/10.1038/ng1089

Jafri, M. A., Ansari, S. A., Alqahtani, M. H., & Shay, J. W. (2016). Roles of telomeres and telomerase in cancer, and advances in telomerase-targeted therapies. *Genome Medicine 2016 8:1*, *8*(1), 1–18. https://doi.org/10.1186/S13073-016-0324-X

Ji, Z., He, L., Rotem, A., Janzer, A., Cheng, C. S., Regev, A., & Struhl, K. (2018). Genome-scale identification of transcription factors that mediate an inflammatory network during breast cellular transformation. *Nature Communications 2018 9:1*, *9*(1), 1–13. https://doi.org/10.1038/s41467-018-04406-2

Kalayda, G. V., Wagner, C. H., Buß, I., Reedijk, J., & Jaehde, U. (2008). Altered localisation of the copper efflux transporters ATP7A and ATP7B associated with cisplatin resistance in human ovarian carcinoma cells. *BMC Cancer*, *8*(1), 1–12. https://doi.org/10.1186/1471-2407-8-175/TABLES/4

Kanafi, M. M., & Tavallaei, M. (2022). Overview of advances in CRISPR/deadCas9 technology and its applications in human diseases. *Gene*, *830*, 146518. https://doi.org/10.1016/J.GENE.2022.146518

La Fontaine, S., & Mercer, J. F. B. (2007). Trafficking of the copper-ATPases, ATP7A and ATP7B: Role in copper homeostasis. *Archives of Biochemistry and Biophysics*, *463*(2), 149–167. https://doi.org/10.1016/J.ABB.2007.04.021

Lam, S. S., Martell, J. D., Kamer, K. J., Deerinck, T. J., Ellisman, M. H., Mootha, V. K., & Ting, A. Y. (2014). Directed evolution of APEX2 for electron microscopy and proximity labeling. *Nature Methods 2014 12:1*, *12*(1), 51–54. https://doi.org/10.1038/nmeth.3179

Lee, T. I., & Young, R. A. (2013). Transcriptional Regulation and Its Misregulation in Disease. *Cell*, *152*(6), 1237–1251. https://doi.org/10.1016/J.CELL.2013.02.014

Li, H. L., Song, J., Yong, H. M., Hou, P. F., Chen, Y. S., Song, W. B., … Zheng, J. N. (2016). PinX1: structure, regulation and its functions in cancer. *Oncotarget*, *7*(40), 66267. https://doi.org/10.18632/ONCOTARGET.11411

Li, T., Fu, J., Zeng, Z., Cohen, D., Li, J., Chen, Q., … Liu, X. S. (2020). TIMER2.0 for analysis of tumor-infiltrating immune cells. *Nucleic Acids Research*, *48*(W1), W509. https://doi.org/10.1093/NAR/GKAA407

Linz, R., & Lutsenko, S. (2007). Copper-transporting ATPases ATP7A and ATP7B: Cousins, not twins. *Journal of Bioenergetics and Biomembranes*, *39*(5–6), 403–407. https://doi.org/10.1007/S10863-007-9101-2/METRICS

Liu, H. (2022). Pan-cancer profiles of the cuproptosis gene set. *American Journal of Cancer Research*, *12*(8), 4074. Retrieved from /pmc/articles/PMC9442004/

Liu, W. L., Guan, Q., Wen, D., Ma, B., Xu, W. B., Hu, J. Q., … Ji, Q. H. (2021). PRDM16 Inhibits Cell Proliferation and Migration via Epithelial-to-Mesenchymal Transition by Directly Targeting Pyruvate Carboxylase in Papillary Thyroid Cancer. *Frontiers in Cell and Developmental Biology*, *9*. https://doi.org/10.3389/fcell.2021.723777

Loudianos, G., Dessi, V., Lovicu, M., Angius, A., Figus, A., Lilliu, F., … Cao, A. (1999). Molecular Characterization of Wilson Disease in the Sardinian Population-Evidence of a Founder Effect. *HUMAN MUTATION*, *14*, 294–303. https://doi.org/10.1002/(SICI)1098-1004(199910)14:4

Lukanović, D., Herzog, M., Kobal, B., & Černe, K. (2020). The contribution of copper efflux transporters ATP7A and ATP7B to chemoresistance and personalized medicine in ovarian cancer. *Biomedicine & Pharmacotherapy*, *129*, 110401. https://doi.org/10.1016/J.BIOPHA.2020.110401

Mangala, L. S., Zuzel, V., Schmandt, R., Leshane, E. S., Halder, J. B., Armaiz-Pena, G. N., … Sood, A. K. (2009). Therapeutic Targeting of ATP7B in Ovarian Carcinoma. *Clinical Cancer Research : An Official Journal of the American Association for Cancer Research*, *15*(11), 3770. https://doi.org/10.1158/1078-0432.CCR-08-2306

Mashal, R. D., Koontz, J., & Sklar, J. (1995). Detection of mutations by cleavage of DNA heteroduplexes with bacteriophage resolvases. *Nature Genetics*, *9*(2), 177–183. https://doi.org/10.1038/NG0295-177

Mayer, G., & Bendayan, M. (1997). Biotinyl-tyramide: A novel approach for electron microscopic immunocytochemistry. *Journal of Histochemistry and Cytochemistry*, *45*(11), 1449–1454. https://doi.org/10.1177/002215549704501101/ASSET/IMAGES/LARGE/10.1177_002215549704501101-FIG5.JPEG

Messeguer, X., Escudero, R., Farré, D., Núñez, O., Martínez, J., & Albà, M. M. (2002). PROMO: detection of known transcription regulatory elements using species-tailored searches. *Bioinformatics*, *18*(2), 333–334. https://doi.org/10.1093/BIOINFORMATICS/18.2.333

Myers, S. A., Wright, J., Peckner, R., Kalish, B. T., Zhang, F., & Carr, S. A. (2018). Discovery of proteins associated with a predefined genomic locus in living cells via dCAS9-APEX-mediated proximity labeling. *Nature Methods*, *15*(6), 437. https://doi.org/10.1038/S41592-018-0007-1

Nakayama, K., Kanzaki, A., Terada, K., Mutoh, M., Ogawa, K., Sugiyama, T., … Takebayashi, Y. (n.d.). Prognostic Value of the Cu-Transporting ATPase in Ovarian Carcinoma Patients Receiving Cisplatin-Based Chemotherapy. Retrieved from http://aacrjournals.org/clincancerres/article-pdf/10/8/2804/1956749/zdf00804002804.pdf

Oh, W. J., Kim, E. K., Park, K. D., Hahn, S. H., & Yoo, O. J. (1999). Cloning and Characterization of the Promoter Region of the Wilson Disease Gene. *Biochemical and Biophysical Research Communications*, *259*(1), 206–211. https://doi.org/10.1006/BBRC.1999.0732

Oksuz, O., Henninger, J. E., Warneford-Thomson, R., Zheng, M. M., Erb, H., Vancura, A., … Young, R. A. (2023). Transcription factors interact with RNA to regulate genes. *Molecular Cell*, *83*(14), 2449-2463.e13. https://doi.org/10.1016/J.MOLCEL.2023.06.012

Ovcharenko, I., Loots, G. G., Nobrega, M. A., Hardison, R. C., Miller, W., & Stubbs, L. (2005). Evolution and functional classification of vertebrate gene deserts. *Genome Research*, *15*(1), 137. https://doi.org/10.1101/GR.3015505

Park, P. J. (2009). ChIP–seq: advantages and challenges of a maturing technology. *Nature Reviews Genetics 2009 10:10*, *10*(10), 669–680. https://doi.org/10.1038/nrg2641

Pérez-Salvia, M., & Esteller, M. (2017). Bromodomain inhibitors and cancer therapy: From structures to applications. *Epigenetics*, *12*(5), 323. https://doi.org/10.1080/15592294.2016.1265710

Petruzzelli, R., Mariniello, M., De Cegli, R., Catalano, F., Guida, F., Di Schiavi, E., & Polishchuk, R. S. (2022). TFEB Regulates ATP7B Expression to Promote Platinum Chemoresistance in Human Ovarian Cancer Cells. *Cells*, *11*(2). https://doi.org/10.3390/cells11020219

Polishchuk, R., & Lutsenko, S. (2013). Golgi in copper homeostasis: A view from the membrane trafficking field. *Histochemistry and Cell Biology*, *140*(3), 285–295. https://doi.org/10.1007/S00418-013-1123-8/FIGURES/3

Poujois, A., & Woimant, F. (2019). Challenges in the diagnosis of Wilson disease. *Annals of Translational Medicine*, *7*(Suppl 2), S67–S67. https://doi.org/10.21037/ATM.2019.02.10

Ray, P. D., Huang, B. W., & Tsuji, Y. (2012). Reactive oxygen species (ROS) homeostasis and redox regulation in cellular signaling. *Cellular Signalling*, *24*(5), 981. https://doi.org/10.1016/J.CELLSIG.2012.01.008

Saad, S. Y., Najjar, T. A. O., & Alashari, M. (2004). Role of non-selective adenosine receptor blockade and phosphodiesterase inhibition in cisplatin-induced nephrogonadal toxicity in rats. *Clinical and Experimental Pharmacology and Physiology*, *31*(12), 862–867. https://doi.org/10.1111/J.1440-1681.2004.04127.X

Saifaldeen, M., Al-Ansari, D. E., Ramotar, D., & Aouida, M. (2020). CRISPR FokI Dead Cas9 System: Principles and Applications in Genome Engineering. *Cells 2020, Vol. 9, Page 2518*, *9*(11), 2518. https://doi.org/10.3390/CELLS9112518

Santos-Barriopedro, I., van Mierlo, G., & Vermeulen, M. (2021). Off-the-shelf proximity biotinylation for interaction proteomics. *Nature Communications 2021*

12:1, *12*(1), 1–12. https://doi.org/10.1038/s41467-021-25338-4

Sarode, G. V., Neier, K., Shibata, N. M., Shen, Y., Goncharov, D. A., Goncharova, E. A., … Medici, V. (2021). Wilson Disease: Intersecting DNA Methylation and Histone Acetylation Regulation of Gene Expression in a Mouse Model of Hepatic Copper Accumulation. *CMGH*, *12*(4), 1457–1477. https://doi.org/10.1016/j.jcmgh.2021.05.020

Schneider, C. A., Rasband, W. S., & Eliceiri, K. W. (2012). NIH Image to ImageJ: 25 years of image analysis. *Nature Methods 2012 9:7*, *9*(7), 671–675. https://doi.org/10.1038/nmeth.2089

Schoeberl, A., Gutmann, M., Theiner, S., Corte-Rodríguez, M., Braun, G., Vician, P., … Koellensperger, G. (2022). The copper transporter CTR1 and cisplatin accumulation at the single-cell level by LA-ICP-TOFMS. *Frontiers in Molecular Biosciences*, *9*, 1055356. https://doi.org/10.3389/FMOLB.2022.1055356/BIBTEX

Seale, P., Bjork, B., Yang, W., Kajimura, S., Chin, S., Kuang, S., … Spiegelman, B. M. (2008). PRDM16 controls a brown fat/skeletal muscle switch. *Nature*, *454*(7207). https://doi.org/10.1038/nature07182

Seto, E., & Yoshida, M. (2014). Erasers of Histone Acetylation: The Histone Deacetylase Enzymes. *Cold Spring Harbor Perspectives in Biology*, *6*(4). https://doi.org/10.1101/CSHPERSPECT.A018713

Solomon, E. R., Caldwell, K. K., & Allan, A. M. (2021). A novel method for the normalization of ChIP-qPCR data. *MethodsX*, *8*, 101504. https://doi.org/10.1016/J.MEX.2021.101504

Stalke, A., Pfister, E. D., Baumann, U., Illig, T., Reischl, E., Sandbothe, M., … Skawran, B. (2020). MTF1 binds to metal-responsive element e within the ATP7B promoter and is a strong candidate in regulating the ATP7B expression. *Annals of Human Genetics*, *84*(2), 195–200. https://doi.org/10.1111/AHG.12355

Sun, Y., Tao, W., Huang, M., Wu, X., & Gu, J. (2017). Genetic variants in telomere-maintenance genes are associated with ovarian cancer risk and outcome. *Journal of*

Cellular and Molecular Medicine, *21*(3), 510. https://doi.org/10.1111/JCMM.12995

Suphapeetiporn, K., Greally, J. M., Walpita, D., Ashley, T., & Bale, A. E. (2002). MEN1 tumor-suppressor protein localizes to telomeres during meiosis. *Genes, Chromosomes & Cancer*, *35*(1), 81–85. https://doi.org/10.1002/GCC.10113

Tan, B., Peng, S., Yatim, S. M. J. M., Gunaratne, J., Hunziker, W., & Ludwig, A. (2020). An Optimized Protocol for Proximity Biotinylation in Confluent Epithelial Cell Cultures Using the Peroxidase APEX2. *STAR Protocols*, *1*(2), 100074. https://doi.org/10.1016/J.XPRO.2020.100074

Tavera-Montañez, C., Hainer, S. J., Cangussu, D., Gordon, S. J. V., Xiao, Y., Reyes-Gutierrez, P., … Padilla-Benavides, T. (2019). The classic metal-sensing transcription factor MTF1 promotes myogenesis in response to copper. *FASEB Journal : Official Publication of the Federation of American Societies for Experimental Biology*, *33*(12), 14556–14574. https://doi.org/10.1096/FJ.201901606R

Telianidis, J., Hung, Y. H., Materia, S., & Fontaine, S. La. (2013). Role of the P-Type ATPases, ATP7A and ATP7B in brain copper homeostasis. *Frontiers in Aging Neuroscience*, *5*(AUG), 44. https://doi.org/10.3389/FNAGI.2013.00044/BIBTEX

Tian, X. P., Jin, X. H., Li, M., Huang, W. J., Xie, D., & Zhang, J. X. (2017). The depletion of PinX1 involved in the tumorigenesis of non-small cell lung cancer promotes cell proliferation via p15/cyclin D1 pathway. *Molecular Cancer*, *16*(1). https://doi.org/10.1186/S12943-017-0637-4

Tian, X. P., Qian, D., He, L. R., Huang, H., Mai, S. J., Li, C. P., … Xie, D. (2014). The telomere/telomerase binding factor PinX1 regulates paclitaxel sensitivity depending on spindle assembly checkpoint in human cervical squamous cell carcinomas. *Cancer Letters*, *353*(1), 104–114. https://doi.org/10.1016/J.CANLET.2014.07.012

Trinkle-Mulcahy, L. (2019). Recent advances in proximity-based labeling methods for interactome mapping. *F1000Research*, *8*.

https://doi.org/10.12688/F1000RESEARCH.16903.1

Tuladhar, R., Yeu, Y., Tyler Piazza, J., Tan, Z., Rene Clemenceau, J., Wu, X., … Lum, L. (2019). CRISPR-Cas9-based mutagenesis frequently provokes on-target mRNA misregulation. *Nature Communications 2019 10:1*, *10*(1), 1–10. https://doi.org/10.1038/s41467-019-12028-5

Ummethum, H., & Hamperl, S. (2020). Proximity Labeling Techniques to Study Chromatin. *Frontiers in Genetics*, *11*, 450. https://doi.org/10.3389/FGENE.2020.00450/BIBTEX

Varnavides, G., Madern, M., Anrather, D., Hartl, N., Reiter, W., & Hartl, M. (2022). In Search of a Universal Method: A Comparative Survey of Bottom-Up Proteomics Sample Preparation Methods. *Journal of Proteome Research*, *21*(10), 2397–2411. https://doi.org/10.1021/ACS.JPROTEOME.2C00265/SUPPL_FILE/PR2C00265_SI_005.ZIP

Vichai, V., & Kirtikara, K. (2006). Sulforhodamine B colorimetric assay for cytotoxicity screening. *Nature Protocols 2006 1:3*, *1*(3), 1112–1116. https://doi.org/10.1038/nprot.2006.179

Wang, H. bin, Wang, X. wei, Zhou, G., Wang, W. qiang, Sun, Y. gang, Yang, S. ming, & Fang, D. chun. (2010). PinX1 inhibits telomerase activity in gastric cancer cells through Mad1/c-Myc pathway. *Journal of Gastrointestinal Surgery*, *14*(8), 1227–1234. https://doi.org/10.1007/S11605-010-1253-4/FIGURES/4

Wang, L., Leite de Oliveira, R., Huijberts, S., Bosdriesz, E., Pencheva, N., Brunen, D., … Bernards, R. (2018). An Acquired Vulnerability of Drug-Resistant Melanoma with Therapeutic Potential. *Cell*, *173*(6), 1413-1425.e14. https://doi.org/10.1016/J.CELL.2018.04.012

Wang, Z., Zang, C., Cui, K., Schones, D. E., Barski, A., Peng, W., & Zhao, K. (2009). Genome-wide Mapping of HATs and HDACs Reveals Distinct Functions in Active and Inactive Genes. *Cell*, *138*(5), 1019–1031. https://doi.org/10.1016/j.cell.2009.06.049

Wingender, E., Dietze, P., Karas, H., & Knüppel, R. (1996). TRANSFAC: A Database on Transcription Factors and Their DNA Binding Sites. *Nucleic Acids Research*, *24*(1), 238–241. https://doi.org/10.1093/NAR/24.1.238

Wu, G., Liu, D., Jiang, K., Zhang, L., Zeng, Y., Zhou, P., … Zheng, Y. (2014). PinX1, a novel target gene of p53, is suppressed by HPV16 E6 in cervical cancer cells. *Biochimica et Biophysica Acta*, *1839*(2), 88–96. https://doi.org/10.1016/J.BBAGRM.2014.01.004

Yimit, A., Adebali, O., Sancar, A., & Jiang, Y. (2019). Differential damage and repair of DNA-adducts induced by anti-cancer drug cisplatin across mouse organs. *Nature Communications 2019 10:1*, *10*(1), 1–11. https://doi.org/10.1038/s41467-019-08290-2

Yoo, J. E., Oh, B. K., & Park, Y. N. (2009). Human PinX1 mediates TRF1 accumulation in nucleolus and enhances TRF1 binding to telomeres. *Journal of Molecular Biology*, *388*(5), 928–940. https://doi.org/10.1016/J.JMB.2009.02.051

Yuan, K., Li, N., Jiang, K., Zhu, T., Huo, Y., Wang, C., … Yao, X. (2009). PinX1 Is a Novel Microtubule-binding Protein Essential for Accurate Chromosome Segregation. *The Journal of Biological Chemistry*, *284*(34), 23072. https://doi.org/10.1074/JBC.M109.001990

Zablewska, B., Bylund, L., Mandic, S. A., Fromaget, M., Gaudray, P., & Weber, G. (2003). Transcription Regulation of the Multiple Endocrine Neoplasia Type 1 Gene in Human and Mouse. *The Journal of Clinical Endocrinology & Metabolism*, *88*(8), 3845–3851. https://doi.org/10.1210/JC.2003-030288

Zhang, H., Zheng, J., Fu, Y., Ling, J., Liu, Z. S., Lin, X., … Xie, G. (2023). Overexpression of POU3F2 promotes radioresistance in triple-negative breast cancer via Akt pathway activation. *Breast Cancer Research and Treatment*, *198*(3), 437–446. https://doi.org/10.1007/S10549-023-06876-5/METRICS

Zhao, S., Jiang, E., Chen, S., Gu, Y., Shangguan, A. J., Lv, T., … Yu, Z. (2016). PiggyBac transposon vectors: the tools of the human gene encoding. *Translational Lung Cancer Research*, *5*(1), 120. https://doi.org/10.3978/J.ISSN.2218-

6751.2016.01.05

Zhou, X. Z., Huang, P., Shi, R., Lee, T. H., Lu, G., Zhang, Z., … Lu, K. P. (2011). The telomerase inhibitor PinX1 is a major haploinsufficient tumor suppressor essential for chromosome stability in mice. *The Journal of Clinical Investigation*, *121*(4), 1266–1282. https://doi.org/10.1172/JCI43452

Zhou, X. Z., & Lu, K. P. (2001). The Pin2/TRF1-Interacting Protein PinX1 Is a Potent Telomerase Inhibitor. *Cell*, *107*(3), 347–359. https://doi.org/10.1016/S0092-8674(01)00538-4